UNIVERSITÀ
DI PAVIA

Dipartimento di Medicina Molecolare

Unità di Immunologia e Patologia Generale

Role of DDB2^{PCNA-} protein, unable to directly interact with PCNA, in UV-irradiated cells: from molecular mechanisms to cellular behaviour

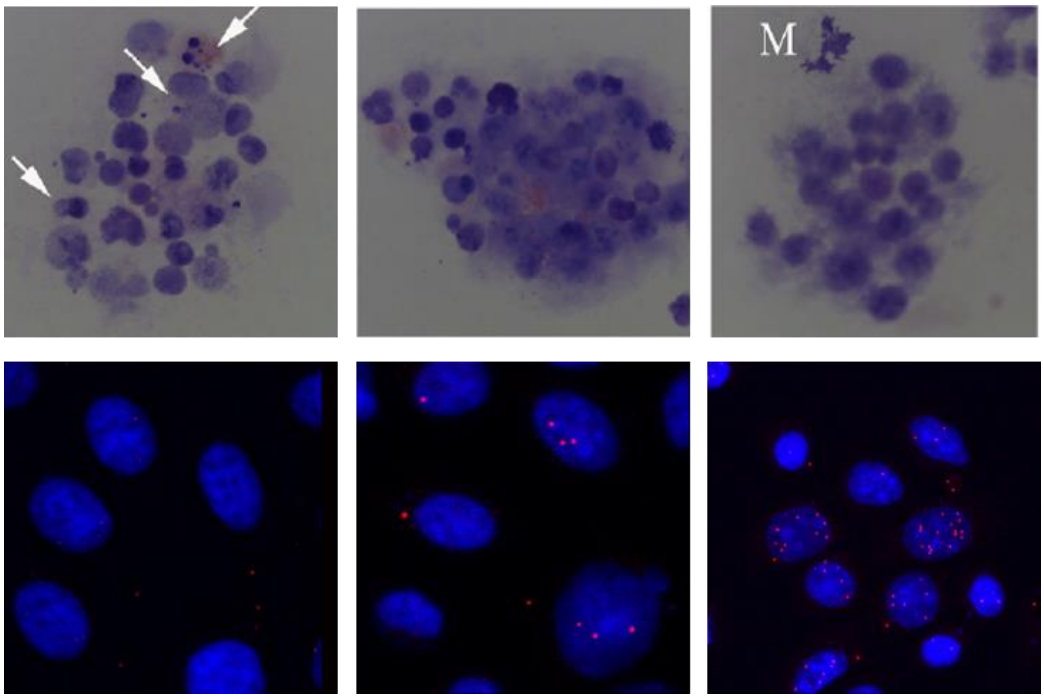

Elisabetta Bassi

Dottorato di Ricerca in
Genetica, Biologia Molecolare e Cellulare
Ciclo XXXII – A.A. 2016-2019

UNIVERSITÀ
DI PAVIA

Dipartimento di Medicina Molecolare
Unità di Immunologia e Patologia Generale

Role of DDB2^{PCNA-} protein, unable to directly interact with PCNA, in UV-irradiated cells: from molecular mechanisms to cellular behaviour

Elisabetta Bassi

Supervised by Prof.ssa Ornella Cazzalini

Dottorato di Ricerca in
Genetica, Biologia Molecolare e Cellulare
Ciclo XXXII – A.A. 2016-2019

Abstract

Nucleotide excision repair (NER) is one of the repair processes, involved in DNA damage response (DDR), which is able to remove DNA damages caused by UV radiation.
DNA damage binding protein 2 (DDB2) is involved in the recognition step of Global Genome-NER (GG-NER), a subpathway of this mechanism. It was previously demonstrated that cells expressing $DDB2^{PCNA-}$ protein, unable to directly interact with PCNA, showed a delay in DDR.

Starting from this evidence, in the first part of my PhD thesis, it was demonstrated that DDB2 mutated protein has an inefficient DNA binding affinity to UV photolesions, highlighting that the loss of DDB2-PCNA association affects the GG-NER mechanism.

Hereafter, mutated DDB2 protein confers to cells an unexpected proliferation advantage and an increased UV resistance, suggesting that these cells are more prone to proliferate. Interestingly, analyzing the morphological features of mitoses, a significant presence of atypical mitoses was found in cells stably expressing $DDB2^{PCNA-}$ protein, leading to speculate that these cells could be more prone to acquire a tumour-like phenotype. Moreover, I demonstrated, using different approaches, that $DDB2^{PCNA-}$ protein is able to interact with Polymerase η, an enzyme involved in the Translesion DNA Synthesis (TLS), after UV-C exposure.

Next, wound healing experiment and Boyden chamber assay have highlighted marked migration ability in the presence of mutated protein, suggesting a possible correlation to an aggressive cell phenotype.
Besides, the modified expression levels of E-cadherin and Vimentin proteins together with an increased activity of two metalloproteinases (MMP-2 and MMP-9), in the presence of mutated protein, leaving to speculate a possible $DDB2^{PCNA-}$ protein involvement in the epithelial to mesenchymal transition (EMT) process.

Finally, in the last section of my PhD project, I have investigated whether DDB2 protein may be involved in other steps of DDR, suggesting a possible cooperation between GG-NER and Transcription Coupled-NER (TC-NER).

In conclusion, it was demonstrated that:

- the loss of DDB2-PCNA interaction affects the mainly steps of GG-NER mechanism;
- the presence of a $DDB2^{PCNA-}$ protein confers to cells not only an increased UV resistance, but also proliferation and motility advantages characterizing an aggressive behaviour and suggesting that mutated cells could be more prone to acquire a tumour-like phenotype;
- the Polymerase η-DDB2 mutated protein interaction leads to consider a possible correlation between $DDB2^{PCNA-}$ positive cells and genomic instability;
- the inability of DDB2 to directly interact with PCNA also affects the repair process of actively transcribed genes, speculating a possible cooperation between GG-NER and TC-NER processes.

Acknowledgements

I would like to thank my supervisor Prof.ssa Ornella Cazzalini for the opportunity she gave me to work on this project, she mentored and guided me during these three years of my PhD research experience, sharing her experience and clarifying my potential doubts.

My heartfelt thanks to Dr. Paola Perucca for her precious recommendations she transmitted me and for always being helpful in every situation, not only work-related.

My grateful goes to Prof.ssa Lucia Anna Stivala, research team head, for her expertise and useful comments that have contributed to improve this research project.

I also would like to thank my colleague Dr. Isabella Guardamagna for teaching me the different laboratory techniques at the beginning of my PhD program, then, for her support that she never missed to give me.

I am grateful to have been a part of this peerless research group that let me to perceive a stimulating and open to dialogue atmosphere from the very beginning.

I would like to thank the Unit of Immunology and General Pathology of University of Pavia, in particular Dr. Maristella Maggi and Dr. Greta Pessino for their kind helpfulness.

Finally, I also would like to thank Prof. Ennio Prosperi for his support to the present project; Dr. Patrizia Vaghi for help in confocal microscopy analysis; Dr. Emmanuele Crespan and Dr. Simone Sabbioneda for their technical advices.

Abbreviations

6-4 Photoproducts (6-4 PPs)
ALDH Aldehyde dehydrogenase
AMP Ampicillin
APS Ammonium persulfate
ATM Ataxia telangiectasia mutated kinase
ATR Ataxia telangiectasia RAD3-related kinase
BER Base excision repair
BSA Bovine Serum Albumin
CAK Cdk activating kinase
CB Chromatin bound
COP9/CSN Constitutive photomorphogenesis 9 signalosome
CPDs Cyclobutane Pyrimidine Dimers
CRA Colorectal adenoma
CRC Colorectal cancer
CS *Cockayne syndrome*
CSA *Cockayne Syndrome* group A protein
CSB *Cockayne Syndrome* group B protein
CSCs Cancer stem cells
CUL4 Cullin 4
DCAF Chromatin associated factor
DDB1 DNA damage-binding protein 1
DDB2 DNA damage-binding protein 2
DDR DNA Damage Response
DMEM Dulbecco's modified Eagle's *medium*
DTT Dithiothreitol
E. COLI *Escherichia coli*
ECM Extracellular matrix
EDTA Ethylenediaminetetraacetic acid
EGTA Ethylene glycol tetraacetic acid
EMSA Electrophoretic mobility shift assay
EMT Epithelial to mesenchymal transition
FAM Carboxyfluorescin
FBS Foetal Bovine Serum
GFP Green Fluorescent Protein
GG-NER Global Genome-Nucleotide Excision Repair
HCR Host cell reactivation
HR Homologous recombination

IGM-CNR Istituto di Genetica Molecolare-Centro Nazionale delle Ricerche
MEFs Mouse embryonic fibroblasts
MFI Mean fluorescence intensity
MMPs Metalloproteinases
MMR Mismatch repair
MnSOD Manganese superoxide dismutase
NER Nucleotide excision repair
NHEJ Non-homologous end joining
PBS Phosphate-buffered saline
PBST PBS and 0.2% Tween 20
PCNA Proliferating cell nuclear antigen
PFA Paraformaldehyde
PIP-box PCNA-protein interacting box
PLA Proximity Ligation Assay
PMSF Phenylmethane sulfonyl fluoride
Pol η-GFP Polymerase η-GFP
RFC Replication factor C
RFP Red Fluorescent Protein
RIR REV1-interacting region
ROC1 Regulator of Cullin 1
RT Room Temperature
S Soluble
SDS Sodium Dodecyl Sulfate
TBE Tris-borate-EDTA
TC-NER Transcription-Coupled Nucleotide Excision Repair
TEMED Tetramethylethylenediamine
TFIIH Transcription factor II H
TLS Translesion DNA synthesis
TTD *Trichothiodystrophy*
UBD Ubiquitin-binding domain
UBM Ubiquitin-binding motif
UBZ Ubiquitin-binding zinc domain
USP7 Ubiquitin-specific peptidase 7
UV-DDB Ultraviolet DNA damage binding protein
UVSSA UV-sensitive scaffold protein A
XP *Xeroderma pigmentosum*
XP-V *Xeroderma pigmentosum* variant

Contents

Abstract I
Acknowledgements III
Abbreviations IV
1. Introduction 1
1.1 DNA damage and DNA damage response 1
1.2 Nucleotide excision repair 2
1.2.1 Global genome-nucleotide excision repair 5
1.2.2 Transcription-coupled nucleotide excision repair 9
1.3 Nucleotide excision repair-related human diseases 11
1.4 Translesion DNA synthesis 13
1.5 DDB2 and its multiple facets 16
2. Aims of the research 20
3. Materials and methods 22
3.1 Cell lines 22
3.2. Stable transfection of HEK293 or transient transfection of HeLa cells with pcDNA3.1-DDB2^{Wt} or pcDNA3.1-DDB2^{PCNA-} constructs 22
3.3 Electrophoretic mobility shift assay 25
3.3.1 EMSA with recombinant proteins 25
3.3.1.1 Extraction and purification of recombinant DDB2^{PCNA-} protein with Ni-His tagged resin (QIAGEN) 25
3.3.1.2 pEGFP-N1 plasmid (Clontech) UV irradiation 30
3.3.1.3 EMSA on agarose gel 31
3.3.2 EMSA with cell extracts derived from HEK293 DDB2^{Wt} or DDB2^{PCNA-} 32
3.3.2.1 HEK293 DDB2^{Wt} or DDB2^{PCNA-} cell extracts 33
3.3.2.2 EMSA on acrylamide gel 34
3.4 Interaction between DDB2 and XPG at UV-damaged sites 37
3.4.1 DDB2 and XPG colocalization 37
3.4.1.1 UV-C local irradiation 37
3.4.1.2 Paraformaldehyde fixation protocol 38
3.4.1.3 Immunofluorescence staining 38
3.4.1.4 Immunoprecipitation assay and immunoblot analysis 39
3.5 Evaluation of proliferation ability 42
3.5.1 Clonogenic assay 42
3.5.2 Study of mitoses 43

3.6 Study of DDB2-Polymerase η interaction 44
3.6.1 Co-transfection of HeLa cells with pcDNA3.1-DDB2^{Wt} or pcDNA3.1-DDB2^{PCNA-} and Polymerase η-GFP constructs and local UV-irradiation 44
3.6.2 Fixation and lysis protocol 45
3.6.3 Immunostaining and immunoprecipitation experiments..... 45
3.6.4 Proximity Ligation Assay 46
3.7 Wound healing assay 47
3.8 Influence of DDB2 protein on cell migration ability 48
3.8.1 Western blot analysis of E-cadherin and Vimentin proteins 49
3.8.2 Zymography assay..... 49
3.8.3 Boyden chamber assay 51
3.9 Other possible role of DDB2..... 52
3.9.1 Host cell reactivation assay and *in vivo* cytofluorimetric analysis..... 53
3.9.2 Evaluation of DDB2 and Polymerase II co-localization by immunofluorescence and confocal microscopies 54
4. Results..... 55
I. DDB2^{PCNA-} in global genome-nucleotide excision repair 55
4.1 Delay in the recognition of UV-DNA lesions 55
4.2 Evaluation of DDB2 binding affinity to DNA lesions 55
4.2.1 EMSA on agarose gel..... 56
4.2.2 EMSA on acrylamide gel..... 57
4.3 Influence of DDB2 protein in the late NER phases 60
II. Influence of DDB2-PCNA interaction on cell proliferation after UV-damage 66
4.4 Study of cell proliferation ability..... 66
4.5 Study of mitoses and cell viability..... 68
4.6 Evaluation of DDB2-Polymerase η interaction 71
4.6.1 Evaluation of DDB2 and Polymerase η co-localization by confocal analysis..... 71
4.6.2 Study DDB2 and Polymerase η interaction by immunoprecipitation assay..... 74
4.6.3 Study of direct interaction between DDB2 and Polymerase η through Proximity Ligation Assay approach..... 77
III. Study of cell migration after UV-damage..... 81
4.7 Wound healing assay 81
4.8 Involvement of DDB2 protein in epithelial to mesenchymal transition 84
4.8.1 Evaluation of E-cadherin and Vimentin expression after UV damage 84

4.8.2 Detection of metalloproteinases 2 and 9 by gelatin zymography 88
4.9 Evaluation of migration capability in irradiated HEK293 92
IV. A novel possible role of DDB2 95
4.10 A novel putative role of DDB2 95
4.10.1 Evaluation of DNA Damage Response to UV lesions 95
4.10.2 Study of co-localization between DDB2 and Polymerase II proteins 99
5. Discussion 104
6. Conclusions and perspectives 110
References 112
List of original manuscripts 131
My contribution to manuscripts 132
Original manuscripts 133

1. Introduction

1.1 DNA damage and DNA damage response

Several DNA damaging agents constantly threaten our genetic heritage. Alkylating chemicals and metabolically-derived aldehydes or reactive oxygen species produced by cellular metabolism and spontaneous replication errors are endogenous damaging factors; whereas, the ultraviolet radiation (UV), ionizing rays, environmental chemicals and chemotherapeutic agents are considered the exogenous mutagens.

When a DNA lesion has occurred, cells carry out several strategies to preserve the integrity of genetic information and to overcome the accumulation of mutations that can leads to genome instability (Gillet LC and Schärer OD 2006; Roos WP *et al*. 2016).

Following a DNA lesion, mammalian cells activate checkpoint control systems that arrest cell cycle progression to repair DNA damage or, if the lesion is too severe, to induce cell death program (Plesca D *et al*. 2008).

When the lesion is repairable, the DNA damage response (DDR) is activated to remove DNA adducts, which are toxic for cells causing the arrest of polymerases during the replication or transcription phases (Hoeijmakers JH 2001; Roos WP *et al*. 2016).

Depending on the type of DNA lesion and on the type of activated signalling pathway, the mainly mechanisms which are involved in the DDR are the DNA repair by non-homologous end joining (NHEJ), homologous recombination (HR), mismatch repair (MMR), base excision repair (BER) and nucleotide excision repair (NER) (**Figure 1**) (Ashour ME *et al*. 2015; Stingele J *et al*. 2015, Chatterjee N and Walker GC 2017).

Furthermore, when the replication fork is stalled, there is a mechanism of

DNA damage tolerance, known as translesion DNA synthesis (TLS), that can bypass the DNA lesion but it is not error free (**Figure 1**) (Roos WP *et al*. 2009; Waters LS *et al*. 2009; Sale JE 2012; Goodman MF and Woodgate R 2013).

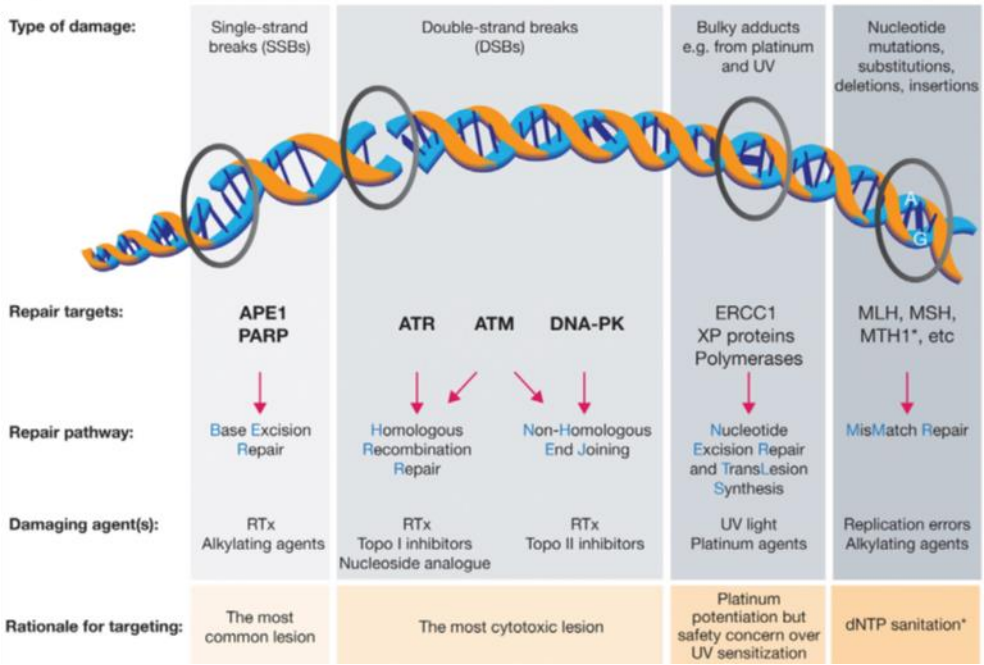

Figure 1 DNA damage response pathways (O' Connor MJ 2015)

1.2 Nucleotide excision repair

In eukaryotic organisms the NER mechanism is a highly conserved versatile pathway, which is able to remove a broad variety of DNA damages (e.g. modifications of one or more nucleotides in purine or pyrimidine bases, chemically induced bulky adducts); this process is particularly specialised in UV-lesion removal caused by UV irradiation (Paul D *et al*. 2019).

UV rays, originated from sunlight, are severe DNA mutagens and the most frequent UV-lesions on chromatin are cyclobutane pyrimidine dimers (CPDs) and 6-4 photoproducts (6-4 PPs) which are constituted by covalent linkages

between two adjacent pyrimidines (Friedberg EC *et al*. 2006; Ganesan A and Hanawalt P 2017; Mao P *et al*. 2017; Cadet J and Douki T 2018) and cause DNA helix distortion (Figure 2).

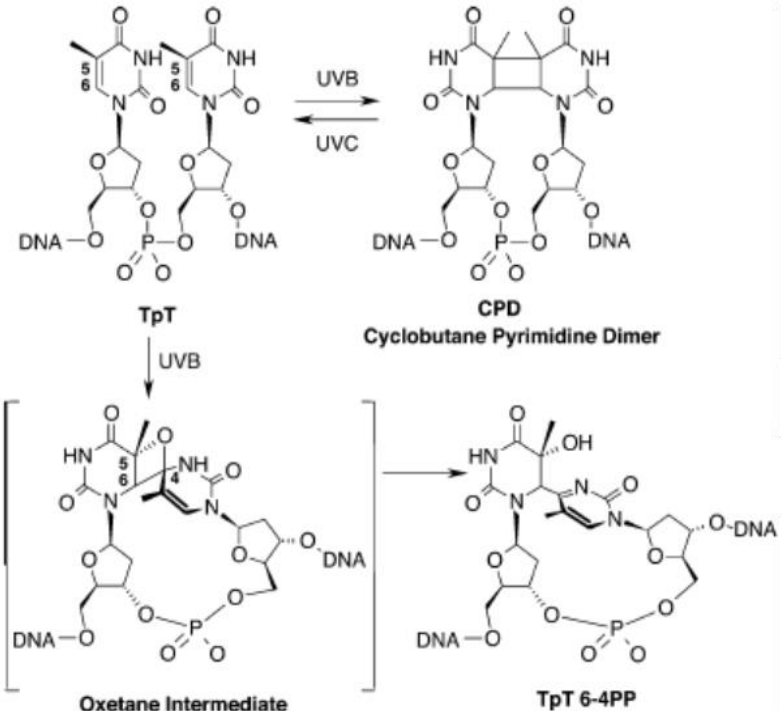

Figure 2 CPD and 6-4 PP chemical structures and formation (Gillet LC and Schärer OD 2006)

The frequency of CPD or 6-4 PP formation depends on the type of UV wavelength, the dose and the region of DNA damaged (Friedberg EC *et al*. 2006; Besaratinia A *et al*. 2011). Generally, if unrepaired, the mainly mutagen and cancerous photolesions are CPDs molecules, which occur 3-4 fold more than 6-4 PPs upon UV-C or UV-B rays with a $\lambda \leq 296$ nm (You YH *et al*. 2001); however, a DNA containing 6-4 PPs damages exhibits a structural distortion more pronounced than a DNA-harbouring CPDs lesions (Park H *et al.* 2002; Dehez F *et al*. 2017).

Depending on the early recognition step of DNA lesions, NER process is divided in two subpathways: the global genome-NER (GG-NER) and the transcription-coupled NER (TC-NER) (Schärer OD 2013; Spivak G 2015).

The GG-NER process operates and eliminates photolesions in the entire genome, included the untranscribed and silent regions (Petruseva IO *et al*. 2014); whereas, the TC-NER removes DNA damage in actively transcribed genes followed the RNA polymerases stalling (**Figure 3**) (Brueckner F *et al*. 2007; Li W *et al*. 2014; Xu J *et al*. 2017; Sanz-Murillo M *et al*. 2018).

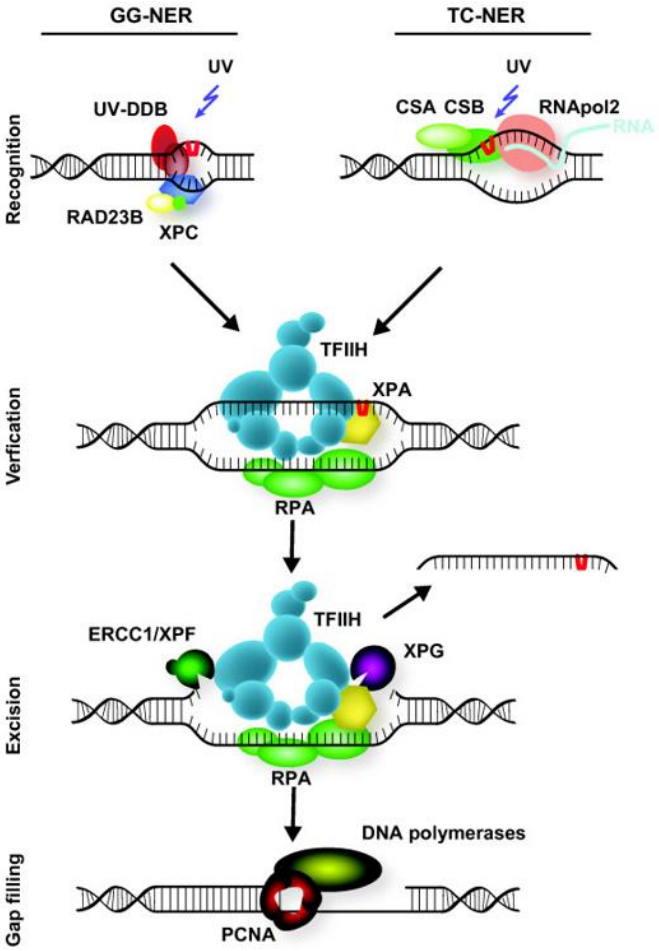

Figure 3 NER subpathways: GG-NER and TC-NER (Lans H *et al*. 2012)

1.2.1 Global genome-nucleotide excision repair

GG-NER, a "cut and patch" process, in eukaryotic cells is orchestrated by 30 proteins which are sequentially involved in damage recognition, dual incision and excision of damaged fragment, gap-filling new DNA synthesis and ligation steps (**Figure 4**) (Aboussekhra A *et al*. 1995; Mu D *et al*. 1995; Araujo SJ *et al*. 2000).

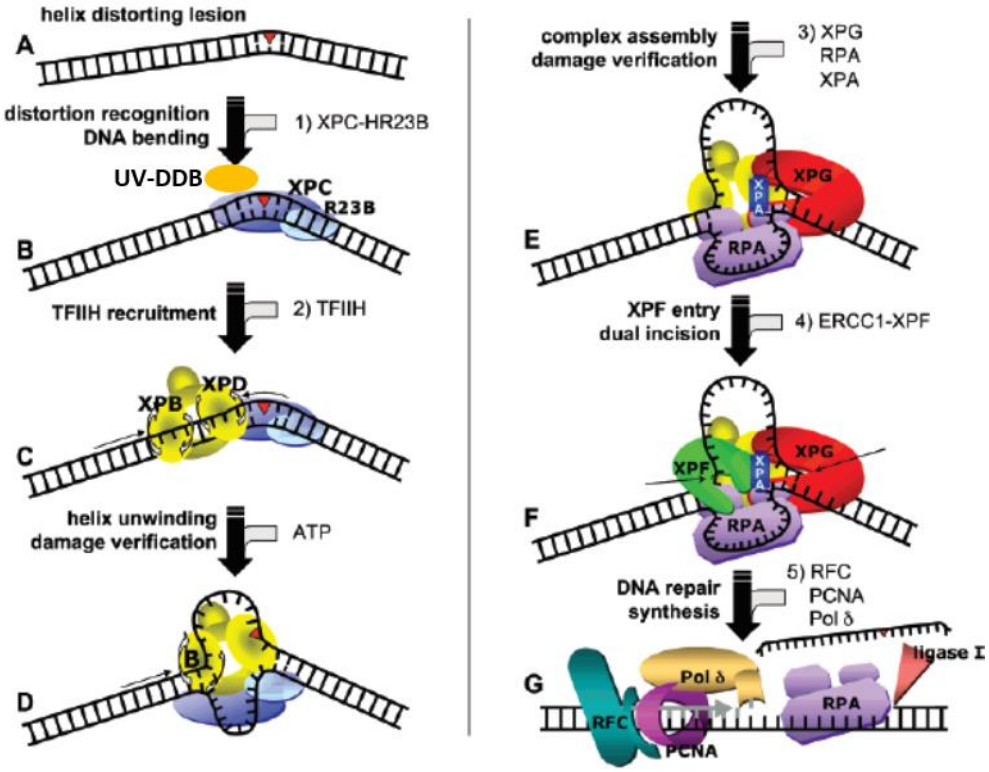

Figure 4 Molecular mechanism of GG-NER. (**A**) DNA containing lesion; (**B**) recognition of damage; (**C**) TFIIH complex recruitment; (**D**) DNA helix unwinding; (**E**) "preincision complex" assembling; (**F**) dual incision; (**G**) synthesis of a new DNA fragment and ligation steps (Gillet LC and Schärer OD 2006, modified)

The heterotrimeric complex formed by XPC-hHR23B-Centrin-2 (XPC complex) detects the DNA damage in a multistep manner (Sugasawa K *et al*. 1998; Araki M *et al*. 2001; Sugasawa K *et al*. 2001; Sugasawa K *et al*. 2002). It directly interacts with the damaged DNA producing a well-defined DNA conformation

to enhance the recruitment of the next NER factor TFIIH (Transcription factor II H) (Yokoi M *et al*. 2000; Volker M *et al*. 2001; Janicijevic A *et al*. 2003).
It was demonstrated that hH23B stabilizes and protects XPC from proteasome 26S degradation, inhibiting its polyubiquitination (Ortolan TG *et al*. 2000; Ng JM *et al*. 2003).
Interestingly, the XPC complex poorly recognizes CPDs lesions (Kusumoto R *et al*. 2001; Sugasawa K *et al*. 2001; Reardon JT and Sancar A 2003), thus, this function is carried out by UV-DDB (Ultraviolet DNA damage binding protein) complex (**Figure 5**) (Wakasugi M *et al*. 2002; Fitch ME *et al*. 2003) that facilitates the following recruitment of XPC (Sugasawa K *et al*. 2005).

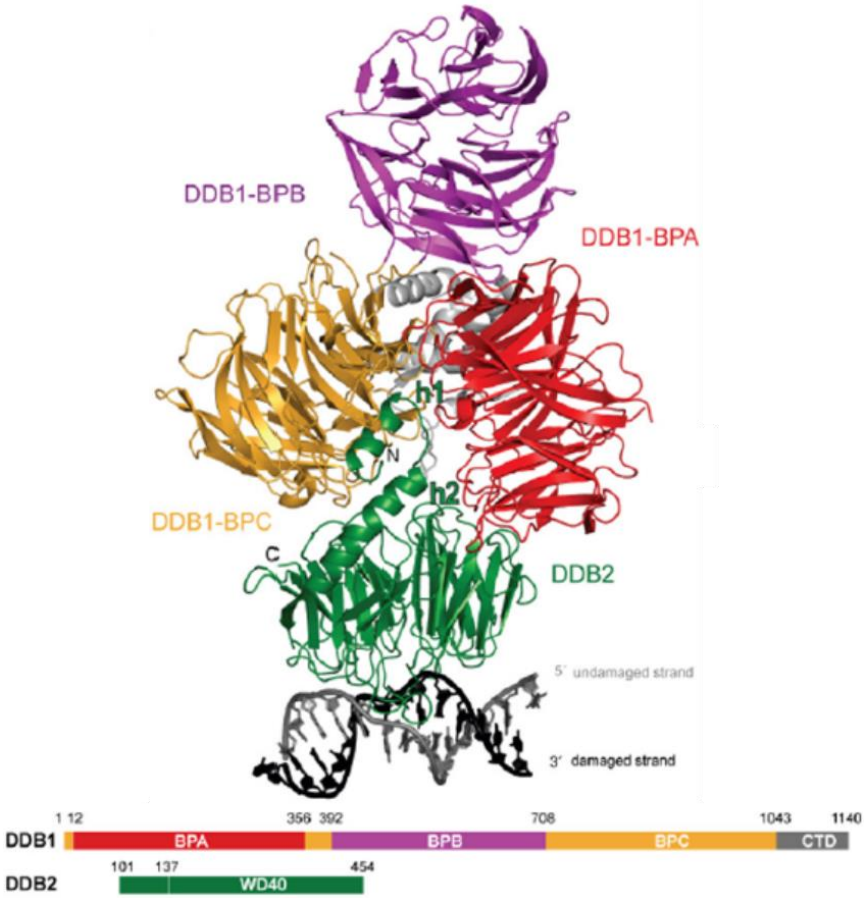

Figure 5 Molecular structure of UV-DBB complex (Scrima A *et al*. 2008)

This complex is composed by DDB1 (DNA damage-binding protein 1) and DDB2 (DNA damage-binding protein 2) proteins (Wittschieben BØ *et al*. 2005; Feltes BC and Bonatto D 2015; Sugasawa K 2016); DDB1 protein forms a complex with CUL4 (Cullin 4) and ROC1 (Regulator of Cullin 1) E3 ubiquitin ligase (Groisman R *et al*. 2003); thus, the complex transfers ubiquitin molecules to target protein, such as DDB2, XPC or histones for chromatin relaxation (Kapetanaki MG *et al*. 2006; Jackson S and Xiong Y 2009; Zhu Q *et al*. 2009).

Upon UV *stimuli*, DDB2 translocates DDB1 into the nucleus and all together form the UV-DDB complex. Then, DDB2 directly interacts with CPDs photolesions with its suitable binding pocket (Schärer OD and Campbell AJ 2009); it seems that the presence of DDB1 protein allows the stabilization of the complex to photolesions (Wittschieben BØ *et al*. 2005; Feltes BC and Bonatto D 2015; Sugasawa K 2016). After damage recognition, DDB2 is ubiquitinated by DDB1-CUL4-ROC1 complex, causing the loss of its DNA binding affinity and its proteasomal-mediated degradation. It was "*in vivo*" demonstrated that DDB2 degradation not only facilitates but also is necessary for XPC recruitment to damaged sites (Sugasawa K *et al*. 2005; Wang QE *et al*. 2005; El-Mahdy MA *et al*. 2006).

Moreover, several studies have demonstrated that UV-DDB complex is able to interact with chromatin remodelling factors or histone modification enzymes to promote chromatin accessibility to the following NER factors (Groisman R *et al*. 2003; Sugasawa K *et al*. 2005; Kapetanaki MG *et al*. 2006; Wang H *et al*. 2006; Fischer ES *et al*. 2011; Luijsterburg MS *et al*. 2012; Osakabe A *et al*. 2015).

TFIIH factor is composed by ten subunits which are assemble in a ring-like structure, the "core" complex, constituted by XPB, XPD, p62, p44, p34, p52, p8 and a cdk activating kinase (CAK) subunit (Mat1, Cdk7, CyclinH).

Together with XPC, TFIIH verifies the damage by a so-called bipartite selection system (Hess MT *et al*. 1997):

1) XPC detects DNA distortion ("base pairing disruption");
2) TFIIH complex confirms the presence of a "chemical modification".

Specifically, as first step TFIIH is loaded at the 5' damaged strand through a direct interaction with XPC in an ATP-independent manner (Araujo SJ *et al*.

2001; Uchida A *et al*. 2002; Riedl T *et al*. 2003; Tapias A *et al*. 2004); then, thanks to XPB and XPD motor components, TFIIH translocates along the chromatin; when a DNA lesion is detected, XPB and XPD helicases stall in the area of the lesion and begin to unwind the chromatin in ATP-dependent manner to allow the DNA helix opening and the recruitment of subsequent NER proteins (Drapkin R *et al*. 1994).

After the preliminary proofreading activity of TFIIH, the "pre-incision complex" composed by RPA, XPA and XPG protein, is recruited to damaged DNA. At the arrival of XPG, it was demonstrated that XPC loses its damage DNA binding activity (Wakasugi M and Sancar A. 1998; Riedl T *et al*. 2003).
RPA, through its recruitment to undamaged strand close to DNA bubble, allows the accurate positioning of XPG and ERCC1-XPF (de Laat WL *et al*. 1998).
XPA is a small protein and it appears to have a key role in probing the proper assemble of the "pre-incision complex"; furthermore, XPA interacts with several NER proteins (RPA, ERCC1-XPF, TFIIH, XPC) (Gillet LC and Schärer OD 2006).

Next, to remove 24-32 nucleotides containing DNA photolesion, a dual incision is performed by two endonucleases: XPG, which is already recruited with "pre-incision complex" and XPF-ERCC1. The second one cuts on 5' side of DNA, followed by the incision on 3' end carried out by the nucleases XPG that leaves a free 3' OH terminus (Sijbers AM *et al*. 1996; Evans E *et al*. 1997; Gillet LC and Schärer OD 2006; Tsodikov OV *et al*. 2007; Staresincic L *et al*. 2009).

Then, the gap-filling occurs with the synthesis of a new DNA fragment by polymerases. In particular, this step is divided in two separated pathways. In the first one, polymerases δ and κ are recruited by RFC (Replication factor C) complex or ubiquitinated PCNA (Proliferating cell nuclear antigen) with XRCC1 molecules, respectively. Both polymerases intervene when the repair synthesis is difficult, due to damaged chromatin structure: for example, it was supposed that polymerases κ, that is involved in TLS process, is recruited when two lesions are closely spaced.

In the second pathway, which occurs in 50% of human cells, polymerase ε operates quickly with CTF18-RFC complex when the damaged site is in accessible conformation (Ogi T *et al*. 2010).

Finally, the nick is sealed by specific DNA ligases (Araujo SJ *et al*. 2000; Moser J *et al*. 2007).

1.2.2 Transcription-coupled nucleotide excision repair

The TC-NER is the other subpathway involved in NER that differs from GG-NER in the early step of the repair process, during the recognition of the lesion. Conversely to GG-NER, this pathway removes CPDs and 6-4 PPs with an equal and efficient repair ability (van Hoffen A *et al*. 1995).
Following a UV photolesion formation, the RNA polymerase II blocked at the damaged site of actively transcribed strand, is the signal that triggers a cascade of events that leads to the assembling of an efficient repair machinery (**Figure 6**) (Vermeulen W and Fousteri M 2013).

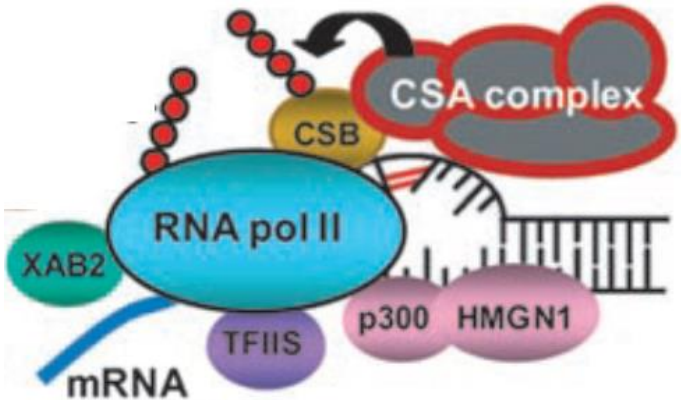

Figure 6 DNA damage recognition factors in TC-NER (Auclair Y *et al*. 2009, modified)

Importantly, the accessibility to damaged chromatin is a critical step in this repair process, thus, several TC-NER factors coordinate their activity and recruit some enzyme which are involved in histone modifications and chromatin remodelling (Lans H *et al*. 2012).

The principal factors involved in TC-NER in mammalian cells are: CSB (Cockayne Syndrome group B protein), CSA (Cockayne Syndrome group A protein), UVSSA (UV-sensitive scaffold protein A) and USP7 (Ubiquitin-specific peptidase 7), XAB2 and HMGN1.

CSB factor dynamically interacts with RNA polymerase II with a great binding affinity; upon UV damage, this interaction is stabilized (van den Boom V *et al*. 2004). CSB, defined as the master coordinator of TC-NER, remodels the chromatin in an ATP-dependent manner (Citterio E *et al*. 2000) to allow the following recruitment of CSA, p300 and the other NER factors (TFIIH, XPG, XPA, RPA, and XPF/ERCC1) (Groisman R *et al*. 2003; Beerens N *et al*. 2005; Fousteri M *et al*. 2006). In the structure of this protein there is the ubiquitin-binding domain, which is essential for the regulation and the activity of CSB (Anindya R *et al*. 2010): its binding to an ubiquitylated factor allows the release of CSB from damaged sites at late phase of TC-NER enhancing the repair activity (Vermeulen W and Fousteri M 2013).

CSA protein, recruited by CSB, is the dedicated substrate receptor (DCAF) of the complex DDB1-CUL4-RX1 (CRL4) E3-ubiquitin ligase associated with COP9 (Constitutive photomorphogenesis 9) signalosome (CNS). The complex is involved in the regulation of TC-NER process through the ubiquitination of some NER factors. At early time upon UV damage, CNS inhibits the ubiquitination activity of CRL4 complex (Groisman R *et al*., 2003; Fousteri M *et al*. 2006); when CNS is dissociated from CSA, the latter is activated. Consequently, CSB, the substrate for the CRL4 complex, is ubiquitylated and degraded by proteasome to permit the subsequent steps of repair process (Groisman R *et al*. 2006; Li JM and Jin J 2012).

The recently identified UVSSA forms a complex with USP7 and all together stabilize and protect CSB and RNA polymerase II complex, preventing their polyubiquitination and, consequently, degradation (Fei J and Chen J 2012; Schwertman P *et al*. 2012; Zhang X *et al*. 2012).

XAB2 protein binds to RNA polymerase II stalled *via* CSA- and UV-dependent manner (Fousteri M *et al*. 2006); it is considered as a scaffold protein for the

proper TC-NER complex formation (Nakatsu Y *et al*. 2000) and also for the restoration of RNA synthesis upon UV-damage induction (Kuraoka I *et al*. 2008).

Another important factor for TC-NER is HMGN1. The protein interacts with UV-blocked RNAPII through CSA-dependent manner (Fousteri M *et al*. 2006). This protein is not essential for the incision complex assembly, but it is supposed that HMGN1 might enhances the dual incision helping p300 to remodel the chromatin (Trieschmann L *et al*. 1998; Lim JH *et al*. 2005).

Both "*in vitro*" and "*in vivo*" experiments have demonstrated that the stalled RNA polymerase II, after the damage sensing, is dislocated to allow the accessibility and the correct assembly of the following factors involved in the repair pathway (Donahue BA *et al*. 1994; Sigurdsson S *et al*. 2010; Cheung AC and Cramer P 2011). The "backtracking" of the polymerase is related to a transcription cleavage of the nascent RNA: any mismatch between RNA and DNA hybrid stimulates the backtracking elongation to allow the removal of RNA-containing the error (Vermeulen W and Fousteri M 2013).

Finally, after the recognition of the lesion, the following steps and factors are the same of the GG-NER (**Figure 4** from step **C**).

1.3 Nucleotide excision repair-related human diseases

Three rare autosomal recessive diseases, *Xeroderma pigmentosum* (XP), *Trichothiodystrophy* (TTD) and *Cockayne syndrome* (CS), are associated with mutations in NER genes (Bukowska B and Karwowski T 2018).

Xeroderma pigmentosum (from the Greek words *xero* – dry and *derma* – skin) is characterized by extreme sunlight sensitiveness (Hebra F and Kaposi M 1874) and a significantly increased frequency to develop skin cancer (Tofuku Y *et al*. 2015). It has been reported that XP patients are more prone to carcinogenesis; in fact, they shown deficient antioxidant enzyme activity and,

moreover, several mutations in tumour suppressor genes were identified (Vuillaume M *et al*. 1986; Giglia G *et al*. 1998; Hayashi M *et al*. 2005). In two third of patients, clinical manifestations occurred in the early months of life, and the main symptom is hypersensitivity to sunlight which is characterized by the manifestations of freckling, redness and blistering. In the other patients, the first clinical evidence is an increased number of lentigines in the UV-exposed skin areas (Lehmann AR *et al*. 2011). Moreover, sun exposure leads to premature skin ageing.

Depending on which gene is impaired in NER process, the syndrome is classified in seven complementation groups (from XP-A to XP-G) (Cleaver JE 1968); additionally, XP-V variant was described by Lehmann and colleagues (Lehmann AR *et al*. 1975). The severity of symptoms and the main organs that are affected depend on the type of gene alterations. All XP patients are predisposed to skin abnormalities; indeed, 30% of them develops neurological impairments and 40% of XP patients are related to ophthalmologic diseases (Kraemer KH *et al*. 2007; Karass M *et al*. 2015).

Among the seven complementation groups, XP-E is characterized by mutations in DDB2 gene; it is the least severe type of disease with mild skin symptoms, but the risk to develop skin cancer at later age is high. Neurological pathologies have not been diagnosed in these patients (Lehmann AR *et al*. 2011).

Trichothiodystrophy (TTD) (from Latin *tricho-thio-dys-trophe* means hairsulphur-faulty-nourishment) is a very rare disease with a prevalence of 1:1000000, to date about only 100 patients are diagnosed (Faghri S *et al*. 2008). Principal clinical manifestations are photosensitivity, ichthyosis, brittle hair, intellectual disability, decreased fertility and short stature (Crovato F *et al*. 1983). Brittle and fragile hair, caused by a lack of sulphure, is the typical diagnostic hallmark of this syndrome (Stefanini M *et al*. 2010). Moreover, several TTD patients are affected by neurological pathologies such as developmental retardation, altered motor control, hearing impairment and growth retardation (Faghri S *et al*. 2008).

The main mutated genes, XPB, XPD, TTDA, which are normally involved in TFIIH formation, are responsible for developmental retardation as consequence of transcription impairment (Fois A *et al*. 1988; Botta E *et al*.

1998; Bergmann E and Egly JM 2001).
A distinct small group of TTD patients, who carried mutations in TTDN1 gene, is characterized by non-photosensitive type of disease with a proper formation and expression of TFIIH factor (Fois A *et al*. 1988; Botta E *et al*. 1998; Bergmann E and Egly JM 2001).

Cockayne syndrome (CS) is identified by a huge variety and severity of clinical manifestations, such as neurological impairment, growth failure, microcephaly and mental retardation; for this reason, it is divided in three groups. The type 1 is the classical form and it is diagnosed in one year newborn child. Mutations in CSA gene are responsible for the phenotype of this group (Karikkineth AC *et al*. 2017). Type 2 is more severe than type 1, with an early-onset of symptoms. It is related to CSB gene mutations which cause a grave retarded neurological development. Type 3 is the mildest form with a late onset of the disease (Karikkineth AC *et al*. 2017).
CS patients also manifested a premature accelerated ageing. Among the complicated mechanisms underlying ageing, the authors suggested an impairment in the activity of mitochondrial RNA polymerase, involving CSB protein in the proper function of this organelle (Scheibye-Knudsen M *et al*. 2012).
Despite its severe outcome, it is difficult to detect CS disease and, contrary to XP and TTD syndromes, a prenatal diagnosis test is not available (Wilson BT *et al*. 2016).

1.4 Translesion DNA synthesis

As mentioned in Paragraph 1.1, translesion DNA synthesis (TLS) is a conserved DNA damage tolerance process, which occurs after replicative DNA polymerases blocking following a DNA lesion (Quinet A *et al*. 2018).
The mechanism is activated to overcome the prolonged stalling of polymerases to avoid fork collapse and DNA strand breaks (both double and single) (Waters LS *et al*. 2009; Goodman MF and Woodgate R 2013).

Currently, 11 TLS polymerases are known: REV1, Pol η, Pol ι, Pol κ, Pol ζ, Pol μ, Pol λ, Pol β, Pol ν, Pol θ which are distributed in four families (Y, B, X and A) and PrimPol (Chatterjee N and Walker GC 2017).

These polymerases are able to displace replicative polymerases from damaged sites, insert new nucleotides in the opposite strand and past the lesions; then, DNA is displaced from TLS enzyme to allow the replacement of a high fidelity DNA polymerases (Sale JE 2013).

These enzymes are characterized by a more spacious and malleable active site compared to replicative polymerases; this characteristic allows to better fit several DNA damaged templates, although they have a lower DNA binding affinity (Rothwell PJ and Waksman G 2005; Waters LS and Walker GC 2006; Silverstein TD *et al*. 2010; Zhao Y *et al*. 2012; Sale JE 2013). However, TLS polymerases are generally related to mutagenesis because of their low fidelity activity to incorporate nucleotides, without a 3'-5' exonuclease proofreading ability (Kunkel TA 2003).

Two models have been proposed to explain the TLS polymerases activity: "two steps" and "central step".

In the first mechanism, which is both error-free and error prone, two polymerases are involved: the inserter and the extender (Shachar S *et al*. 2009). The earlier, generally Pol η, ι or κ, is able to add a single nucleotide in the DNA strand opposite to the lesion, then, the extender enzyme, usually Pol ζ, takes place of the inserter and extends the primer template (Washington MT *et al*. 2002; Korzhnev DM and Hadden MK 2016).

In the "central or multistep model", REV1 acts as a scaffold protein to unify both inserter and extender activity. One inserter TLS polymerase (η, ι or κ) interacts with the REV1 interface through the RIR (REV1-interacting region) sequence, simultaneously Pol ζ4 binds to the other REV1 interface to extend the DNA strand (Wojtaszek J *et al*. 2012a; Wojtaszek J *et al*. 2012b; Pustovalova Y *et al*. 2016).

Pol η, which belong to Y family, is the best known specialized polymerase to bypass the two main UV-lesions, CPDs and 6-4 PPs (Yoon JH *et al*. 2015; Quinet A *et al*. 2016). This family is characterized by the presence of PIP-boxes (PCNA-protein interacting) and several ubiquitin-binding domains (UBDs) in the C-terminal region, known as UBZ (ubiquitin-binding zinc domain) and UBM (ubiquitin-binding motif) (Yang W and Woodgate R 2007).

TLS polymerases are able to bind to PCNA through their PIP-box sequence, even though these interactions are weak. Thus, to strengthen this binding, the protein Rad18, an E3 ubiquitin ligase, ubiquitinates PCNA on Lysine 164 after UV damage, promoting the binding of TLS polymerases to monoubiquitinated PCNA, by their UBD domains (Watanabe K *et al*. 2004; Bi X *et al*. 2006).

Conversely, to inhibit and block this interplay in undamaged cells, it was demonstrated by "*in vivo*" experiments, that polymerases are ubiquitinated themselves (Bienko M *et al*. 2005; Guo C *et al*. 2006; Plosky BS *et al*. 2006; Bienko M *et al*. 2010; Jung YS *et al*. 2011).

Regarding CPDs, Pol η directly interact, through its PIP-box, with stalled monoubiquitinated-PCNA (Kannouche PL *et al*. 2004) and acts both as inserter and extender enzyme by adding three nucleotides past the lesion (Johnson RE *et al*. 1999b) with a very efficient and quite accurate ability (Biertümpfel C *et al*. 2010; Su Y *et al*. 2015). For this reason, this polymerase is considered as a protector of mammal cells from UV-induced carcinogenesis (Stary A *et al*. 2003).

Indeed, patients who carried mutations in POLH gene, which encodes for polymerase η, are characterized with an extremely sensitivity to sunburn and a higher risk to develop skin cancers compared to normal populations. This very rare, recessive genetic disease is the eighth form of XP, also known as *Xeroderma pigmentosum* variant (XP-V) (Johnson RE *et al*. 1999a; Masutani C *et al*. 1999).

Conversely, when a 6-4 PP lesion occurs, the "two steps" model is triggered: REV1 acts as a scaffold protein for pol η, which inserts a nucleotide in the opposite strand, and pol ζ that promotes the gap-filling across the damage (Johnson RE *et al*. 2001; Bresson A and Fuchs RP 2002; Yoon JH and Prakash L 2010). In this model, "*in vivo*" and "*in vitro*" studies have demonstrated that pol η acts in an error-prone manner (Johnson RE *et al*. 2001; Bresson A and Fuchs RP 2002; Yoon JH and Prakash L 2010; Quinet A *et al*. 2016).

1.5 DDB2 and its multiple facets

DDB2 is a protein composed by 427 amino acid residues (48 kDa) that is encoded by the XPE gene located to 11p12-p11 (Takao M *et al*. 1993; Dualan R *et al*. 1995). Structurally, DDB2 is characterized by seven WD-40 repeats, which are associated to a family of proteins involved in chromatin remodelling (Neuwald A and Poleksic A 2000).

The expression of this protein depends on p53, thanks to the presence, in the 5' untranslated sequence of DDB2 gene, of a consensus binding site for p53 (Tan D and Chu G 2002). It was demonstrated that, in the absence of p53, basal expression levels of DDB2 are dramatically reduced, and the expression does not increase even after the exposure to UV or IR irradiation (Hwang BJ *et al*. 1999).

DDB2 is mainly localized into the nucleus, both in undamaged and damaged cells; whereas DDB1, in normal conditions, is located both in the nucleus and cytoplasm and, after UV *stimuli*, DDB1 is mainly recruited into the nucleus by DDB2 translocation (Otrin V *et al*. 1997; Shiyanov P *et al*. 1999; Liu W *et al*. 2000).

As reported in the Paragraph 1.2.1, DDB2 is directly involved in the GG-NER pathway, recognizing UV photolesions.
However, DDB2 is also indirectly implicated in DDR pathway, in particular in chromatin remodelling.
For instance, Kapetanaki and colleagues have demonstrated that DDB2, together with Cul4A-DDB1 ligase complex, promotes the monoubiquitination of the H2A histone, speculating the possible DDB2 role as an adaptor molecule in NER mechanism (Kapetanaki MG *et al*. 2006). Indeed, another study has demonstrated the same role of DDB2 for the ubiquitination of H3 and H4 histones, suggesting a possible support for XPC recruitment upon UV irradiation (Wang H *et al*. 2006).
Moreover, DDB2 also interacts, both "*in vivo*" and "*in vitro*", with the histone acetyltransferase p300/CBP proteins (Datta A *et al*. 2001; Rapic-Otrin V *et al*. 2002).

DDB2 plays also an important role in the modulation of p53 and p21 expression. p53 protein is a crucial molecule for cell cycle arresting upon UV damage: it ensures that damaged cells do not proceed into cell cycle until the repair of lesions, preventing the accumulation and propagation of DNA mutations.

p53 is phosphorylated by Ataxia telangiectasia mutated kinase (ATM) and Ataxia telangiectasia RAD3-related kinase (ATR) after UV damage (on serine 15 or 18 in humans or mice, respectively) to stimulate its stability (Chao C *et al*. 2003). When mouse embryonic fibroblasts (MEFs) were exposed to low UV dose, DDB2 favoured $p53^{S18P}$ ubiquitin proteasome-mediated degradation (Stoyanova T *et al*. 2008) through Cul4a-DDB1 ligase complex, enhancing the nuclear accumulation of DDB1 protein that is responsible for p53 proteolysis (Stoyanova T *et al*. 2009). Moreover, its proteolysis is fundamental to maintain p21 expression at low levels to promote the NER process activation (Stoyanova T *et al*. 2008).

Conversely, the exposure at high UV-dose causes unrepairable cell damages and inhibits the DDB2 ubiquitination activity on p53, allowing the activation of the apoptotic pathway inducing the expression of specific pro-apoptotic factors such as Bax, PUMA and NOXA (Nakano K and Vousden KH 2001). In this case, the cell death program is protected from p21 inhibition because DDB2 stimulates the proteasome-mediated degradation of the protein through its ubiquitination.

DDB2 is also implicated in cell cycle regulation thanks to its interaction with E2F1 transcription factor, an important regulator of the expression of molecules that are implicated in DNA replication or S-phase onset (Hayes S *et al*. 1998). This interaction was demonstrated only in undamaged cells; after UV damage, the UV-DDB complex is not able to bind and activate E2F1 since the complex is sequestered by damaged DNA, causing a delay in cell cycle progression (Shiyanov P *et al*. 1999). In addition, the presence of a DDB2 mutated protein ($DDB2^{PCNA-}$), unable to interact with PCNA, determines DDB2 accumulation in cells (Cazzalini O *et al*. 2014) and influences cell cycle progression promoting cell proliferation (Perucca P *et al*. 2015); furthermore, $DDB2^{PCNA-}$ also confers an increase UV-resistance and proliferation advantage to irradiated cells (Perucca P *et al*. 2018).

DDB2 protein is not only correlated to UV damage or DDR pathways; in the last 15 years, several studies have demonstrated that it also plays an important role in cancer biology, although its contribution is still debated.
Interestingly, it was found that DDB2-deficient mice were not only prone to UV-induced carcinogenesis, but they also frequently developed spontaneous malignant tumour in internal organs in the absence of damaging agents, suggesting, for the first time, a hypothetical DDB2 role as tumour suppressor (Yoon T *et al*. 2005).

Furthermore, in several tumours (such as ovarian, breast and lung cancer), a low expression of DDB2 mRNA is frequently associated to a poor prognosis (Ennen M *et al*. 2013; Roy N *et al*. 2013), suggesting a possible involvement of DDB2 in preventing tumour progression and relapse.

In non-invasive breast cancer cells, DDB2 overexpression inhibits the transcription of manganese superoxide dismutase (MnSOD) and reduces the activity of NF-kB enhancing the expression of IkBα (Ennen M *et al*. 2013).
Conversely, in metastatic breast cancer cells DDB2 is not produced, thus the increase of MnSOD expression promotes the invasive capability of cells through the extracellular matrix (ECM) digestion by metalloproteinases 9 (MMP-9). Indeed, the transcription factor NF-kB by the regulation of some target genes expression, confers to metastatic breast cancer cells migration and invasive abilities (Min C *et al*. 2008).

Concerning colon cancer, DDB2 was found overexpressed in colorectal cancer (CRC) and colorectal adenoma (CRA) cells, probably due to the high rate of DNA damage in these cells compared to adjacent non-tumour tissues. Interestingly, a significant downregulation of DDB2 was found in high grade colon cancer cells associated to an aggressive phenotype, suggesting a correlation between DDB2 expression and CRC outcome (Roy N *et al*. 2013; Yang H *et al*. 2018).
Other data, obtained in metastatic colon cancer cells, have demonstrated that, a decrease in DDB2 expression is related to a reduction of E-cadherin expression, suggesting a possible DDB2 involvement in epithelial to mesenchymal transition (EMT) (Roy N *et al*. 2013).
EMT is a conserved mechanism which occurs both in physiological (e.g.

embryonic development) and pathological condition; for instance, in epithelial cancers is often activated during metastatic progression. In EMT, epithelial cells acquire typical feature of mesenchymal cells and, during this process, several changes occur (such as the loss of cell-cell adhesion and apical-basal polarity) to gain motility and migratory advantages (Ye X and Weinberg RA 2015).

Cancer stem cells (CSCs) are key factors for tumour initiation and progression in several solid tumours (Dean M *et al*. 2005; Hermann PC *et al*. 2008; Nguyen LV *et al*. 2012; Han C *et al*. 2014). Moreover, non-CSCs are able to dedifferentiate in CSCs (Friedmann-Morvinski D and Verma IM 2014).
Ovarian CSCs are characterized by a pronounced aldehyde dehydrogenase (ALDH) activity which promotes their cell differentiation to enrich CSCs pool (Vasiliou V and Nebert DW 2005; Silva IA *et al*. 2011).
Cui T and colleagues (Cui T *et al*. 2018), have demonstrated that DDB2 is able to bind to ALDH gene promoter inhibiting the transcriptional activity and, therefore, the amount and self-renewal capabilities of CRCs.

2. Aims of the research

Nucleotide excision repair (NER) is one of the DNA damage response (DDR) mechanisms that is able to remove different DNA lesions, such as distorting helix generated by physical (UV irradiation) or chemical mutagens. The process is divided in two subpathways – global genome-NER (GG-NER) and transcription coupled-NER (TC-NER) - that repair damaged DNA in the entire genome or in actively transcribed genes, respectively. The mechanism is composed by several phases: 1) the recognition of the lesion which differs in the two subpathways, 2) the damaged fragment incision and excision, 3) the gap-filling of new DNA synthesis and 4) the ligation steps.
DNA damage binding protein 2 (DDB2) is an essential factor that recognizes and binds UV photolesions – cyclobutane pyrimidine dimers (CPD) or 6-4 photoproducts (6-4 PPs) – in GG-NER pathway; this protein directly interacts with PCNA by its PCNA-protein interacting box (PIP box) sequence, allowing a correct DDB2 degradation *via* proteasome for the recruitment of following NER factors. In fact, in our laboratory, it was previously demonstrated that a DDB2 mutated protein ($DDB2^{PCNA-}$), unable to interact with PCNA, accumulates in cells.

In my PhD project, I employed, as experimental models, HEK293 and HeLa cell lines stably or transiently transfected with pcDNA3.1-$DDB2^{Wt}$ or pcDNA3.1-$DDB2^{PCNA-}$ constructs and exposed to UV-C irradiation, to study the following proposals:

I. In the first part of my PhD project I studied whether the loss of DDB2-PCNA interaction can influence other steps of GG-NER process. For this purpose, the DDB2 binding affinity to UV photolesions was analysed, using two different electrophoretic mobility shift assays (EMSA), to investigate whether the early phase of repair mechanism could be impaired; then a late step of NER process was dissected through co-localization studies and immunoprecipitation experiments.

II. In the second section of my thesis I investigated, whether the loss of DDB2-PCNA interaction could influence cell proliferation, after UV damage induction; for this purpose, I performed clonogenic assay and study pospho-histone 3 protein level. Furthermore, morphological features of mitoses were considered to identify possible hallmarks of genomic instability.
Starting from an enhanced UV-resistance and highest cell proliferation demonstrated when DDB2-PCNA interaction is lost, it was hypothesized a possible interaction between DDB2 and Polymerase η which is involved in Translesion DNA Synthesis (TLS). For this purpose, HeLa cells were co-transfected with Polymerase η-GFP and $DDB2^{Wt}$ or $DDB2^{PCNA-}$ constructs and co-localization protocols and immunoprecipitation experiments were performed. Moreover, to evaluate whether DDB2 protein could be directly associated to Polymerase η, the Proximity Ligation Assay (PLA), an innovative approach, was performed.

III. In the third part of my project, motility abilities and the possible DDB2 involvement in epithelial to mesenchymal transition (EMT) were taken into account and investigated in irradiated HEK293 cell lines (CTR, $DDB2^{Wt}$ and $DDB2^{PCNA-}$). In particular, wound healing experiments and Boyden chamber assay were used to evaluate cellular environment and motility abilities in response to chemoattractant *stimulus*. Then, the Western blotting analysis was performed to investigate the expression levels of E-cadherin and Vimentin proteins, the main epithelial and mesenchymal markers respectively, and to detect the activity of metalloproteinases (MMPs) 2 and 9.

IV. Finally, I investigated a possible other role of DDB2 in the repair process of actively transcribed genes, evaluating the ability of HEK293 cells ($DDB2^{Wt}$ and $DDB2^{PCNA-}$ stable clones) to repair and restore the expression of a UV-damaged gene by Host Cell Reactivation (HCR) assay. Moreover, co-localization studies between DDB2 and Polymerase II were performed to find a possible cooperation between GG-NER and TC-NER pathways.

3. Materials and methods

3.1 Cell lines

HEK293 (Human Embryonic Kidney) cell line and HeLa S3 (cervical cancer cells) cell line were cultured in Dulbecco's modified Eagle's *medium* (DMEM High glucose 4.5 g/l, Sigma-Aldrich) supplemented with 10% fetal bovine serum (One Shot™ FBS, Gibco™), 2 mM L-Glutamine (Gibco™), 100 U/ml penicillin, 100 µg/ml streptomycin in a 5% CO_2 humidified atmosphere at 37°C in sterile conditions.

3.2. Stable transfection of HEK293 or transient transfection of HeLa cells with pcDNA3.1-DDB2^{Wt} or pcDNA3.1-DDB2^{PCNA-} constructs

To evaluate and analyse the exogenous expression of DDB2 wild-type or mutated form in our cell lines, a standard transfection protocol was performed.

HEK293 cells (50% confluent) were stably transfected with pcDNA3.1-DDB2^{Wt}/His construct kindly provided by Dr. Q.E. Wang (The Ohio State University, Columbus, USA) (Barakat BM *et al*. 2010) or the mutated pcDNA3.1-DDB2^{PCNA-}/His constructs.
The pcDNA3.1-DDB2^{PCNA-}/His construct was previously obtained in our laboratory performing a site-directed mutagenesis in the DDB2 wild type plasmid vector (Invitrogen) (**Figure 7**) (Cazzalini O *et al*. 2014).

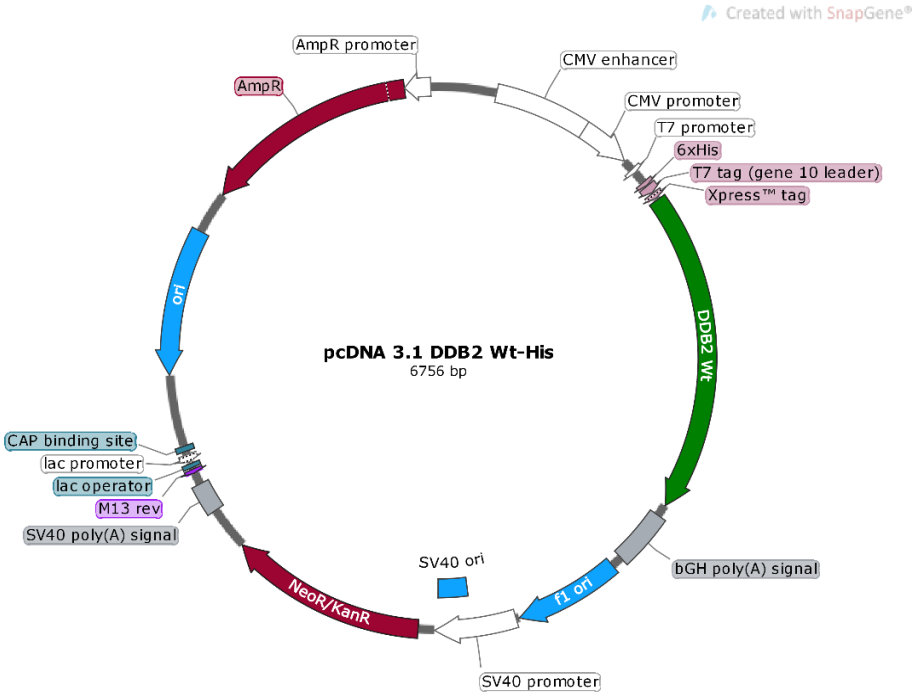

Figure 7 Map of pcDNA3.1 DDB2^{Wt}/His kindly provided by Dr. Wang. The plasmidic vector was employed for the mutagenesis of DDB2^{PCNA-}

DDB2^{PCNA-} protein is mutated in a conserved sequence called PIP-box which is present in many proteins that directly interact with PCNA (**Figure 8**) (Cazzalini O *et al*. 2014).

87-94	VQQGLQQSFL	*H. sapiens*
87-94	LQQGLQKSFL	*M. musculus*
87-94	LQQGLQQSFL	*B. taurus*
79-86	KQRSIVHYLY	*X. tropicalis*
79-86	WQCSIVHYVY	*G. gallus*
68-75	GQTSILHYIY	*D. rerio*
PIP-box:	QxxL/I/MxxFF/FY/YY	
DDB2^{Wt}	P S V Q Q G L Q Q S F L H T	
DDB2^{PCNA-}	P S V A Q G A Q Q S A L H T	

Figure 8 Phylogenetic analysis of aminoacidic sequence of PIP-box in DDB2 among several species. Comparison between DDB2^{Wt} and DDB2^{PCNA-} PIP-box sequence in human: in red the three mutated amino acids

The mutation in this region prevents the association between DDB2 and PCNA, leading to DDB2 accumulation due to its degradation impairment (Cazzalini O *et al*. 2014).
DDB2^{Wt} or DDB2^{PCNA-} HEK293 stable clones were previously selected and maintained in my laboratory by Geneticin® (G418) resistance present in plasmid vector (**Figure 7**).

HeLa S3 cells (70% confluent) were transiently transfected with DDB2 wild-type or mutated construct.
The transfection was performed in sterile conditions using "Effectene Transfection Reagents" (Qiagen) as described below:

- 10^6 cells were seeded in Petri dish (100x20 mm) and incubated at 37°C for 24 h;
- 1 µg of DDB2^{Wt} or DDB2^{PCNA-} DNA was diluted in 100 µl of EC buffer (DNA condensation buffer);
- 8 µl of Enhancer were added, then the mix was vortexed for 1 s and incubated for 5 min at room temperature (RT);
- 25 µl of Effectene were added and gently mixed;
- the mix was incubated for 10 min at RT;

- meanwhile the *medium* was removed from Petri dish, after a gently wash with phosphate-buffered saline (PBS), 9 ml of culture *medium* were added;
- finally, 1 ml of culture *medium* was added to the mix which was distributed on Petri dish.

HeLa cells, previously seeded on coverslips (22x22 mm) contained in Petri dishes (35 mm), were transfected with the same procedure described above but with 0.4 µg of DNA, 3.2 µl of Enhancer and 10 µl of Effectene.

3.3 Electrophoretic mobility shift assay

To study the electrophoretic mobility shift of DDB2 protein complexed with a specific DNA containing UV-damage, two different approaches were performed:

- EMSA on agarose gel with recombinant DDB2 (wild-type and mutated form) protein binds to UV plasmid;
- EMSA on polyacrylamide gel with cell extracts (HEK293 $DDB2^{Wt}$ or $DDB2^{PCNA-}$) complexed to CPDs-oligonucleotide.

3.3.1 EMSA with recombinant proteins

$DDB2^{Wt}$ recombinant protein was previously obtained in my laboratory (Cazzalini O *et al*. 2014).

3.3.1.1 Extraction and purification of recombinant $DDB2^{PCNA-}$ protein with Ni-His tagged resin (QIAGEN)

Escherichia coli (*E. coli*) BL21 were transformed with pET45-$DDB2^{PCNA-}$ construct to produce $DDB2^{PCNA-}$ with a histidine tail (6xHis). This tag allows purifying the protein of interest with a specific resin (His tagged).

50 µl of transformed *E. coli* BL21 cells were inoculated in 50 ml of sterile 2xYT broth with Ampicillin (Amp) [50 µg/ml] (**Table 1**) and grown overnight in a shaking 37°C incubator.

Components	Quantity
Bacto Tryptone	16 g
Bacto Yeast Extract	10 g
NaCl	5 g
Deionized water	to 1 l

Table 1 2xYT *medium* for 1 litre

Next day, the bacterial culture was inoculated in 500 ml of 2xYT broth with Amp [50 µg/ml] and enriched until the obtaining of 0.35 value of optical density at 600 nm (OD_{600}).
To induce $DDB2^{PCNA-}$ expression in *E. coli* BL21, Isopropyl-β-D-1-thiogalactopyranoside (IPTG) [1 mM] was added to bacterial culture and the expression was continued for 3 h.
Then, the bacteria were centrifuged (Avanti™ Centrifuge J-25, Beckman) at 1200 g for 16 min at RT: an aliquot of the pellet was stored at -80°C, whereas the remaining pellet was employed for $DDB2^{PCNA-}$ protein purification.
Pellet was resuspended and vortexed in 2.5 ml of BugBuster HT Protein Extraction Reagent (Novagen), then sample was placed on roller at 4°C for 40 min.
The sample was centrifuged (Allegra 21R, Beckman Coulter) at 5000 g for 10 min at 4°C and the lysate was collected.

In the meantime, to activate the resin for protein purification, a Nickel His-tagged resin (Qiagen) was washed 3 times with purification buffer pH 8.0 (**Table 2**) and it was centrifuged at 2880 g for 15 min at 4 °C each time.

Components	Molarity
NaCl	300 mM
NaH_2PO_4	50 mM

Table 2 Purification buffer

The lysate was incubated with resin on roller at 4°C overnight.

Next day, the mix was centrifuged at 2880 g for 15 min at 4°C and the supernatant was collected as "Waste".
The resin was resuspended with 8 ml of purification buffer (**Table 2**) containing 1 µl of protease inhibitors (Protease Inhibitor Cocktail, Sigma-Aldrich), glycerol 10% and phenylmethane sulfonyl fluoride (PMSF) [1 mM].
After centrifugation at 2880 g for 15 min at 4°C, the resin was loaded into a purification column.
The resin was washed 2 times with 8 ml of purification buffer (**Table 2**) containing 1 µl of protease inhibitors (Protease Inhibitor Cocktail, Sigma), glycerol 10% and PMSF [1 mM], the two washing were collected (Wash 1 and 2).
Several concentrations of imidazole pH 7.2 (diluted in 8 ml of purification buffer) were used to eluate the protein, as reported in **Table 3**. Each elution was collected.

Elution	[Imidazole]
1	25 mM
2	50 mM
3	100 mM
4	250 mM
5	500 mM
6	1 M

Table 3 Imidazole concentrations employed for protein elution

Each elution, Waste sample and Wash 1 and 2 were quantified by spectrophotometer (Eppendorf BioPhotometer® D30) through Bradford method; then, 2.5 µg of each sample resuspended in Mix 3x (**Table 4**) and a

protein marker "Precision Plus Standard Dual Color" (Bio-Rad) were loaded on 10% acrylamide gel (**Table 5**) to evaluate the presence of DDB2^{PCNA-} protein.

Components	Molarity/Concentration
Bromophenol blue	0.06%
SDS	3%
DTT	300 mM
Glycerol	30%
Tris base	150 mM
Deionized water	to volume

Table 4 Composition of Mix 3x for loading samples on acrylamide gels

The acrylamide gel was prepared, as reported in **Table 5**, with the following reagents:

- lower buffer (4x) (Tris pH 8.8; 1.5 mM + SDS 0.4%);
- upper buffer (4x) (Tris pH 6.8; 0.5mM + SDS 0.4%);
- acrylamide/bisacrylamide 30% (37.5:1);
- tetramethylethylenediamine (TEMED, AppliChem);
- ammonium persulfate (APS, AppliChem) al 15%.

PLUG	7.5%	10%
	(µl)	(µl)
Deionized water	1500	1250
Lower buffer	750	750
Acrylamide	750	1000
TEMED	12	9
APS	40	76

RUNNING	7.5%	10%
	(µl)	(µl)
Deionized water	6000	4600
Lower buffer	3000	3000
Acrylamide	3000	4400
TEMED	30	10
APS	120	80

STACKING 5%	5 %
	(µl)
Deionized water	2340
Lower buffer	1000
Acrylamide	660
TEMED	10
APS	30

Table 5 Composition of acrylamide gels used for protein electrophoresis

The protein electrophoresis was performed before at 60 V, then at 120 V under denaturing and reducing conditions with the Migration buffer 1x (from Migration buffer 10x, **Table 6**).

Components	Molarity/Concentration
Tris base	250 mM
Glycine	2 M
SDS	10%
Deionized water	to volume

Table 6 Composition of Migration buffer 10x

The acrylamide gel was stained with Coomassie 0.25% (**Table 7**) overnight to verify the presence of the $DDB2^{PCNA-}$ protein.

Components	Concentration
Brilliant blue	0.25%
Acetic acid	10%
Methanol	45%
Deionized water	45%

Table 7 Coomassie 0.25% staining composition

Then, the purificated protein was concentrated through an Amicon® Ultra Centrifugal Filter (Millipore) with a cutoff of 30 kDa as described below:

- the filter was activated with 8 ml of PBS and glycerol 10% and centrifuged at 4500 g for 15 min at 4°C;
- the eluted $DDB2^{PCNA-}$ protein was loaded on the filter and centrifuged at 4500 g for 15 min at 4°C;
- 2 washing with 8 ml of PBS were performed by several centrifugation at 4500 g for 15 min at 4°C to obtain 250 µl of concentrated protein.

The concentrated protein was quantified by spectrophotometer (Eppendorf BioPhotometer® D30) using Bradford method; then, 2.5 µg of protein resuspended in Mix 3x (**Table 4**) and a protein marker "Precision Plus Standard Dual Color" (Bio-Rad) were loaded on 10% polyacrylamide gel (**Table 5**). After the protein electrophoresis, the acrylamide gel was stained with Coomassie 0.25% (**Table 7**) overnight to verify the correct presence of a protein band with the same molecular weight of $DDB2^{PCNA-}$.

3.3.1.2 pEGFP-N1 plasmid (Clontech) UV irradiation

2.85 ug/µl of pEGFP-N1 plasmid (Clontech), previously quantified by spectrophotometer (Eppendorf BioPhotometer® D30), were resuspended in 10.5 µl of TE buffer pH 8.0 (**Table 8**) and UV-C irradiated at 800 J/m^2 with a lamp (Philips TUV-9) emitting mainly at 254 nm, as measured with a DCRX radiometer (Spectronics).

Components	Molarity
Tris-HCl	10 mM
EDTA	1 mM

Table 8 TE buffer composition

Ethanol at a final concentration of 70% was added to irradiated DNA to enhance its precipitation. After 15 min at -20°C, the sample was centrifuged at 15500 g for 15 min at 4°C (Allegra 21R, Beckman Coulter). The pellet was resuspended in 15 µl of TE buffer pH 8.0 (**Table 8**) and quantified by spectrophotometer (POLARstar Omega, BMG LABTECH).

3.3.1.3 EMSA on agarose gel

The "*in vitro*" assay with recombinant DDB2 protein was performed following the published protocol (Osakabe E *et al.* 2015).
The irradiated pEGFP-N1 plasmid (**Paragraph 3.3.1.2**) was incubated with recombinant $DDB2^{Wt}$ or $DDB2^{PCNA-}$ proteins, previously purified in our laboratory (**Paragraph 3.3.1.1**). The reactions were performed in Binding buffer (**Table 9**) for 30 min (**Table 10**, sample 1, 2 and 3) or 1 h (**Table 10**, sample 4 and 5) at 30°C.

Components	Molarity/Concentration
Sodium phosphate pH 7.5	28 mM
NaCl	150 mM
$MgCl_2$	3.4 mM
EDTA	1.4 mM
Glycerol	2%
BSA (Bovine Serum Albumin)	0.1 mg/ml

Table 9 Composition of Binding buffer employed for "*in vitro*" assay

Mix
Binding buffer
UV-pEGFP-N1

Components	1	2	3	4	5
Binding buffer	+	+	+	+	+
$DDB2^{Wt}$	-	+	-	+	-
$DDB2^{PCNA-}$	-	-	+	-	+
Deionized water	+	+	+	+	+
Final volume (µl)	10	10	10	10	10

Table 10 Schematic representation of EMSA with recombinant $DDB2^{Wt}$ or $DDB2^{PCNA-}$ proteins

Gel electrophoresis was performed on 1% agarose gel in TBE 1x buffer (from TBE 10x, **Table 11**) at 40 V for 3 h.

Components	Molarity
Tris base	0.9 M
Boric acid	0.9 M
EDTA	20 mM

Table 11 Composition of TBE 10x

The DNA was visualized and photographed by transilluminator UST-20M-8E on Darkhood DH-30/32 (Biostep).

3.3.2 EMSA with cell extracts derived from HEK293 $DDB2^{Wt}$ or $DDB2^{PCNA-}$

The electrophoretic mobility shift assay with cell extracts derived from HEK293 $DDB2^{Wt}$ or $DDB2^{PCNA-}$ on polyacrylamide gel was performed following

a published protocol (Tsai C *et al*. 2012).

3.3.2.1 HEK293 DDB2^{Wt} or DDB2^{PCNA-} cell extracts

HEK293 DDB2^{Wt} and DDB2^{PCNA-} cells (2x10^{6} for each sample) were harvested and resuspended in 1 ml of sterile cold PBS. After centrifugation at 13000 g for 1 min at 4°C (Allegra 21R, Beckman Coulter), pellets were resuspended in 100 µl of cold Lysis buffer (**Table 12**) and incubated for 30 min at 4°C on roller.

Components	Molarity/Concentration
NaCl	700 mM
EGTA	1 mM
EDTA	1 mM
β-glycerolphosphate	10 mM
$MgCl_2$	2 mM
KCl	10 mM
Sodium vanadate	1 mM
PMSF	1 mM
DTT	1 mM
Nonidet NP-40	0.1%
Protease inhibitor cocktail	1 µl/ml

Table 12 Lysis buffer composition

Lysates were centrifuged at 13000 g for 30 min at 4°C and the supernatants were stored at -80°C overnight.
Protein concentration of cell extracts was measured by spectrophotometer (Eppendorf BioPhotometer® D30) through Bradford method.
To verify the presence of DDB2 protein, 30 µg of HEK293 DDB2^{Wt} and DDB2^{PCNA-} cell extracts were resuspended in Mix 3x (**Table 4**) and loaded on 10% polyacrylamide gel (**Table 5**). The electrophoresis was performed as previously indicated (**Paragraph 3.3.1.1**)
Proteins were electrotransferred to nitrocellulose membrane by semi-dry transfer cell (Sigma B2529) at 100 mA for 30 min with Transfers buffer (**Table 13**). The Western blot system was assembled as followed described:

- 3 filter papers 3 MM of Whatman soaked in Transfers buffer (**Table 13**);
- nitrocellulose membrane soaked in Transfers buffer (**Table 13**);
- polyacrylamide gel 10%;
- 3 filter papers 3 MM of Whatman soaked in Transfers buffer (**Table 13**).

Components	Quantity/Volume
Tris base	0.3 g
Glycine	1.4 g
Methanol	20 ml
Deionized water	to 100 ml

Table 13 Transfers buffer composition

The nitrocellulose membrane was stained with Ponceau and blocked with 5% non-fat milk in PBS and 0.2% Tween 20 (PBST) buffer for 30 min under constant agitation to reduce background and minimize non-specific binding by primary antibodies.
Membrane was incubated with primary antibody (**Table 14**) for 1 h under constant agitation, following by three washing with PBST 10 min/each. Then, membrane was probed with appropriate HRP-conjugated secondary antibody (**Table 14**) for 30 min. After three washing with PBST, the signal was revealed using enhanced chemiluminescence with ECL kit (Bio-Rad).

Primary antibody	Secondary antibody
anti-DDB2 in rabbit polyclonal (1:500, Novus Biologicals)	anti-rabbit HRP-conjugated (1:10000, KPL)

Table 14 Antibodies employed for immunoblot assay

3.3.2.2 EMSA on acrylamide gel

The oligonucleotide CPD-annealing 5’ labeled with carboxyfluorescin (FAM) group, kindly provided by Dr. E. Crespan (Istituto di Genetica

Molecolare-Centro Nazionale delle Ricerche [IGM-CNR], Pavia), was used as a substrate to evaluate the $DDB2^{Wt}$ or $DDB2^{PCNA-}$ binding affinity.

Each binding reaction was prepared with the following reagents:

- 0.5 µg of cell extracts derived from HEK293 $DDB2^{Wt}$ or $DDB2^{PCNA-}$;
- 40 nM of oligonucleotide CPD-annealing 5' labeled with carboxyfluorescin (FAM) group;
- 40 nM of primer INT2-600 (MWG-Biotech AG) used as a competitor of oligonucleotide CPD for DNase digestion;
- Binding buffer 1x (from Binding buffer 5x, **Table 15**);
- 10 mg/ml of BSA (Albumin fraction V [pH 7.0], Blotting Grade [BioFroxx]).

Components	Molarity/Concentration
Hepes-KOH pH 7.9	12 mM
KCl	60 mM
$MgCl_2$	5 mM
Tris base	4 mM
EDTA	0.6 mM
DTT	1 mM
Glycerol	12%

Table 15 Binding buffer 5x composition

A mix containing the Binding buffer 5x (**Table 15**), the oligonucleotide CPD-annealing, the primer INT2-600 and BSA was prepared and aliquoted in each "*in vitro*" binding reaction. As reported in the following experimental plan (**Table 16**), the experiments were performed in a final volume of 10 µl and conducted at RT for 30 min (**Table 16**, Sample 1, 2 and 4) or 1 h (**Table 16**, Sample 3 and 5), protecting samples by light exposure to preserve the fluorescence of the oligonucleotide-CPD.

Mix
Binding Buffer 5X
Oligonucleotide CPD-annealing
Primer INT2-600
BSA

Components	1	2	3	4	5
Mix	+	+	+	+	+
HEK 293 DDB2^{Wt} cell extracts	-	+	+	-	-
HEK 293 DDB2^{PCNA-}cell extracts	-	-	-	+	+
Deionized water	+	+	+	+	+
Final volume (µl)	10	10	10	10	10

Table 16 Experimental plan of EMSA performed on polyacrylamide gel with HEK293 DDB2^{Wt} or DDB2^{PCNA-} cell extracts

Then, the protein-DNA complexes were resolved from free oligonucleotide in 4% non-denaturing polyacrylamide gel (Table 17); before loading, samples were mixed with 2 µl of loading dye composed by 0.025% of blue bromophenol diluted in Binding buffer 5x (Table 15). The assay was performed in TGE buffer 1x (from TGE buffer 5x, Table 18) at 10 V/cm (70 V) for approximately 90-120 min.

Components	Volume (ml)
Acrylamide	2.8
TGE 5x	4
APS 10%	0.2
TEMED	0.024
Deionized water	13

Table 17 Composition of non-denaturing gel at 4%

Components	Molarity
Tris-HCl pH 8.5	50 mM
Glycine	380 mM
EDTA	2 mM

Table 18 TGE buffer 5x composition

EMSA was revealed by Molecular Dynamics Phosphoimager (Typhoon Trio, GE Healthcare) through the detection of carboxyfluorescin (FAM) group on oligonucleotide-CPD.

The densitometric analysis was performed for each sample comparing protein-DNA complexes bands on total bands (protein-DNA complexes + free oligonucleotide bands) through the public software ImageJ (https://imagej.nih.gov/ij/).

3.4 Interaction between DDB2 and XPG at UV-damaged sites

To verify a possible delay in DNA repair process in the late steps of NER, in particular in HEK293 DDB2^{PCNA-} clone, DDB2 and XPG recruitment was investigated.
In particular, DDB2 and XPG colocalization to DNA damaged sites and their interaction were evaluated.
Then, it was examined the possible DDB2 involvement in translesion DNA synthesis (TLS) focusing on DDB2 and Polymerase η interaction.

3.4.1 DDB2 and XPG colocalization

3.4.1.1 UV-C local irradiation

HeLa cells, previously seeded on coverslips, were transiently

transfected with DDB2^{Wt} or DDB2^{PCNA-} construct (**Paragraph 3.2**). The next day, samples were gently washed with PBS and, after its removal were locally irradiated with a lamp (Philips TUV-9) emitting mainly at 254 nm at 100 J/m^2, by laying on top of cells an Isopore polycarbonate filters (Millipore) with 3 µm pores to induce DNA damage *foci* formation.
After UV-C irradiation, samples were incubated at 37° C and fixed 5, 10, 30 and 60 min later. Not irradiated HeLa cells were used as control.

3.4.1.2 Paraformaldehyde fixation protocol

At the end of specific recovery times, cells were washed twice with cold PBS and lysed with 0.5% Triton X-100 (Sigma-Aldrich) diluted in cold PBS for 30 min at 4°C in shaking. Then, cells were fixed with 2% paraformaldehyde (PFA) for 5 min and 70% ethanol for 20 min at -20°C.

3.4.1.3 Immunofluorescence staining

To detect the protein localization, the following immunostaining standard protocol was applied:

- after the removal of ethanol, cells were washed twice with cold PBS;
- samples were incubated with blocking solution containing 1% of BSA in PBST buffer for 30 min at RT with gentle shaking;
- cells were incubated with primary specific antibodies diluted in PBST/1% BSA for 1 h at RT;
- three washing, for 10 min each, with PBST with shaking were performed;
- the reactions were followed by incubation with secondary antibodies diluted in PBST/1% BSA for 30 min;
- after immunoreactions and three washing with PBST (as previously described), samples were incubated with Hoechst 33258 dye (0.5 µg/ml) for 10 min at RT with mild agitation and then washed in PBS;
- finally, coverslips were mounted in Mowiol (Calbiochem) containing 0.25% 1,4-diazabicyclo-octane (Aldrich) as antifading agent.

Images were acquired with a TCS SP5 II Leica confocal microscope, at 0.3 µm intervals. Image analysis was performed using the LAS AF software.
To detect the presence and the colocalization between DDB2 and XPG, HeLa cells were immunostaining with specific antibodies as reported in **Table 19**. XPG antibody was kindly provided by Dr. E. Prosperi (IGM-CNR, Pavia).

Primary antibodies	Secondary antibodies
anti-DDB2 in mouse monoclonal (1:100, Santa Cruz Biotechnology)	anti-mouse DyLight™ 594 (1:200, Thermo Scientific)
anti-XPG in rabbit polyclonal (1:200, Sigma-Aldrich)	anti-rabbit DyLight™ 488 (1:100, KPL)

Table 19 Antibodies used for DDB2 and XPG immunostaining

3.4.1.4 Immunoprecipitation assay and immunoblot analysis

To evaluate the direct or indirect interaction between DDB2 and XPG after UV damage induction, an immunoprecipitation assay was performed.

For this purpose, HeLa cells were seeded at the density of $1x10^6$. The day after, cells were transiently transfected with $DDB2^{Wt}$ or $DDB2^{PCNA-}$ construct (**Paragraph 3.2**).
24 h later, cells were washed with PBS and irradiated with a lamp (Philips TUV-9) emitting mainly at 254, at a dose of 30 J/m^2 UV-C.
HeLa cells not transfected and not irradiated were employed as control.
After 30 or 60 min recovery times, cells were trypsinized, harvested and pelleted by centrifugation at 200 g for 3 min (Centrifuge 4236, Alc). Pellets were stored at -80°C.

Dynabeads™ Protein G (Invitrogen) were used to immunoprecipitate DDB2 protein and were prepared as follow:

- 180 µl of magnetic beads (corresponding to 900 µg for each sample) were washed twice with 1 ml of Beads washing buffer 1x (from Beads washing buffer 2x, **Table 20**);
- beads were resuspended with 150 µl of Beads washing buffer 1x (from

Beads washing buffer 2x, **Table 20**) and 30 µl of anti-DDB2 in rabbit polyclonal (Santa Cruz Biotechnology) (corresponding to 1 µg of antibody for each sample) were added;

- the mix was placed on roller for 90 min at 4°C to obtain the binding beads-antibody.

Components	Quantity (g)/Volume
Citric acid	0.094
Sodium phosphate bibasic	0.184
Deionized water	10 ml

Table 20 Beads washing buffer 2x composition for 10 ml

In the meantime, pellets were resuspended and lysed with 1 ml of Hypotonic buffer (**Table 21**) for 10 min on ice.

Components	Molarity/Concentration
Tris-HCl, pH 8.0	10 mM
$MgCl_2$	2.5 mM
Nonidet NP-40	0.5%
Na_3VO_4	0.2 mM
DTT	1 mM
PMSF	1 mM
Protease inhibitor cocktail	0.5 µl/ml

Table 21 Hypotonic buffer composition

After centrifugation at 2900 g for 1 min at 4°C (Allegra 21R, Beckman Coulter), supernatants, corresponding to Soluble (S) fraction, were collected and quantified by spectrophotometer (Eppendorf BioPhotometer® D30) through Bradford method. 50 µl of these samples were mixed with 25 µl of Mix 3x (**Table 4**) and stored at -20°C as Soluble fraction of Input.
Pellets were washed in Hypotonic buffer (**Table 21**) and centrifuged at 2900 g for 1 min at 4°C.
Pellets were resuspended and washed with 1 ml of Isotonic buffer (**Table 22**) and centrifuged at 2900 g for 1 min at 4°C.

Components	Molarity/Concentration
Tris-HCl, pH 8.0	10 mM
NaCl	150 mM
PMSF	1 mM
Protease inhibitor cocktail	0.5 µl/ml

Table 22 Composition of Isotonic buffer

Pellets were digested by 1 ml of DNase buffer 1x (Buffer A 2x (**Table 23**), DNase 20 U/µl/10^6 cells and Buffer B 2x (**Table 24**)) (Buffer A and B ratio 1:1) for 20 min at 4°C.

Components	Molarity
Tris-HCl, pH 8.0	20 mM
$MgCl_2$	10 mM

Table 23 Buffer A 2x composition

Components	Molarity
NaCl	20 mM
PMSF	1 mM

Table 24 Buffer B 2x composition

Samples were centrifuged at 16000 g for 1 min at 4°C. 40 µl of supernatants, corresponding to Chromatin Bound (CB) of Input, were collected and mixed with 20 µl of Mix 3x (**Table 4**) and placed at -20°C.
The remainder fraction of CB and 1.5 mg/ml of proteins of S fractions were incubated with 30 µl of the mix composed by magnetic beads and anti-DDB2 (previously obtained) for 3 h at 4°C under constant agitation.
Then, immunocomplexes were washed three times with Isotonic buffer (**Table 22**), resuspended in 60 µl of Mix 3x (**Table 4**) and placed at -20°C.

Samples were resolved by Mini-PROTEAN® TGX™ Precast Gel gradient gel 4-15% (Bio-Rad). 30 µl of immunoprecipitated samples (S fraction and CB) and 30 µg of Input (S fraction and CB) were loaded and a protein marker "Precision Plus Standard Dual Color" (Bio-Rad) was used. Protein

electrophoresis was conducted at 150 V for 45-60 min at 4°C in TGS 1x buffer (Table 25).

Components	Molarity/Concentration
Tris base	25 mM
Glycine	192 mM
SDS	0.1%

Table 25 TGS buffer 1x used as running buffer for protein electrophoresis

The Western blot was performed as reported in Paragraph 3.3.1.1 and the antibodies are indicated in Table 26. The signal was revealed using enhanced chemiluminescence with Azure Biosystem.

Primary antibodies	Secondary antibodies
anti-DDB2 in mouse monoclonal (1:100, Santa Cruz Biotechnology)	anti-mouse HRP-conjugated (1:20000, Sigma-Aldrich)
anti-XPG in rabbit polyclonal (1:1000, Sigma-Aldrich)	anti-rabbit HRP-conjugated (1:10000, KPL)
anti-beta actin in mouse monoclonal (1:1000, Sigma-Aldrich)	anti-mouse HRP-conjugated (1:20000, Sigma-Aldrich)
anti-IgG HRP-conjugated in rabbit polyclonal (1:4000, Amersham Biosciences)	

Table 26 Antibodies employed

3.5 Evaluation of proliferation ability

3.5.1 Clonogenic assay

To investigate, after UV damage, the cells proliferation capability, the clonogenic assay was performed.

HEK293 CTR, DDB2^{Wt} and DDB2^{PCNA-} stable clones were seeded into 100 mm culture dishes and two days later, cells were UV-C irradiated (10 J/m^2), immediately harvested and 5x10^3 cells were re-seeded into 60 mm cell culture dishes in triplicate for each cell line.
To allow cellular growth and colony formation, Petri dishes were incubated at 37°C for 10 days, then cells were fixed and stained with Gentian violet (**Table 27**) for 20 min in agitation and washed several times with deionized water.

Components	Volume/Quantity
Acetic acid	5 ml
Gentian violet	1 g
Aniline oil	1 ml
Ethanol	15 ml
Deionized water	80 ml

Table 27 Gentian violet staining composition

The number of developed colonies was manually counted.

3.5.2 Study of mitoses

To examine the colony formation focusing on the number and morphological features of their mitoses, an immunofluorescence and a May-Grünwald Giemsa staining were performed.
To visualize mitoses, irradiated HEK293 cells (CTR, DDB2^{Wt} and DDB2^{PCNA-}), previously exposed to 10 J/m^2 and seeded on coverslips, were fixed with 3.7 paraformaldehyde three days after UV-radiation treatment and permeabilized with ethanol 70% at -20°C.
Then, samples were immunostained with antibodies reported in the **Table 28** and the procedure is reported in **Paragraph 3.4.1.3**. Cells were incubated with primary antibody for 2 h; the antibody was kindly provided by Dr. C. Mondello (IGM-CNR, Pavia).

Primary antibody	Secondary antibody
anti-pospho-Histone 3 in rabbit polyclonal (1:100, Upstate)	anti-rabbit DyLight™ 488 (1:100, KPL)

Table 28 Antibodies employed to visualize mitoses

HEK293 cells (CTR and both stably transfected clones) were seeded on coverslips. After two days, cells were totally UV-C irradiated (10 J/m^2), trypsinized and reseeded on coverslips (2X10^5 cells).

Three days later, samples were fixed with methanol and acetic acid and stained with May-Grünwald Giemsa using a standard protocol.

Total number of cells per colony, including dead cells and mitoses were counted and photographed by Nikon Eclipse 80i digital microscope with Nikon Digital Sight DS-Fi1 camera.

3.6 Study of DDB2-Polymerase η interaction

To investigate whether DDB2 protein could be involved in TLS, its colocalization with Polymerase η was assessed through confocal analysis and immunoprecipitation assay.
Moreover, using Proximity Ligation Assay (PLA), DDB2 and Polymerase η direct interaction was investigated.

3.6.1 Co-transfection of HeLa cells with pcDNA3.1-DDB2^{Wt} or pcDNA3.1-DDB2^{PCNA-} and Polymerase η-GFP constructs and local UV-irradiation

HeLa cells were co-transfected with Polymerase η-GFP (Pol η-GFP) construct kindly provided by Dr. S. Sabbioneda (IGM-CNR, Pavia) and DDB2^{Wt} or DDB2 mutated construct following the protocol as described in **Paragraph**

3.2.1.

In particular, cells, previously seeded on coverslips, were co-transfected with 0.2 µg of Pol η-GFP and 0.4 µg of $DDB2^{Wt}$ or $DDB2^{PCNA-}$ DNA.

As a positive control of Polymerase η expression, HeLa cells were transfected only with Pol η-GFP construct.

The day after cells were exposed to local UV-C radiation (100 J/m^2), as reported at Paragraph 3.4.1.1.

3.6.2 Fixation and lysis protocol

Cells were fixed and lysed 30 and 60 min later, following a specific protocol published by Soria and colleagues (Soria G *et al*. 2008). Briefly:

- cells were fixed with a solution containing 4% PFA and 4% sucrose diluted in PBS for 15 min at RT;
- then cells were washed with PBS and incubated with 0.1% Triton X-100 diluted in PBS for 10 min under constant agitation at RT;
- finally, after a gently wash with PBS, samples were incubated with ethanol 70% at -20°C for at least 20 min.

3.6.3 Immunostaining and immunoprecipitation experiments

For confocal analysis, cells were immunostained as reported in Paragraph 3.4.1.3.

In Table 29 are reported the antibodies employed for the incubation:

Primary antibodies	Secondary antibodies
anti-XPE/DDB2 in rabbit polyclonal (1:100, Novus Biologicals)	anti-rabbit DyLight™ 488 (1:100, KPL)
anti-Polymerase H in mouse monoclonal (1:100, Santa Cruz Biotechnology)	anti-mouse DyLight™ 594 (1:200, Thermo Fisher Scientific)

Table 29 Antibodies used for DDB2 and Polymerase η (Polymerase H) immunostaining

For immunoprecipitation assay, HeLa cells, previously seeded on Petri dishes, were co-transfected with with 0.8 µg of Pol η-GFP and 1 µg of $DDB2^{Wt}$ or $DDB2^{PCNA-}$ DNA. 24 h later, cells were washed with PBS and irradiated at a dose of 30 J/m^2 UV-C and after 30 min were pelleted.

In addition, as negative and positive controls, HeLa cells were only transfected with GFP (0.5 µg) or Pol η-GFP (0.8 µg) constructs. These samples were not irradiated.

Immunoprecipitation experiment was performed following the protocol reported in **Paragraph 3.4.1.4**, magnetic beads were incubated with anti-GFP in mouse monoclonal (Sigma) and, to immunodetect DDB2 and Polymerase η proteins, the following antibodies were employed (**Table 30**):

Primary antibodies	Secondary antibodies
anti-XPE/DDB2 in rabbit polyclonal (1:500, Novus Biologicals)	anti-rabbit HRP-conjugated (1:10000, Sigma-Aldrich)
anti-Polymerase H in mouse monoclonal (1:500, Santa Cruz Biotechnologies)	anti-mouse HRP-conjugated (1:20000, Sigma-Aldrich)
anti-beta actin in mouse monoclonal (1:1000, Sigma-Aldrich)	anti-mouse HRP-conjugated (1:20000, Sigma-Aldrich)
anti-IgG HRP-conjugated in rabbit polyclonal (1:4000, Amersham Biosciences)	

Table 30 Antibodies used for DDB2 and Polymerase η (Polymerase H) immunoblotting

3.6.4 Proximity Ligation Assay

HeLa cells, previously seeded on coverslips, were transfected with Pol η-GFP only or co-transfected with DDB2 (wild-type or mutated DNA) and Pol η-GFP (**Paragraph 3.6.1**).

After 24 h, cells were irradiated (10 J/m^2) to induce DNA UV-damage and 30 min later samples were lysed (**Paragraph 3.6.2**).

The PLA assay was performed with the kit "Duolink® In Situ PLA" (Sigma-Aldrich), according to the "Fluorescence Protocol" provided by the manufacturer (**Figure 9**).

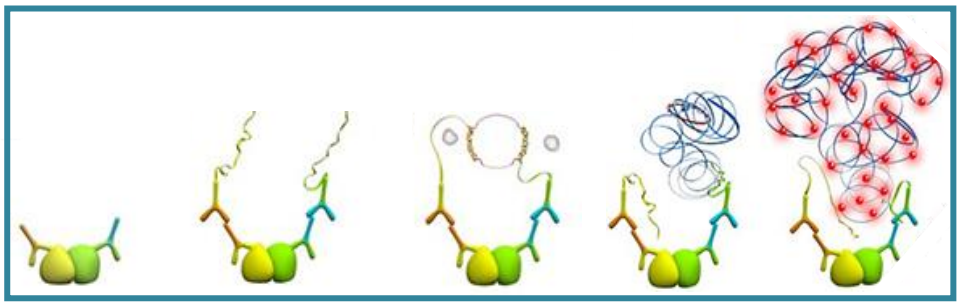

Figure 9 Schematic representation of PLA technique

After the blocking with 1% of BSA, samples were co-incubated for 1 h at RT with the following primary antibodies (**Table 31**):

Primary antibodies
anti-DDB2 in rabbit polyclonal (1:100, Rockland)
anti-GFP in mouse monoclonal (1:100, Sigma-Aldrich)

Table 31 Antibodies used for PLA assay

Finally, images of fixed cells were acquired with a TCS SP5 II Leica confocal microscope, at 0.3 µm intervals. Image analysis was performed using the LAS AF software.

3.7 Wound healing assay

To analyse whether irradiated HEK293 stable clones could acquire

better proliferation and motility capabilities, a wound healing assay was performed.

HEK293 CTR cells, $DDB2^{Wt}$ and $DDB2^{PCNA-}$ stable clones, previously seeded on Petri dishes, were totally irradiated (10 J/m^2 UV-C) immediately trypsinized and counted.
In the meantime, an Ibidi Culture-Insert (Madison, WI), composed by two *septa*, was applicated in a 6 well-plate pre-treated with polylysine that allowing cell adhesion.
Irradiated cells ($7x10^4$) were resuspended in 70 µl of *medium* and seeded in each *septum* of the culture-insert, and incubated at 37° C.
Cells grew until the achievement of a confluent layer, then the culture-insert was carefully removed and a cell-free gap was evident.

The growth and motility of irradiated cells in the gap were daily monitored and photographed starting from day 0 (corresponding to the removal of culture-inserts) until day 10, employing an inverted light microscope equipped with a Canon A590 IS camera (Tokyo, JP).

3.8 Influence of DDB2 protein on cell migration ability

To study whether DDB2 protein (wild-type or mutated form) could be implicated in EMT, the expression levels of E-cadherin and Vimentin proteins and the activity of metalloproteinases (MMPs) 2 and 9 were analysed.

To this purpose, HEK293 CTR and stably transfected clones expressing $DDB2^{Wt}$ or $DDB2^{PCNA-}$ protein were exposed to UV-C irradiation (10 J/m^2).
After several recovery times from UV-induced DNA damage (4, 8, 24, 48, 72, 96 h and 7 d), pelleted cells and supernatants were collected for Western blot analysis and Zymography assay, respectively.
For each cell line, not irradiated cells were employed as negative controls.

3.8.1 Western blot analysis of E-cadherin and Vimentin proteins

30 µg of proteins of each sample were resuspended in Mix 3x (**Table 4**) and separated on 10% polyacrylamide gel (**Table 5**); "Precision Plus Standard Dual Color" (Bio-Rad) was used as protein marker.
The protein electrophoresis was conducted at 120 V for about 90 min with Migration buffer 1x (**Table 6**).
Proteins were electrotransferred to nitrocellulose membrane by semi-dry transfer cell (Sigma B2529) at 100 mA for 30 min with Transfers buffer (**Table 13**).
After the blocking with milk, the membrane was probed with the antibodies reported on **Table 32**.
To detect beta actin, as a loading control protein, a specific antibody for it was used.

Primary antibodies	Secondary antibodies
anti-E cadherin in rabbit polyclonal (1:1000, GeneTex)	anti-rabbit HRP-conjugated (1:10000, KPL)
anti-Vimentin in mouse monoclonal (1:1000, Santa Cruz Biotechnology)	anti-mouse HRP-conjugated (1:20000, Sigma-Aldrich)
anti-beta actin in mouse monoclonal (1:1000, Sigma-Aldrich)	

Table 32 Antibodies employed for Western blot analysis

The signal was revealed using enhanced chemiluminescence with Azure Biosystem.

The densitometric analysis was performed with the public software ImageJ (https://imagej.nih.gov/ij/) and the results were normalized with beta actin.

3.8.2 Zymography assay

The presence and the activity of MMPs-2 and 9, also known as Gelatine

A and B, were investigated by Zymography technique.

Therefore, a 10% acrylamide gel (**Table 5**) containing 1209 µl of gelatin [10 mg/ml] in the Running gel was prepared.
Supernatants were centrifuged (Allegra 21R, Beckman Coulter) at 1100 g for 10 min at 4°C and resuspended in Sample buffer 2x (**Table 33**, ratio 1:1).

Components	Molarity/Concentration
Tris HCl pH 6.8	125 mM
Glycerol	20%
SDS	4%
Bromophenol blue	0.005%
Deionized water	to volume

Table 33 Sample buffer 2x composition

30 µl of each sample and the "Precision Plus Standard Dual Color" (Bio-Rad) protein marker were loaded.
The protein electrophoresis was performed before at 60 V, then at 100 V under denaturing but not reducing conditions with the Migration buffer 1x (from Migration buffer 10x, **Table 6**).

To eliminate SDS and for MMPs renaturation, gel was incubated with Renaturing buffer (2.5 % Triton X-100 diluted in deionized water) for 30 min under stirring.
Next, gel was incubated with Developing buffer 1x (from Developing buffer 10x, **Table 34**) at RT for 30 min and then at 37°C overnight.

Components	Quantity (g)/Concentration
Tris base	12.1
Tris-HCl	63
NaCl	117
$CaCl_2$	7.4
Triton X-100	0.1%
Deionized water	to 1 l

Table 34 Developing buffer 10x composition

Then, gel was dipped in Staining buffer (**Table 35**) for 1 h under constant agitation.
Finally, to detect the digested white bands, gel was incubated 30 min with Destaining buffer (**Table 36**).

Components	Volume (ml)
Methanol	30
Acetic acid	10
Blue Coomassie	0.5
Deionized water	to 100

Table 35 Staining buffer composition

Components	Volume (ml)
Methanol	25
Acetic acid	37.5
Deionized water	to 500

Table 36 Composition of Destaining buffer

The densitometric analysis of each digested bands was performed by the public software ImageJ (https://imagej.nih.gov/ij/).

3.8.3 Boyden chamber assay

Finally, to determine whether DDB2 protein could also be implicated in the migration process of irradiated HEK293 cells, a Boyden assay was performed.

The 48-Well Micro Chemotaxis chamber (Neuro Probe) was composed by a top and bottom plates containing wells, separated by a silicone gasket. Indeed, to analyse migrated cells, a coated polycarbonate membrane with 8µm pores (Neuro Probe) was placed between the bottom plate and silicone gasket. The membrane was incubated with 0.5 M acetic acid at RT overnight; then, after an accurate washing in distilled water, the filter was coated with 100 µg/ml of collagen type 1 (from calf skin, Sigma-Aldrich) solution diluted

in 0.1 M acetic acid for 72 h at RT. Before use, the polycarbonate membrane was left to completely air dry.
For the experiment, HEK293 control line and both stable clones expressing $DDB2^{Wt}$ or $DDB2^{PCNA-}$ protein were exposed to UV irradiation (10 J/m^2) and immediately harvested and counted. 10^5 cells diluted in 50 µl of *medium* without FBS were loaded in each wells of the top plate. For each cell lines, not irradiated cells were used as control.

The protocol was performed as followed described:

- in the bottom wells 30 µl of DMEM containing different FBS concentration (0, 10 and 20%) were loaded to chemoattractant cells;
- the collagen-coated polycarbonate membrane was carefully placed followed by silicone gasket and top of chamber assembly;
- clamps were screwed applying a great pressure to avoid bubble formation;
- Boyden chamber was located at 37°C for 5 min to equilibrate the system;
- irradiated and not irradiated cells were loaded in the top wells;
- the chamber was placed in incubator at 37°C for 24 h;
- the day after, the membrane containing both migrated (on top) and non-migrated cells (bottom) was incubated with fixative (Diff-Quick Fixative) for 2 min, then with the Diff-Quick Solution I for 2.5 min and Diff-Quick Solution II for 1 min and, finally, the filter was placed in distilled water to eliminate the excess dyes;
- then, the filter was set on a clean slide with the migrated cell side down and, with a cotton swab, non-migrated cells were wiped off;
- three coverslips were placed on the membrane with a mounting *media* and cells were visualized and photographed under a digital microscope Nikon Eclipse 80i with a camera Nikon Digital Sight DS-Fi1.

3.9 Other possible role of DDB2

To investigate the possible involvement of DDB2 protein (wild-type and

mutated form) in the TC-NER, the other subpathway of NER, the host cell reactivation (HCR) assay and confocal analysis were performed.

3.9.1 Host cell reactivation assay and "*in vivo*" cytofluorimetric analysis

This assay allows evaluating the DNA repair ability by FACS technology (Burger K *et al*. 2010). To this end, plasmidic DNA was previously irradiated and then transfected.

HEK293 stable transfected clones ($DDB2^{Wt}$ and $DDB2^{PCNA-}$) were co-transfected with 0.4 or 0.6 µg of pmRFP-N2 (as a positive control) kindly provided by Dr. M.C. Cardoso (Technische Universität Darmstadt, Germany) and 0.4 µg of pEGFP-N1 or 0.6 µg of UV-pEGFP-N1 (obtained as previously described on **Paragraph 3.3.1.2**) employing the kit "Effectene Transfection Reagent" (Qiagen) (**Figure 10**).

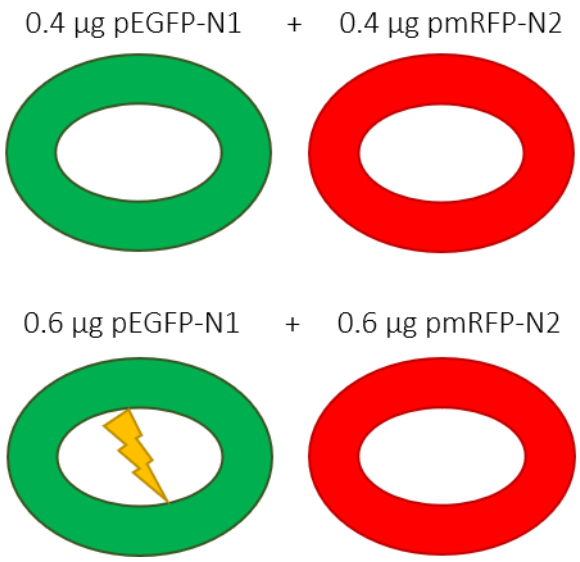

Figure 10 Experimental plan of HCR

After 16 and 48 h respectively, cells were trypsinized, harvested and centrifuged at 200 g for 3 min (Centrifuge 4236, Alc); the pellets were gently

re-suspended in PBS for *"in vivo"* cytofluorimetric assay (CyFlow® SL, Sysmex Partec GmbH).

The analysis was performed only on RFP positive cells and the mean fluorescence intensity (MFI) for the RFP and GFP protein was calculated. After normalization (MFI GFP/MFI RFP), the relative expression of GFP protein was computed by comparing the normalized MFI UV to the normalized MFI not irradiated.

3.9.2 Evaluation of DDB2 and Polymerase II co-localization by immunofluorescence and confocal microscopies

HeLa cells previously seeded on coverslips, were transfected with $DDB2^{Wt}$ or $DDB2^{PCNA-}$ construct, as described in **Paragraph 3.2**.
The day after, cells were exposed to local UV-C irradiation (100 J/m^2, as previously described at **Paragraph 3.4.1.1**), and 30 or 60 min later were fixed (**Paragraph 3.4.1.2**).
Then, following the procedure described in **Paragraph 3.4.1.3**, cells were immunostained with the antibodies reported in the **Table 37** and observed by immunofluorescence and confocal microscopies.
Anti-RNA Polymerase II was kindly provided by Dr. T. Nardo (IGM-CNR, Pavia).

Primary antibodies	Secondary antibodies
anti-DDB2 in rabbit polyclonal (1:100, Novus Biologicals)	anti-rabbit DyLight™ 488 (1:100, KPL)
anti-RNA Polymerase II in mouse monoclonal (1:100, Covance)	anti-mouse DyLight™ 594 (1:200, Thermo Scientific)

Table 37 Antibodies employed for DDB2 and Polymerase II co-localization studies

4. Results

I. DDB2^{PCNA-} in global genome-nucleotide excision repair

4.1 Delay in the recognition of UV-DNA lesions

In the laboratory in which I have conducted my PhD project, previous studies have demonstrated that DDB2^{PCNA-} protein, which is unable to directly interact with PCNA, shows a delayed recruitment at DNA damaged sites, after UV-C radiation, compared to DDB2 wild-type protein. These time course experiments were performed by immunofluorescence staining and confocal analysis (Perucca P *et al*. 2018). In order to clarify the molecular mechanism that determines this delay, I performed new experiments applying different approaches.

4.2 Evaluation of DDB2 binding affinity to DNA lesions

Firstly, I investigated whether the mutation in DDB2 sequence may affects the protein binding affinity to DNA photolesions.
To test the DDB2-DNA interaction "*in vitro*", two different electrophoretic mobility shift assays (EMSA) were performed:

- EMSA on agarose gel with recombinant DDB2 (wild-type or mutated form) protein incubated with an UV-irradiated plasmid;

- EMSA on acrylamide gel with HEK293 cell extracts ($DDB2^{Wt}$ or $DDB2^{PCNA-}$ stable clones) and CPDs-oligonucleotide.

Both approaches allow to visualize a band shift when a DNA/protein complex is formed.

4.2.1 EMSA on agarose gel

EMSA on agarose gel was performed to evaluate the binding ability of recombinant DDB2 (wild-type or mutated form) proteins to irradiated plasmid containing DNA UV photolesions. $DDB2^{Wt}$ recombinant protein was purified in our laboratory (Cazzalini O *et al*. 2014) and, the protocol used to produce a recombinant $DDB2^{PCNA-}$ protein is reported in Materials and Methods (**Paragraph 3.3.1.1**).

Figure 11 shows gel electrophoresis and staining of DDB2 (wild-type and mutated form) concentrated protein. The blue evident band in lane 2 of each gel, between 37 and 50 kDa, highlighted the correct presence of DDB2 recombinant proteins (molecular weight 48 kDa).

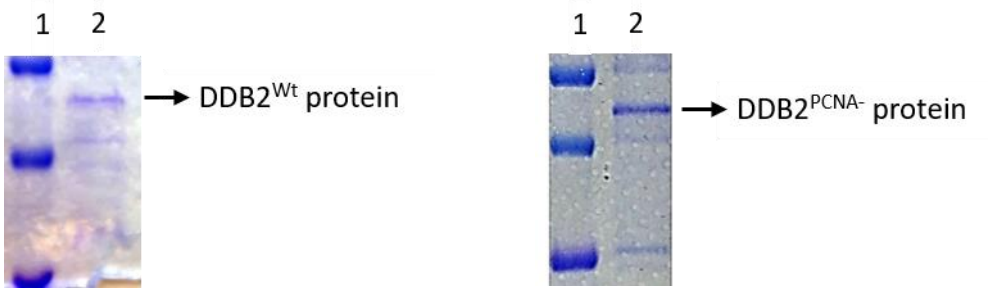

Figure 11 Precision Plus Standard Dual Color protein marker (50, 37 and 25 kDa; lane 1), protein electrophoresis of recombinant $DDB2^{Wt}$ and $DDB2^{PCNA-}$ proteins stained with Coomassie (48 kDa, lane 2)

The irradiated plasmid was incubated "*in vitro*" with recombinant DDB2 (wild-type or mutated form) proteins for 30 or 60 min at 30° C; then, DNA/protein complexes were resolved by an agarose gel electrophoresis (**Figure 12**) (Perucca P *et al*. 2018).

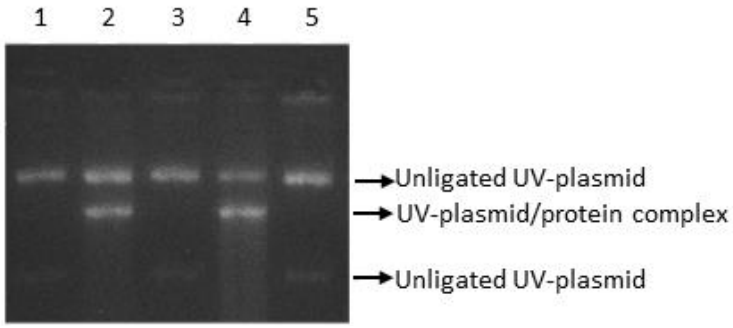

Figure 12 Gel electrophoretic mobility shift assay. Damaged plasmidic DNA (lane 1), UV-damaged DNA incubated with recombinant DDB2^{Wt} protein for 30 or 60 min, respectively (lane 2 and 4), UV-damaged DNA incubated with recombinant DDB2^{PCNA-} protein for 30 or 60 min, respectively (lane 3 and 5)

DDB2^{PCNA-} proteins was not able to bind to the irradiated UV-plasmid both 30 and 60 min after the incubation (lane 3 and 5): in fact, these lanes showed the same banding pattern of lane 1 in which the free irradiated plasmid was loaded, as negative control.
Conversely, the presence of recombinant DDB2^{Wt} protein allowed to form a UV-plasmid/protein complex already 30 min after incubation (lane 2) and this bound persisted 1 h later, as demonstrated by the band shift (lane 4).
The results shown that DDB2^{PCNA-}, unlike DDB2^{Wt} protein, is not able to recognize and bind the lesions present on UV-irradiated DNA plasmid demonstrating an inefficient binding affinity.

4.2.2 EMSA on acrylamide gel

To investigate whether the ectopically DDB2 expression in both HEK293 stable clones may also modify the binding affinity to UV-induced photolesions, an "*in vitro*" reaction was prepared.

First of all, HEK293 (DDB2^{Wt} and DDB2^{PCNA-}) were lysed in order to obtain cell extracts. Next, to verify the presence of DDB2 protein in both cell extracts, a Western blot analysis, with a specific DDB2 antibody, was performed (**Figure 13**).

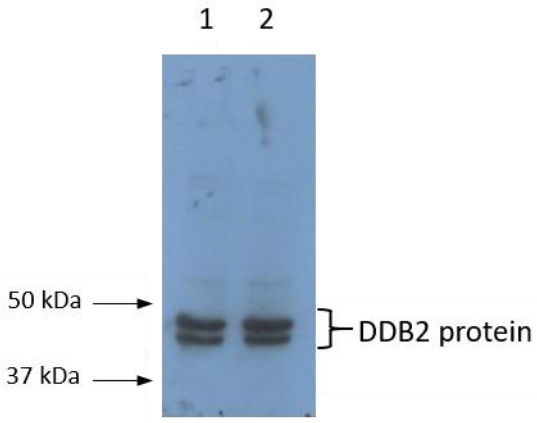

Figure 13 Western blot analysis of DDB2 protein in HEK293 cell extracts: DDB2^{Wt} (lane 1) and DDB2^{PCNA-} (lane 2)

Then, HEK293 DDB2^{Wt} or DDB2^{PCNA-} cell extracts were incubated with CPDs-oligonucleotides, labeled with FAM probe, for 30 min or 1 h. The protein-DNA complexes were resolved by electrophoresis and revealed by Typhoon.

In both HEK293 cell extracts (DDB2^{Wt} or DDB2^{PCNA-}) the CPDs oligonucleotide-protein complex formation has occurred, as demonstrated by the band shifts in **Figure 14**.

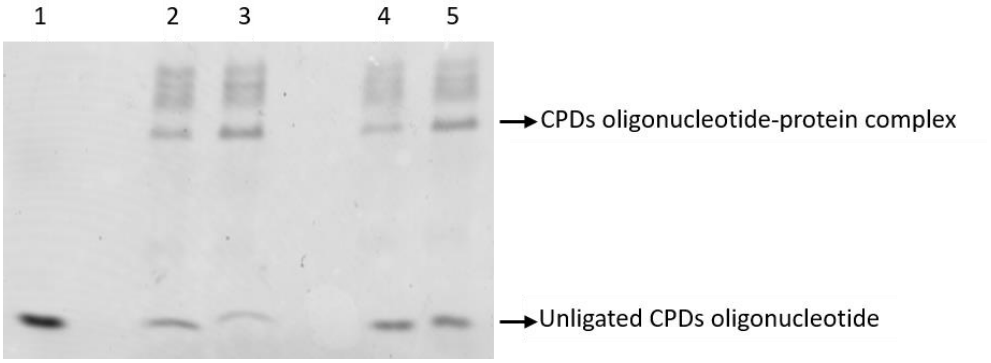

Figure 14 Representative image of EMSA on acrylamide gel. Unbound CPDs oligonucleotide (lane 1), HEK293 DDB2^{Wt} cell extracts incubated with CPDs oligonucleotide for 30 min or 1 h, respectively (lane 2 and 3), HEK293 DDB2^{PCNA-} incubated with CPDs oligonucleotide for 30 min or 1 h, respectively (lane 4 and 5). Results from n=3 independent experiments

However, the DDB2 ability to recognize specific CPDs lesions was different: in HEK293 DDB2^{PCNA-} extracts the binding affinity was less evident, as demonstrated by the marked presence of unbound CPDs oligonucleotide both 30 min and 1 h later from the incubation (lanes 4 and 5, respectively). On the contrary, the wild-type DDB2 protein was able to bind CPDs lesions, as highlighted by the decrease of free CPDs oligonucleotide bands (30 min or 1 h of incubation, lane 2 and 3 respectively).

Finally, to confirm these data, densitometric and statistical analysis were performed (**Figure 15**). HEK293 DDB2^{Wt} extracts showed a significant binding affinity to DNA lesions compared to DDB2^{PCNA-} cell extracts 30 min after incubation. Moreover, although the DDB2 mutated protein binding affinity was increased 1 h later, the statistical difference with the wild-type protein is still maintained.

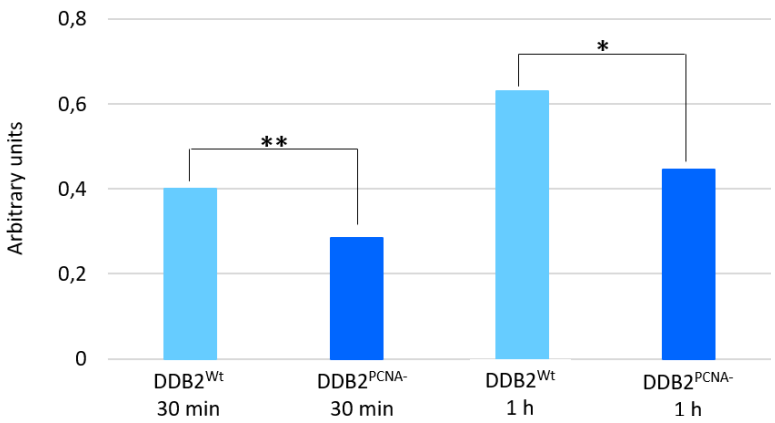

Figure 15 Densitometric and statistical analysis of $DDB2^{Wt}$ (light blue bar) and $DDB2^{PCNA-}$ (blue bar) extracts performed on EMSA with acrylamide gel experiments. N=3 independent experiments; HEK293 $DDB2^{Wt}$ extracts *vs*. HEK293 $DDB2^{PCNA-}$ extracts, * $p < 0.05$ and ** $p < 0.01$

All these collected data demonstrate that the expression of a mutated DDB2 protein confers a lower capability to bind UV DNA lesions, compared to $DDB2^{Wt}$ protein.

4.3 Influence of DDB2 protein in the late NER phases

In previous studies carried out in my laboratory, it was demonstrated that $DDB2^{PCNA-}$ protein co-localized later with XPC, another key protein involved in the recognition of DNA lesions, compared to DDB2 wild-type protein (Perucca P *et al*. 2018). This observation suggested a delay in the initiation of the repair process in cells expressing the mutated DDB2.

Therefore, it was evaluated whether this defective delay may also be evident in a late step of NER, focusing on DDB2 and XPG co-localization and interaction.

To study this aspect, I performed co-localization experiments in HeLa cells, transiently transfected with $DDB2^{Wt}$ or $DDB2^{PCNA-}$ constructs; the next day cells were locally irradiated using a polycarbonate filter with 3 µm pores and fixed after several minutes from UV-C damage. The results were obtained using immunofluorescence techniques, visualized by fluorescence and/or confocal microscopies.

Figure 16 shows representative images of DDB2-XPG co-localization: the best result, in cells expressing DDB2 wild-type protein, was found 10 min after local UV irradiation (**Figure 16 A**, upper panel), whereas DDB2 mutated protein postponed its co-localization with XPG and the signals were evident only 30 min later (**Figure 16 B**, lower panel) (Bassi E *et al*. 2019).

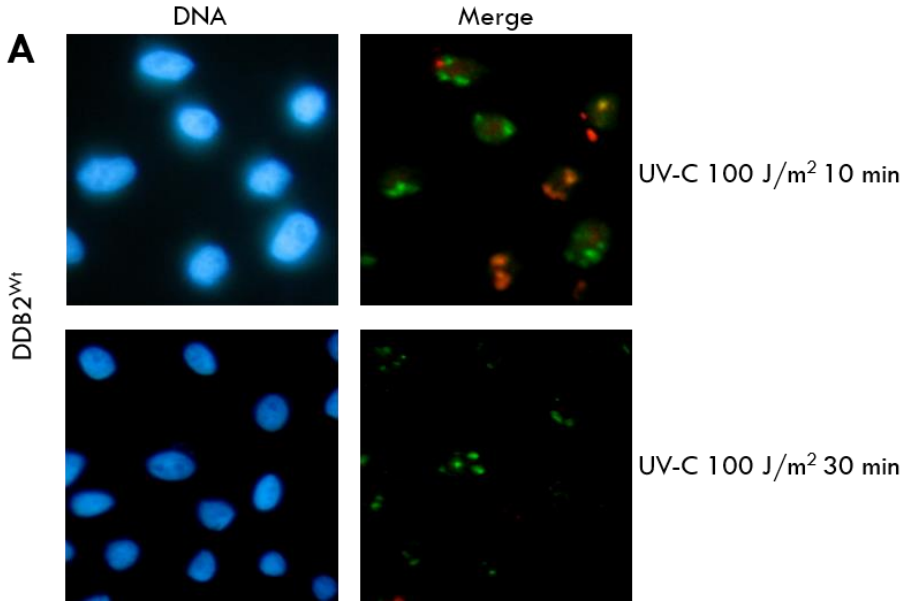

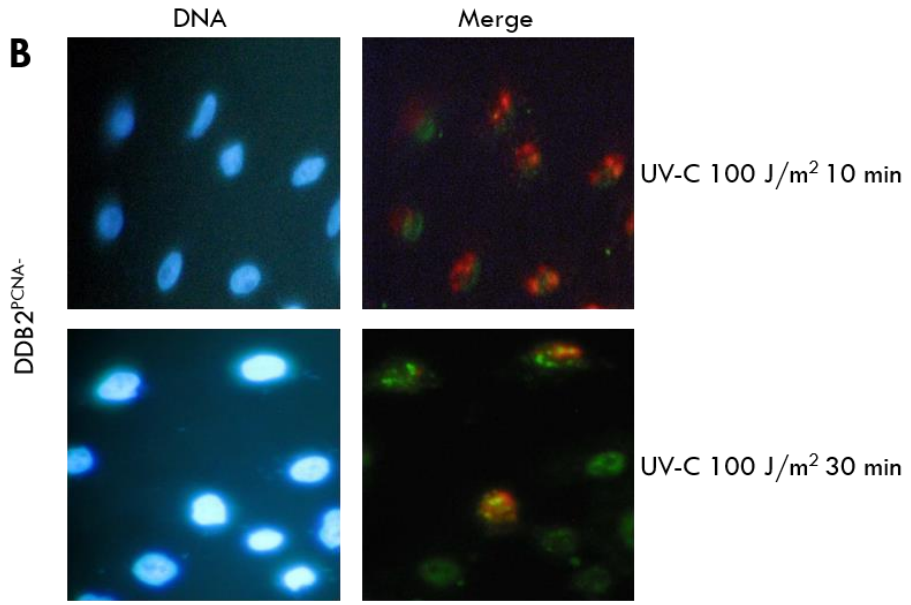

Figure 16 Representative images of DDB2 and XPG co-localization. Cells expressing $DDB2^{Wt}$ (**A**) or $DDB2^{PCNA-}$ (**B**) protein were analysed after 10 or 30 min from UV-C local exposure (100 J/m^2). HeLa nuclei were stained with blue DAPI, XPG (green) and DDB2 (red)

To study in depth the co-localization between XPG (green signal) and DDB2 (red signal) proteins, confocal analysis was performed. **Figure 17 A** and **B** shown the specific co-localization study performed in representative nuclei (Bassi E *et al*. 2019). In particular, in $DDB2^{Wt}$ positive cells the two peaks related to DDB2 and XPG signals were perfectly overlapped 10 min after UV irradiation (**Figure 17 A**).

On the contrary, as shown in the pixel profile (**Figure 17 B**), the DDB2 mutated peak was not coincident with XPG peak even 30 min from UV-damage, demonstrating that the two proteins were in proximity to each other but not completely overlapped.

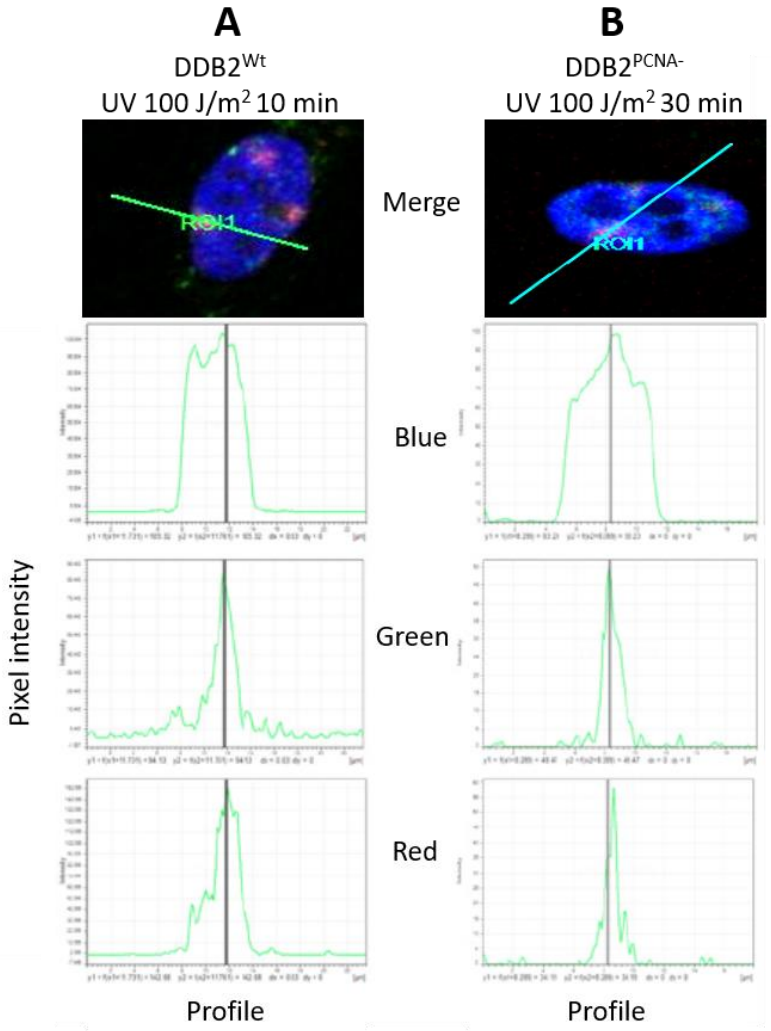

Figure 17 Representative images of confocal co-localization analysis between XPG and DDB2 proteins. HeLa nuclei were stained with blue DAPI, XPG (green) and DDB2 (red). (A) and (B) $DDB2^{Wt}$ (A) or $DDB2^{PCNA-}$ (B) positive cells. Scale bar 13.54 µm. N=3 independent experiments

To verify whether the co-localization was an evidence of an interaction between DDB2 and XPG, an immunoprecipitation assay was performed. For this purpose, a specific DDB2 antibody was used to the immunoprecipitation

reaction and then, both Soluble (S) and Chromatin Bound (CB) fractions were analysed.

In the S fraction, XPG protein was not immunoprecipitated with DDB2 wild-type or mutated protein 30 min after UV irradiation, although the presence of both proteins in the Input S was demonstrated (**Figure 18**, upper panel). Otherwise, DDB2 proteins (both wild-type and mutated) associated to CB fraction were able to pull-down XPG, as shown in the lower panel of **Figure 18**.

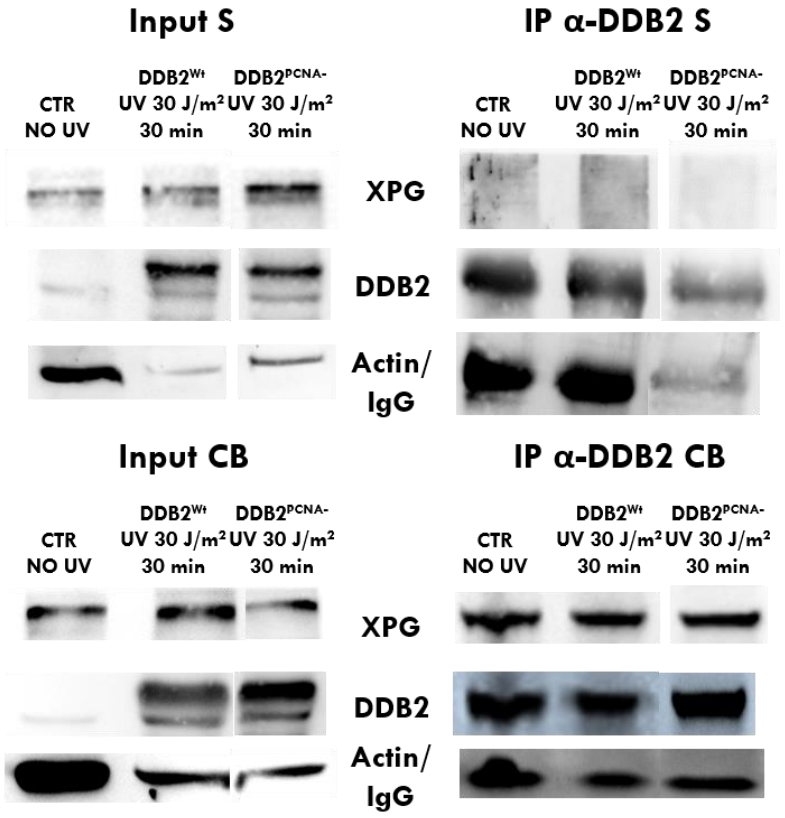

Figure 18 DDB2 interaction with XPG, representative images: results were separated in Soluble (S) or Chromatin Bound (CB) fractions, upper panel and lower panel, respectively; a DDB2 antibody was used to immunoprecipitate samples (IP). IP and Input fractions were analysed by Western blot. Molecular weights: XPG 133 kDa, DDB2 48 kDa, Actin 42 kDa, IgG light chains 25 kDa. N > 3 independent experiments

This evidence not only confirms the results obtained with immunofluorescence analysis but highlighted that the presence of a mutated DDB2 protein affects several steps of NER process.

Furthermore, previous studies have demonstrated that cells stably expressing $DDB2^{PCNA-}$ protein shown a lower efficiency in CPDs removal, the ultimate purpose of the NER process, compared to $DDB2^{Wt}$ stable clone or control cell line (Perucca P *et al*. 2018).

II. Influence of DDB2-PCNA interaction on cell proliferation after UV-damage

4.4 Study of cell proliferation ability

It was previously demonstrated that the stable expression of a mutated DDB2 protein in HEK293 cells allows an increased cell proliferation compared to HEK293 $DDB2^{Wt}$ or control cell lines (Perucca P *et al*. 2015).
Starting from this evidence, it was investigated whether DDB2 protein could influence the cellular growth of HEK293 cell lines, after UV irradiation. To this end, a clonogenic assay has been performed.

Irradiated HEK293 (CTR, $DDB2^{Wt}$ and $DDB2^{PCNA-}$) were seeded at a low density to avoid colony confluence; then, the cellular growth and the colony formation were daily checked and, after 10 days, cells were fixed and stained for manual colony counting.

Figure 19 A displays representative images of the assay: the highest number of colonies was evident in cells stably transfected with $DDB2^{PCNA-}$ construct; moreover, these colonies showed larger dimensions than those obtained with other cell lines (Perucca P *et al*. 2018).
The $DDB2^{Wt}$ clone was able to form colonies, although these cells shown an increased sensitivity to UV rays, as demonstrated by the lower number of developed colonies compared to the mutated clone.
Instead, in the control cell line (HEK293 CTR) the few formed colonies appeared faded, thus confirming the poor resistance to UV irradiation of these cells.

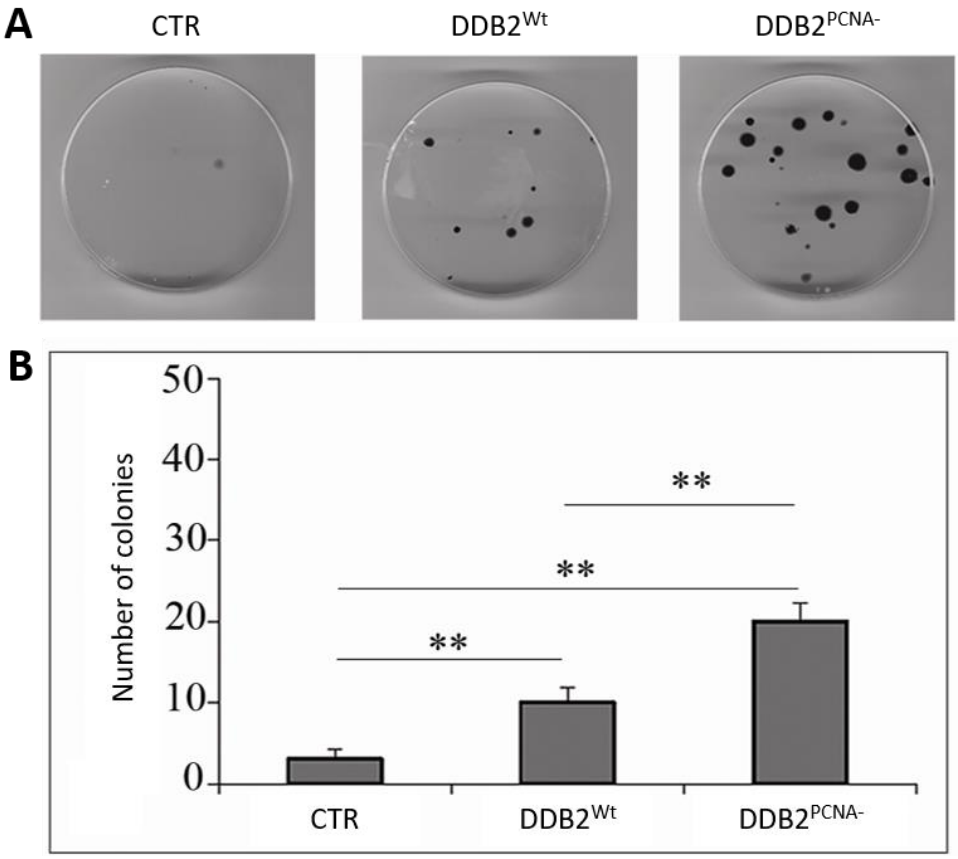

Figure 19 Clonogenic assay of HEK293 (CTR, $DDB2^{Wt}$ and $DDB2^{PCNA-}$ stable clones) after UV-induced DNA damage (10 J/m^2). (**A**) Representative images of colonies formed after Gentian violet staining. (**B**) Number of colonies grown. Mean values (± S.D.) are reported from 3 independent experiments. ** $p < 0.01$

The data obtained and the statistical analysis are summarized in **Figure 19 B**: cells expressing the exogenous DDB2 protein, both wild-type and even more, the mutated form, acquired an unexpected and significant increased UV resistance, compared with control cell line (Perucca P *et al*. 2018). Moreover, comparing both stable clones, the ability to develop colonies was significantly marked in the mutated one.

4.5 Study of mitoses and cell viability

To examine in depth the number and morphological features of mitoses in HEK293 cells (CTR, DDB2^{Wt} and DDB2^{PCNA-} stable clones), an immunofluorescence and a May-Grünwald Giemsa staining were performed.

To visualize the number of mitoses, not irradiated and irradiated HEK293 cells were fixed after three days and incubated with a specific pospho-Histone 3 antibody. Not irradiated cells were used as positive control (data not shown). In Figure 20 are reported the results obtained from the immunostaining analysis.

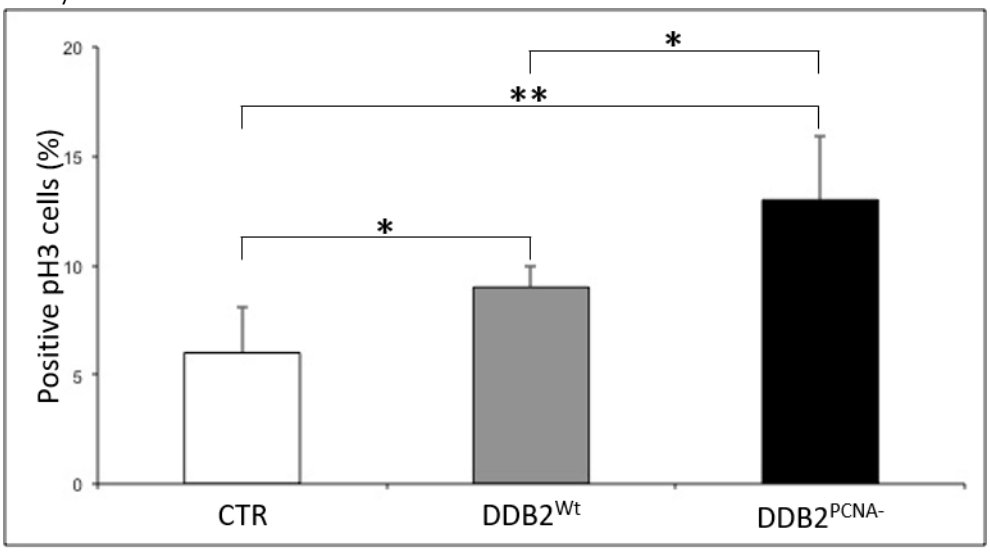

Figure 20 Immunofluorescence analysis of positive pH3 cells expressed in percentage. Irradiated HEK293 CTR (white bar), DDB2^{Wt} (grey bar) and DDB2^{PCNA-} (black bar) stable clones were fixed, immunostained with pospho-Histone 3 (pH3) antibody and manually counted. Mean values (± S.D.) are reported from 3 independent experiments, * $p < 0.05$ and ** $p < 0.01$

The mutated clone showed the highest percentage of pH3-positive irradiated cells, confirming not only its increased resistance to UV-C radiation but also its predisposition to proliferate. On the contrary, few cells of the control line were immunostained, suggesting that a lower number of cells was able to enter in mitosis, after UV DNA damage.

To evaluate the morphological features, three days after seeding, when irradiated cells were grown but they have not yet formed multilayer and confluent colonies, samples were stained with May-Grünwald Giemsa. Total number of cells per colony, including dead cells and mitoses, were counted and photographed.
In particular, the attention was focused on the presence of atypical mitoses, which are a specific hallmark frequently observed in cancer cells (Batistatou A 2004).

Some representative images show the morphological features of colonies (**Figure 21 A**) and their sorting on mitoses, atypical mitoses and dead cells (**Figure 21 B**) (Perucca P *et al*. 2018).

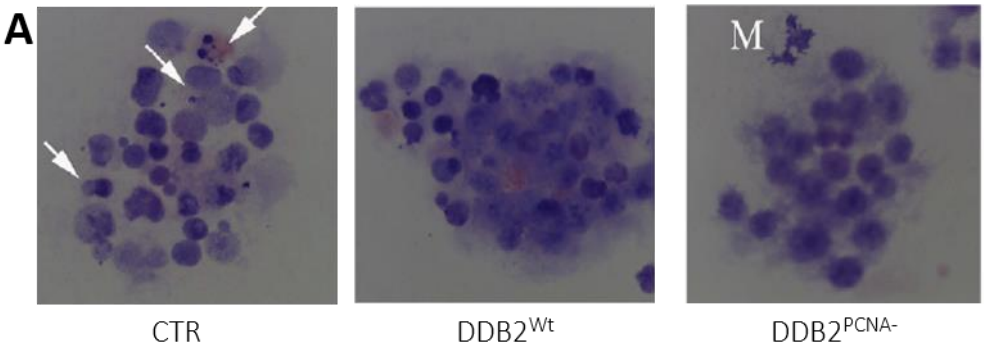

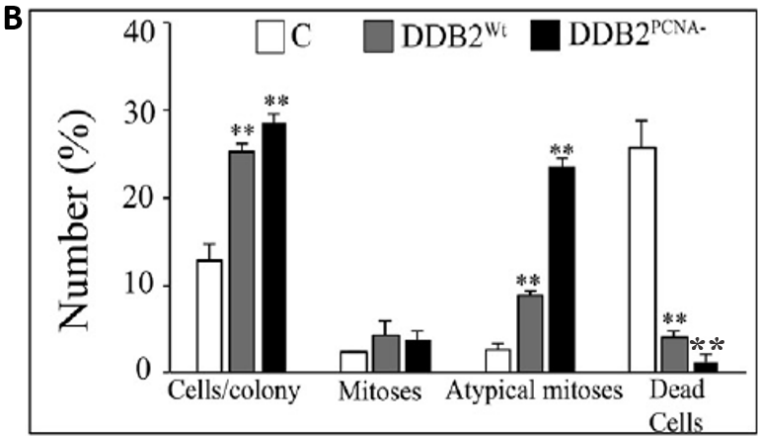

Figure 21 May-Grünwald Giemsa staining in control HEK293 (CTR), $DDB2^{Wt}$ and $DDB2^{PCNA-}$ stable clones after UV-C radiation (10 J/m^2), representative images. (**A**) Morphological features of growing colonies of $DDB2^{Wt}$ and $DDB2^{PCNA-}$ clones *vs*. control cell line. Arrows pointed dead cells; representative atypical mitoses (M) in cells expressing $DDB2^{PCNA-}$ protein. (**B**) Percentages of cells per colony, mitoses, atypical mitoses and dead cells in control HEK293 (white bar), $DDB2^{Wt}$ (grey bar) and $DDB2^{PCNA-}$ (black bar) stable clones, respectively. Mean values (± S.D.) are reported from 3 independent experiments, ** $p < 0.01$

Cells expressing $DDB2^{PCNA-}$ produced more colonies with larger size compared to $DDB2^{Wt}$ stably transfected clone and control cell line (**Figure 21 A**), as it was also demonstrated with the clonogenic assay above. Although the number of mitoses was comparable in $DDB2^{PCNA-}$ and $DDB2^{Wt}$ clones, in cells expressing DDB2 mutated protein, a higher and significant percentage of atypical mitoses (**Figure 21 B**) was found (indicated with letter M in **Figure 21 A**.

Both clones showed an increased UV resistance, as demonstrated by the poor presence of dead cells in samples but, in mutated clone, the number was strongly reduced (**Figure 21 B**).

Conversely, the number of dead cells (highlighted with arrows in **Figure 21 A**) in control cell line was very high, confirming a low resistance to UV-C radiation. In some of control cells, apoptotic bodies were also observed.

4.6 Evaluation of DDB2-Polymerase η interaction

The previously collected data have demonstrated that cells expressing DDB2 mutated protein acquired an unexpected proliferation advantage after UV damage. Moreover, these cells developed an increased resistance to UV irradiation and showed specific morphological features, such as atypical mitoses, underlying genomic instability.

Starting from this evidence it was explored whether DDB2 is involved in Trans-Lesion DNA Synthesis (TLS). In particular, it was investigated the possible interaction between DDB2 protein and Polymerase η, the protein involved in TLS.

4.6.1 Evaluation of DDB2 and Polymerase η co-localization by confocal analysis

For this purpose, HeLa cells were transiently co-transfected with Pol η-GFP and $DDB2^{Wt}$ or $DDB2^{PCNA-}$ constructs. Cells transfected only with Pol η-GFP construct represent negative control. After UV-C local irradiation, cells were lysed and immunostained with specific antibodies; the analysis was performed by confocal microscopy.

In **Figure 22** are reported some representative images. First of all, it was verified the proper *foci* formation of Polymerase η after UV irradiation (**Figure 22,** upper panel) and that the expression of DDB2 protein (both wild-type and mutated) was homogeneous in all the samples (**Figure 22**, representative images middle and lower panel).
Confocal analysis evidenced the co-localization between DDB2 and Pol η only in the presence of mutated form, suggesting their possible interaction.

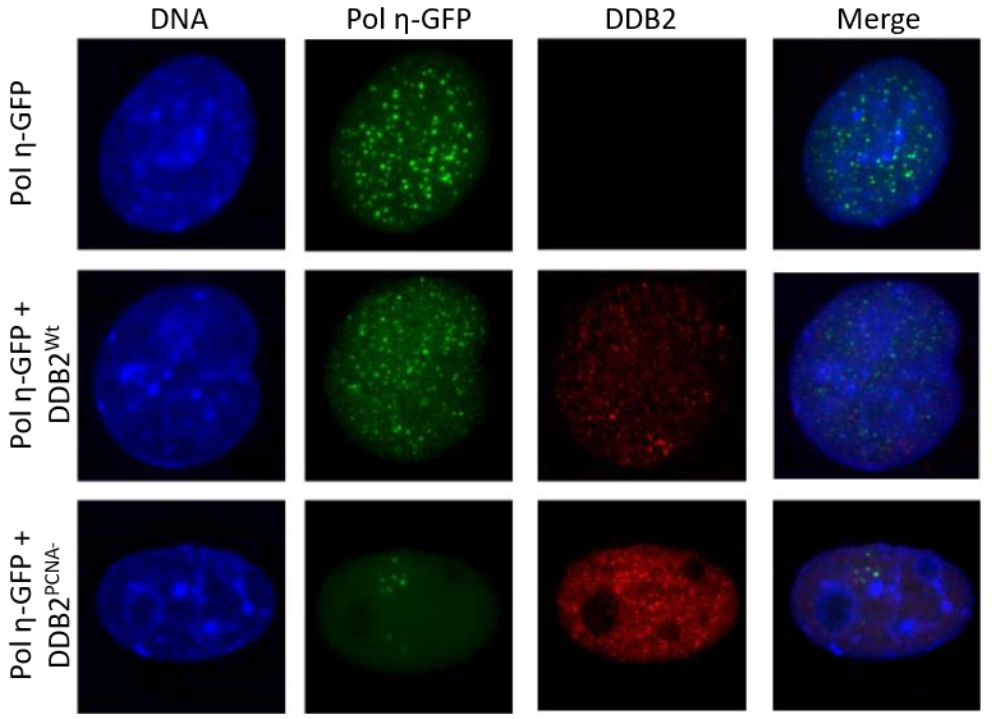

Figure 22 Representative images of confocal analysis of Pol η-GFP and DDB2 recruited to DNA damage sites after UV irradiation. Recruitment of Pol η-GFP (green fluorescence), upper panel; recruitment of Pol η-GFP and DDB2 (red fluorescence) wild-type or mutated form, middle and lower panel, respectively. Nuclei were stained with Hoechst 33258 dye

To study in depth the possible co-localization between Polymerase η and DDB2, it was analysed the pixel intensity of both proteins by confocal microscopy.

Regarding the recruitment to UV photolesions of Polymerase η and DDB2 wild-type protein, no co-localization was observed.
Interestingly, the Polymerase involved in TLS and $DDB2^{PCNA-}$ protein were overlapped (**Figure 23**).

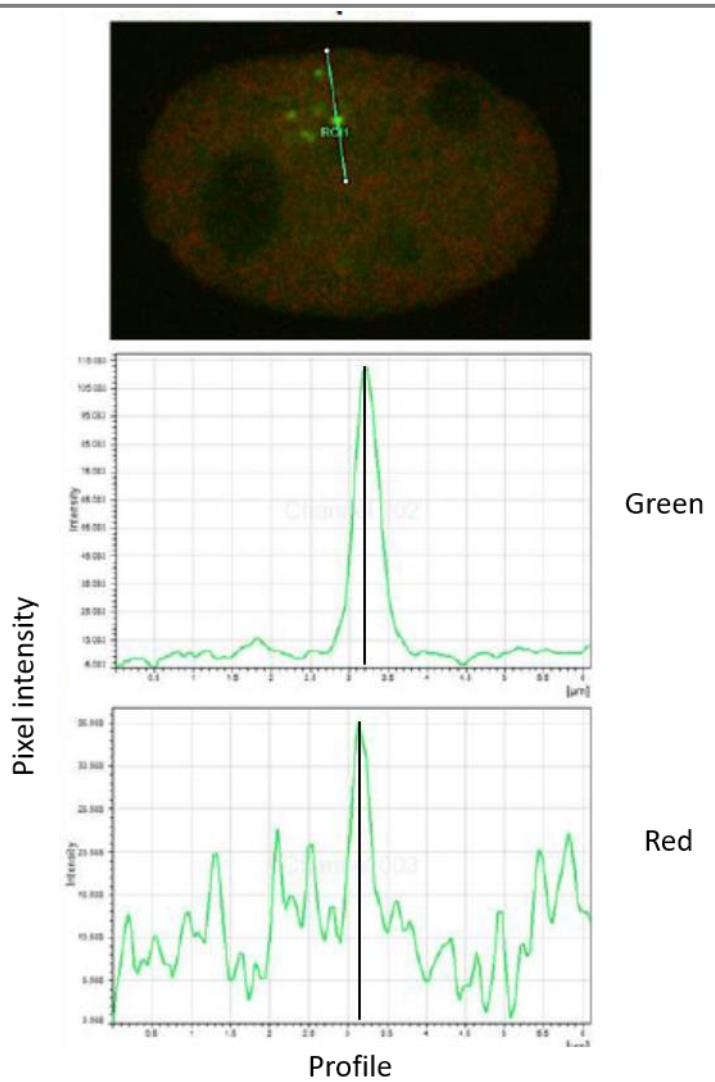

Figure 23 Confocal co-localization analysis of Polymerase η and DDB2^{PCNA-} proteins, representative image. Pixel intensity representation of Polymerase η (green fluorescence) and DDB2^{PCNA-} (red fluorescence) recruited to DNA lesions upon UV irradiation. N=3 independent experiments

4.6.2 Study DDB2 and Polymerase η interaction by immunoprecipitation assay

To verify the possible interaction between Polymerase η and DDB2 proteins, immunoprecipitation experiments were performed.

For this purpose, HeLa cells were transiently co-transfected with Pol η-GFP and pcDNA3.1-DDB2^{Wt} or pcDNA3.1-DDB2^{PCNA-} constructs and exposed to UV irradiation (30 J/m^2). As negative and positive controls, two samples were only transfected with GFP or Pol η-GFP constructs. Then, GFP protein was immunoprecipitated and, from each sample, a Chromatin Bound (CB) fraction was obtained and analysed.

Figure 24 shows representative images of the immunoprecipitation assay. DDB2 protein was only immunoprecipitated in co-transfected samples (both input and IP fractions), suggesting that endogenous DDB2 protein in HeLa cells was not detected.
As expected, Polymerase η was found in co-transfected samples and in positive control. In particular, it seems that the interaction between the Polymerase involved in TLS and mutated DDB2 protein was more evident compared to DDB2 wild-type.
In the negative control (GFP sample) no immunocomplexes between GFP and Pol η or DDB2 proteins were detected.

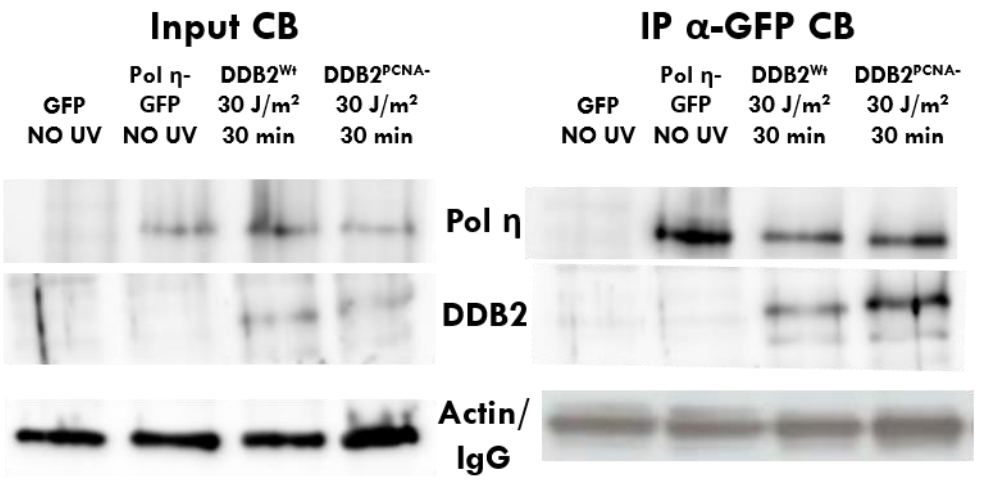

Figure 24 DDB2 interaction with Polymerase η, representative images of Chromatin Bound (CB) fractions. A GFP antibody was used to immunoprecipitate samples (IP). IP and Input fractions were analysed by Western blot. Molecular weights: Polymerase η 78 kDa, DDB2 48 kDa, Actin 42 kDa, IgG light chain 25 kDa. N=3 independent experiments

These observations were confirmed by a densitometric analysis of Polymerase η and DDB2 bands performed by ImageJ software (Figure 25).

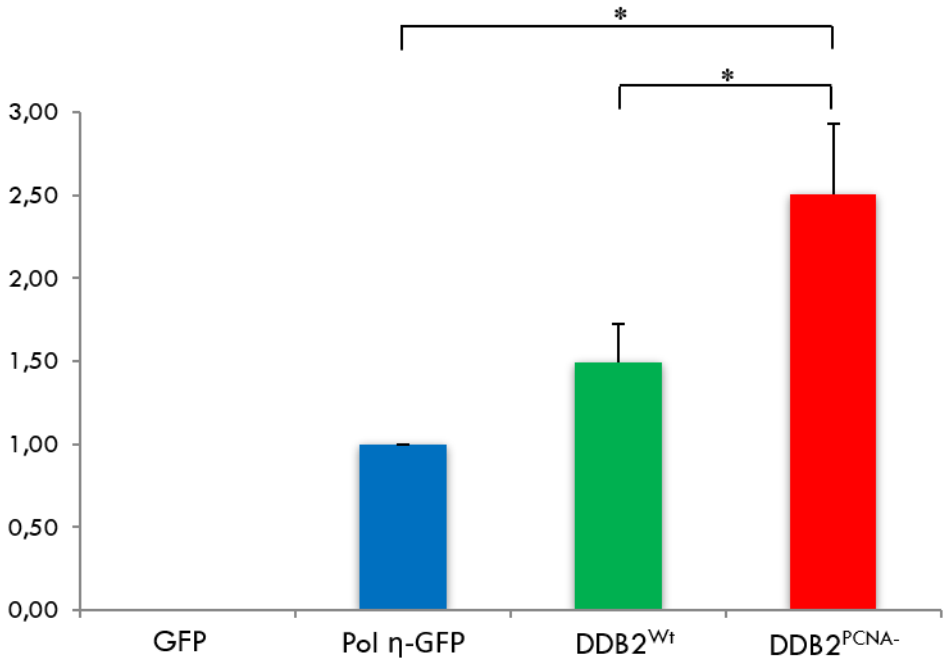

Figure 25 Band densitometric analysis of Polymerase η compared to DDB2 protein in HeLa GFP, Pol η-GFP (light blue bar), $DDB2^{Wt}$ (green bar) and $DDB2^{PCNA-}$ (red bar) samples. N=3 independent experiments; data are mean ± S.D. $DDB2^{PCNA-}$ *vs*. $DDB2^{Wt}$ or Pol η-GFP samples, * $p < 0.05$

The interaction between $DDB2^{Wt}$ and Polymerase η was quite comparable to positive control sample (Pol η-GFP): the presence of exogenous DDB2 wild-type protein did not notably influence the possible cooperation with the Polymerase involved in TLS.
On the contrary, DDB2 mutated protein was more able to interact with Polymerase η. The interaction between the above proteins was 2.5 fold higher than positive control and the statistical analysis confirmed that this protein interaction is significant, suggesting a possible involvement of mutated DDB2 protein in TLS process.

4.6.3 Study of direct interaction between DDB2 and Polymerase η through Proximity Ligation Assay approach

Finally, it was investigated the possible interaction with the PLA, an innovative and powerful technique. This approach allows to determine, with an immunofluorescence signal, a direct interaction between two target proteins that are in close proximity (no more than 40 nm).
For this purpose, HeLa cells were transiently co-transfected with Pol η-GFP and DDB2 wild-type or mutated constructs and UV-totally irradiated. Cells transfected only with Pol η-GFP was employed as negative control. 30 min later, cells were lysed and immunostained according to the PLA manufacturer protocol and visualized by confocal microscopy.

Representative images of PLA technique are reported in **Figure 26**:

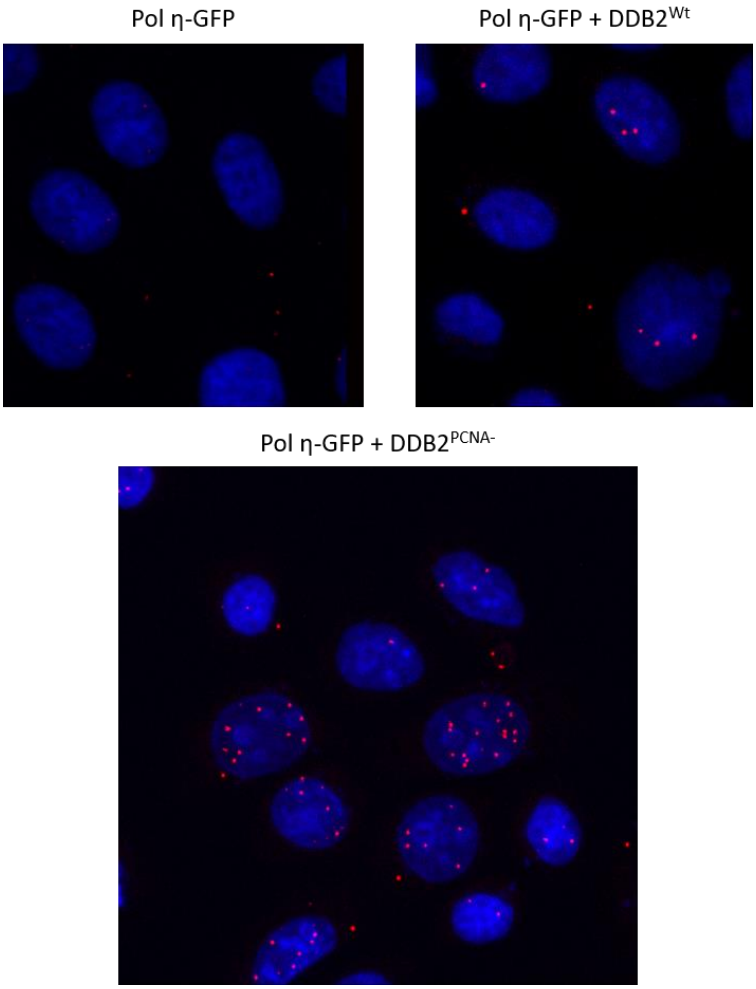

Figure 26 Confocal analysis of PLA assay performed on locally irradiated HeLa cells only transfected with Pol η-GFP or co-transfected with Pol η-GFP and $DDB2^{Wt}$ or $DDB2^{PCNA-}$ constructs; cells were lysed 30 min after UV damage. Nuclei were stained with Hoechst 33258 dye. N=3 independent experiments

As expected, in cells only transfected with Polymerase η a positive result was not obtained. The few signals detected in the samples are only background (as explained by the manufacturer) (**Figure 26**).
In samples co-transfected with DDB2 protein, both wild-type and, even more, the mutated one, the red spots were detected, confirming a positive direct

interaction between the two target proteins. As expected, these spots were mainly localized in the nuclei of HeLa cells, confirming the proper recruitment of Polymerase η and DDB2 proteins to damaged DNA.
In the wild-type sample, the amplification of the signal, which is related to a positive result, was detected in few cells compared to the mutated sample. Moreover, when the mutated DDB2 protein was present, several red spots were found in each cell that was analysed, suggesting a strong interaction between these proteins (Figure 26).

The collected data of PLA were also analysed with GraphPad Prism software (Figure 27).

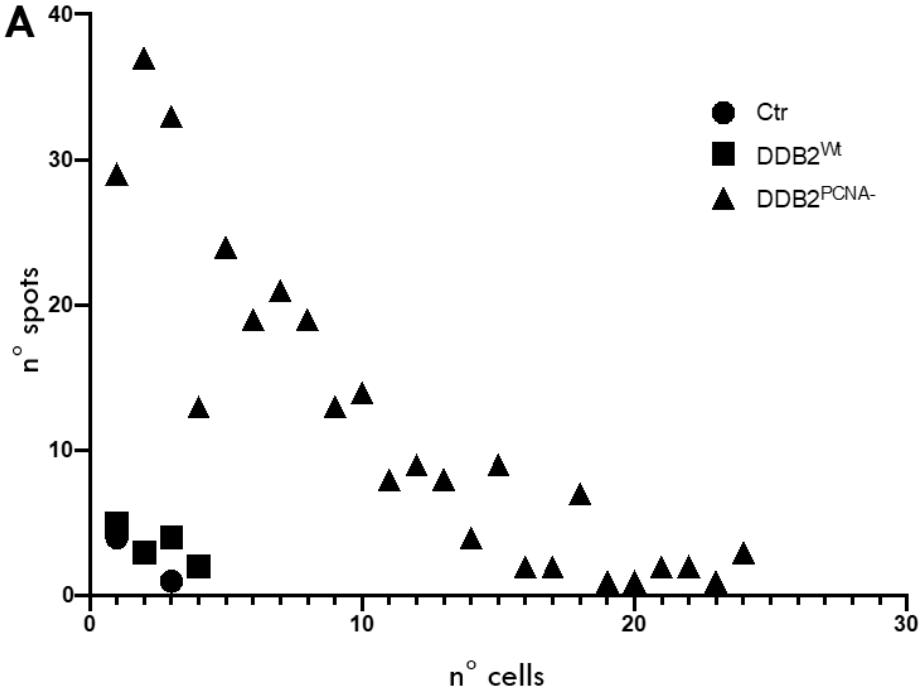

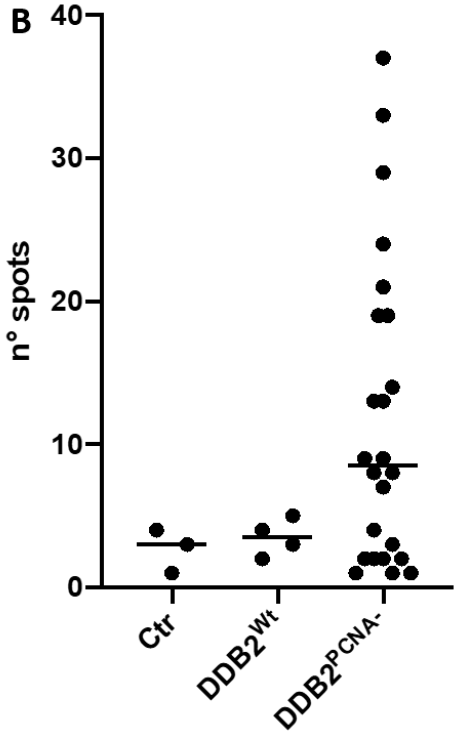

Figure 27 GraphPad Prism analysis of PLA technique. (A) Correlation between number of red spots and number of positive cells in irradiated HeLa cells only transfected with Pol η-GFP (CTR), or co-transfected with Pol η-GFP and pcDNA3.1-DDB2^{Wt} (DDB2^{Wt}) or pcDNA3.1-DDB2^{PCNA-} (DDB2^{PCNA-}) samples. (B) Distribution of positive events in HeLa CTR, DDB2^{Wt} and DDB2^{PCNA-} samples transfected only with Pol η-GFP (CTR), or co-transfected with Pol η-GFP and DDB2^{Wt} and DDB2^{PCNA-}. The straight line depicts the average value of each sample

In Figure 27 A the number of analysed cells was correlated with the number of red spots that were counted. In control and DDB2^{Wt} samples it was found a similarity. Only few positive cells with 2 or 3 red spots for cell were observed; whereas in the majority of cells not positive results were found.
Conversely, in the mutated sample, several cells confirmed the direct interaction between Polymerase η and DDB2^{PCNA-} protein.
Moreover, in this sample it was found a wide heterogeneity in the number of positive events: although the majority of cells contained an average number

of 10 spots, in several nuclei until 40 red spots were counted, as demonstrated in Figure 27 B.

All together these results have demonstrated that the mutated DDB2 protein directly interacted with Polymerase η, suggesting that the mutated DDB2 protein may be involved in the TLS process.

III. Study of cell migration after UV-damage

4.7 Wound healing assay

To investigate whether the exogenous expression of DDB2 protein ($DDB2^{Wt}$ or $DDB2^{PCNA-}$) could confers to irradiated HEK293 cells both proliferation and migration advantages, a wound healing experiment was carried out.

Briefly, HEK293 CTR, $DDB2^{Wt}$ and $DDB2^{PCNA-}$ stable clones were irradiated and seeded in each *septum* of the culture-insert. The culture-insert was removed when cells have reached a confluent layer, leaving a cell-free gap. The growth and motility of cells were checked and photographed starting from day 0 (corresponding to removal of culture-inserts) until day 9.

Some representative images of the time course experiments are displayed in Figure 28 A (Perucca P *et al*. 2018).

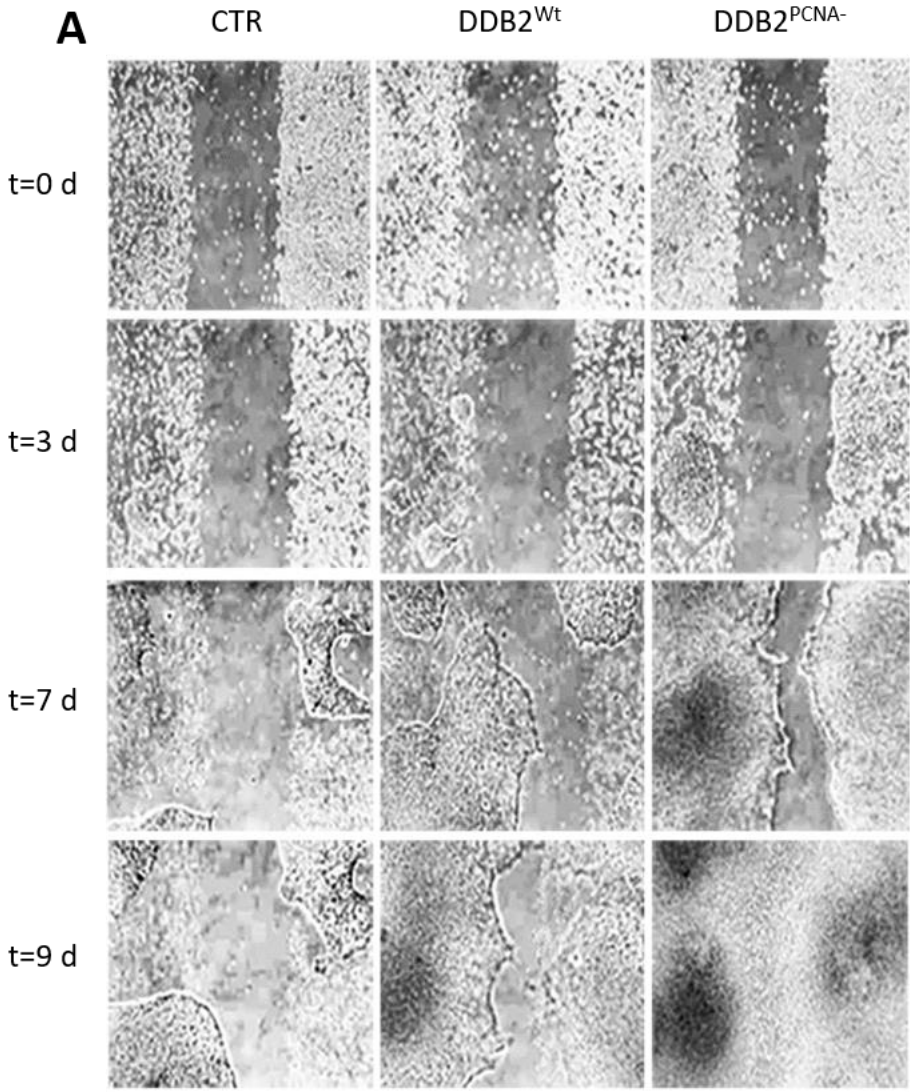
A
CTR
DDB2Wt
DDB2PCNA-
t=0 d
t=3 d
t=7 d
t=9 d

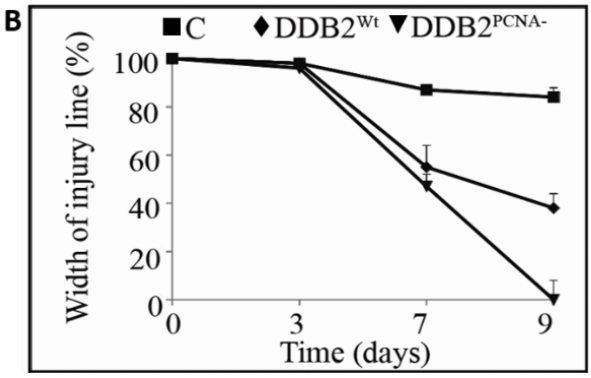

Figure 28 Wound healing assay in HEK293 CTR (C), $DDB2^{Wt}$ and $DDB2^{PCNA-}$ stably transfected clones after UV-induced DNA damage. (**A**) Representative images of cell proliferation and motility (×10 magnification objective) after 0, 3, 7 and 9 days from the removal of culture-insert. (**B**) Migration rate quantification. N>3 independent experiments; data are mean ± S.D.

The first column shows the behaviour of irradiated control cells, while in the second and in the third column, cells stably expressing $DDB2^{Wt}$ or DDB2 mutated protein were shown, respectively.
Until day 3, the width of injury was similar in all the three cell lines, suggesting that cells were initially affected by UV damage.
7 days after UV-C irradiation, the distance between two sets was significantly reduced in both stably transfected clones, in particular in the mutated one; whereas in control cells the migration rate was only 10% (**Figure 28 B**) (Perucca P *et al*. 2018).
At 9th day after the removal of culture-inserts, $DDB2^{PCNA-}$ stable clone closed entirely the gap; moreover, these cells exhibited not only a higher cell motility and growth but they were able to form an unexpected compact multilayer of growing cells, evident in both cellular walls in **Figure 28 A**.
Indeed, in $DDB2^{Wt}$ stable clone the gap between the two *septa* was still visible and the size of injury line was almost 40% (**Figure 28 B**), thus the wild-type clone confirmed a lower rate of cell proliferation and motility compared to the mutated clone.
As expected, in HEK293 control line, it was observed a reduced cell motility as reported in **Figure 28 B**; indeed, the width of injury line, after 9 days from

UV irradiation, was still 80%.

4.8 Involvement of DDB2 protein in epithelial to mesenchymal transition

By clonogenic experiments and wound healing assay it was demonstrated that the exogenous expression of DDB2 protein, both wild-type and, even more, the mutated one, confers proliferation and motility advantages in irradiated HEK293 cells, suggesting a possible implication of DDB2 in cancer biology.

Starting from this evidence, it was investigated whether DDB2 protein could be implicated in EMT process, an important step of cancer progression; to this end, E-cadherin and Vimentin protein expression levels were analysed by Western blot. E-cadherin and Vimentin proteins are the main epithelial and mesenchymal markers, respectively. Furthermore, it was also evaluated the presence and activity of MMPs-2 and 9 by gelatin zymography assay.

4.8.1 Evaluation of E-cadherin and Vimentin expression after UV damage

Briefly, HEK293 CTR cell line and cells stably expressing $DDB2^{Wt}$ or $DDB2^{PCNA-}$ protein were irradiated and harvested after several times. For each cell line, not irradiated cells were employed as negative control. After protein electrophoresis, Western blot analysis using specific E-cadherin and Vimentin antibodies was performed.

Figure 29 shows the expression levels of E-cadherin protein starting from 48 h upon UV damage. The protein expression levels after 4, 8 and 24 h after UV-C exposure were analysed, but not significant results were obtained (data not shown in the underlying graph).
The highest E-cadherin expression levels were found in control cell line; besides, the production of E-cadherin protein in irradiated control cells remained always higher compared to its negative control. In particular, 96 h

after UV-damage, the protein production increased almost 3-fold compared to its basal level with a very significant statistical value.

Conversely, cells stably expressing DDB2^{PCNA-} protein had an instable trend and the lowest protein levels compared to DDB2^{Wt} cells and, even more, to control HEK293 cells. In particular, 96 h after UV-induced DNA damage, E-cadherin levels in the mutated clone were the lowest that we have ever found, representing a very or extremely significant values compared to its negative control.

Furthermore, it was observed that also DDB2^{Wt} stable clone expressed a lower E-cadherin protein level than its basal level and, even more, compared to irradiated control cells.

The alteration of E-cadherin expression levels in cells expressing DDB2^{Wt} or, even more, DDB2^{PCNA-} protein, suggested that in both clones the cell-cell adhesion was decreased upon UV-damage.

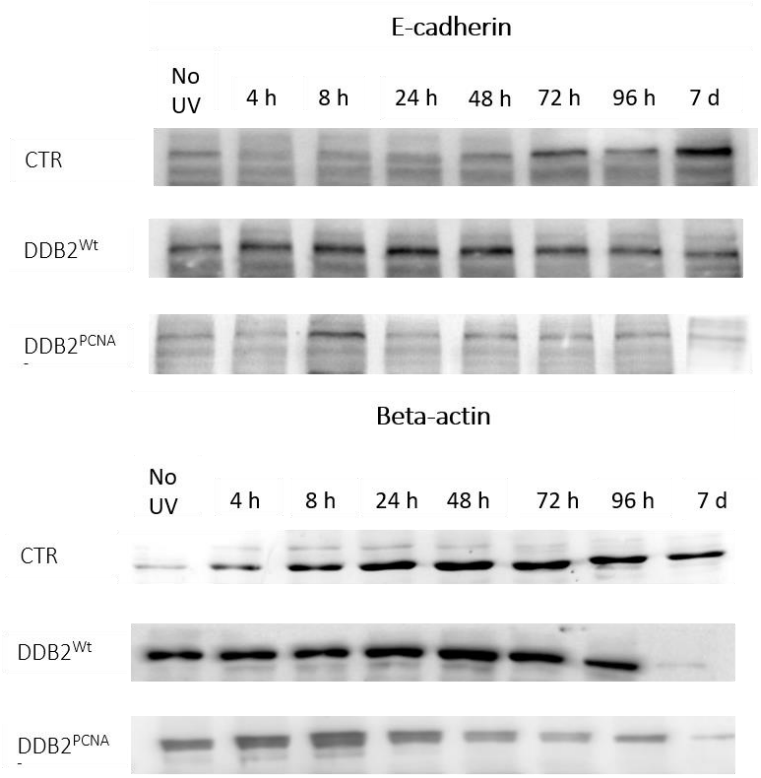

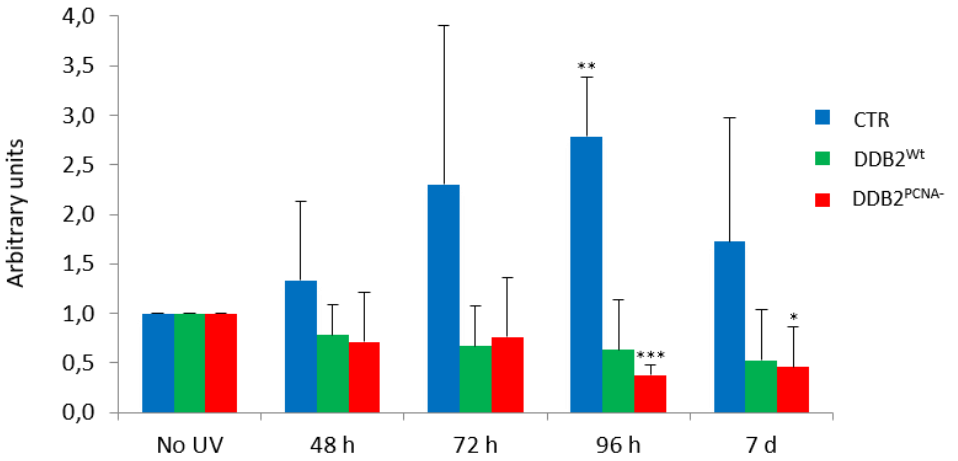

Figure 29 Evaluation of E-cadherin expression levels in HEK293 CTR (blue bar), $DDB2^{Wt}$ (green bar) and $DDB2^{PCNA-}$ (red bar) stably transfected clones after UV-induced DNA damage by Western blot analysis. All the three cell lines were seeded ($1x10^6$) in 100 mm cell culture dishes, irradiated (10 J/m^2 UV-C) and harvested at different times (No UV, 4 h, 24 h, 48 h, 72 h, 96 h and 7 d). E-cadherin expression was normalized with beta actin. N>3 independent experiments; data are mean ± S.D., UV irradiated cells *vs*. not irradiated cells * $p < 0.05$, ** $p < 0.01$, *** $p < 0.0001$

The results about Vimentin expression levels are illustrated in **Figure 30**. In the underlying graph, only values obtained starting from 48 h after UV damage were showed.

The highest values of the protein were found in $DDB2^{PCNA-}$ clone, although the levels were similar to its basal level, suggesting that the trend remained almost stable during all the time course in this clone. In particular, starting from 48 h until 7 d after UV-induced DNA damage, the protein values were statistically significant compared to not irradiated $DDB2^{PCNA-}$ cells.

On the contrary, in the other two cell lines, it was observed a reduction in Vimentin expression; in particular, 7 d after UV irradiation, decrease on protein level was evident.

These results suggest that in DDB2 mutated clone cell-cell adhesion is affected.

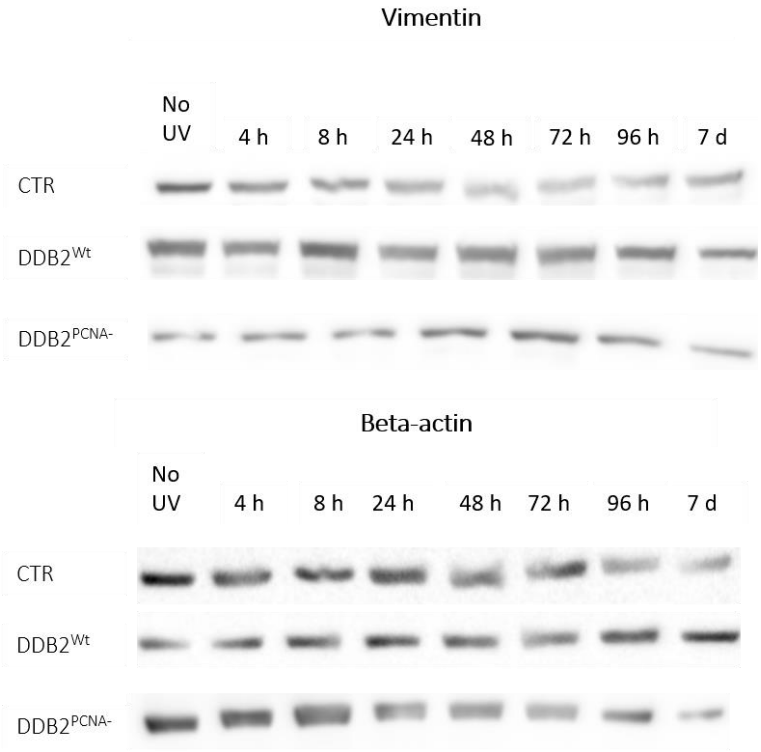
Vimentin
No UV
4 h
8 h
24 h
48 h
72 h
96 h
7 d
CTR
DDB2Wt
DDB2PCNA-
Beta-actin
No UV
4 h
8 h
24 h
48 h
72 h
96 h
7 d
CTR
DDB2Wt
DDB2PCNA-

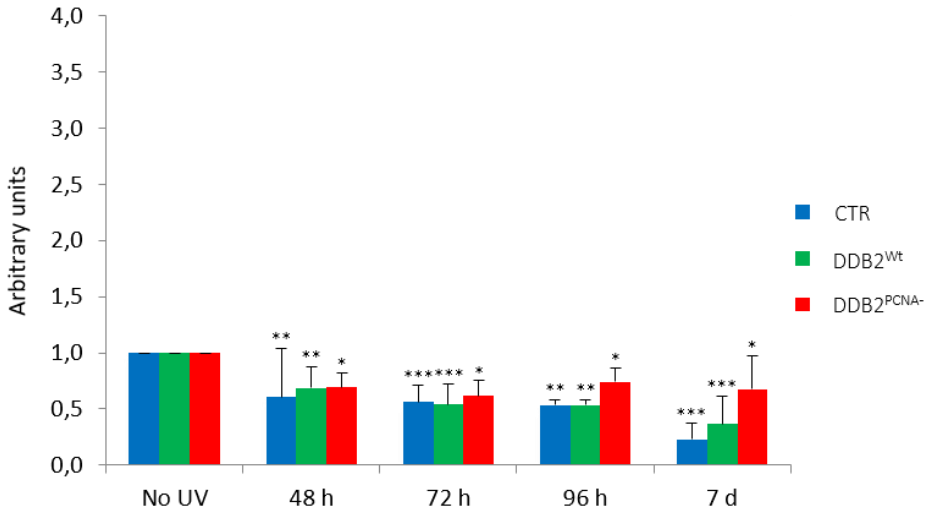

Figure 30 Evaluation of Vimentin expression levels in HEK293 CTR (blue bar), DDB2^{Wt} (green bar) and DDB2^{PCNA-} (red bar) stable transfected clones after UV-induced DNA damage by Western blot analysis. All the three cell lines were plated (1x10^6) in 100 mm cell culture dishes, then were irradiated (10 J/m^2 UV-C) and harvested at different times (No UV, 4 h, 24 h, 48 h, 72 h, 96 h and 7 d). Vimentin expression was normalized with beta actin. N>3 independent experiments; data are mean ± S.D., UV irradiated cells *vs*. not irradiated cells * $p < 0.05$, ** $p < 0.01$, *** $p < 0.0001$

Taking together all the data collected by the Western blot analysis, demonstrate that the modification of E-cadherin and Vimentin expression level leads to speculate that DDB2^{Wt} and, even more, the mutated stable clone might be more prone to activate the EMT process.

4.8.2 Detection of metalloproteinases 2 and 9 by gelatin zymography

The activation of MMPs is a crucial event in EMT and tumour progression since these proteases are responsible for the degradation of extracellular matrix (Chambers AF and Matrisian LM 1997; Duffy MJ *et al*. 2008). This is a key step in invasion and metastatic processes. In particular, MMPs-2 and 9, also known as gelatinases, are involved in cancer progression (Gialeli C *et al*. 2011); for these reasons, it was investigated their activity in irradiated HEK293 stable clones using a gelatin zymography assay.

For this purpose, the culture *media* of irradiated HEK293 CTR, $DDB2^{Wt}$ and $DDB2^{PCNA-}$ stable clones were collected at different time recovery after UV-induced DNA damage. For each cell line, cells not irradiated were employed as negative control. After electrophoresis, the gel was incubated with several buffers in order to visualized and analysed the digested bands, as reported in Materials and Methods section.

Figure 31 shows some representative images of the results obtained by time course experiments: the white bands (corresponding to digested gelatin) at 62 kDa and 84 kDa confirmed the presence and the activation of MMPs-2 and 9, respectively.

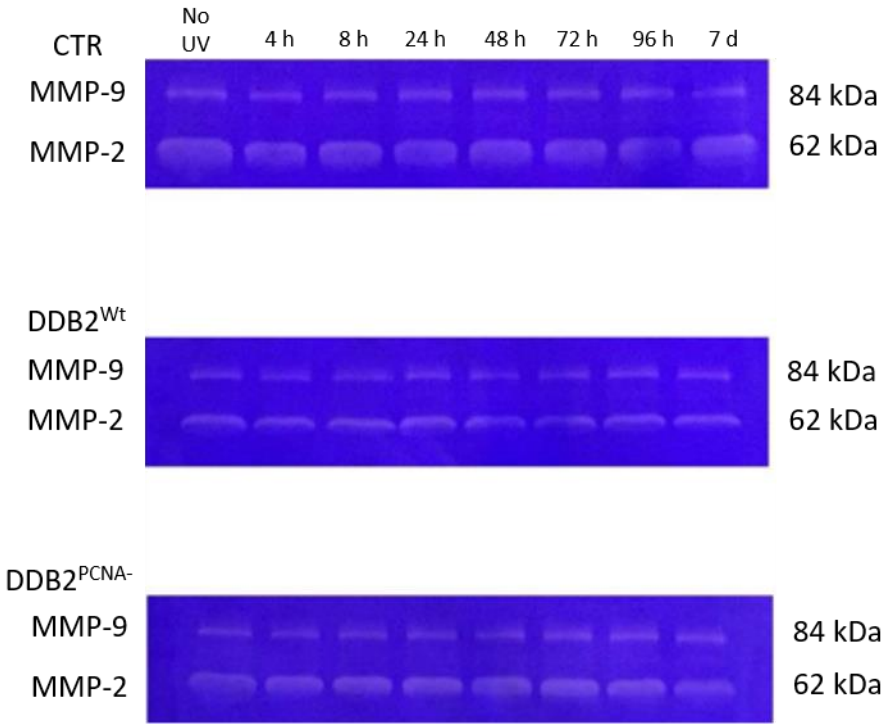

Figure 31 Evaluation of MMPs-2 and 9 activity in HEK293 CTR, $DDB2^{Wt}$ and $DDB2^{PCNA-}$ stable clones by gelatin zymography technique after UV-C exposure. Cells culture *media* were harvested at different times (No UV, 4 h, 8 h, 24 h, 48 h, 72 h, 96 h and 7 d). Supernatants were mixed with sample buffer 2x (ratio 1:1). After protein electrophoresis, gel was incubated with Renaturing, Developing, Staining and Destaining buffers to visualized gelatin digestion (white stripes) due to MMPs-2 (62 kDa) and 9 (84 kDa) activation.

The results of MMPs-2 and 9 digestion and their statistical analysis are reported in **Figure 32**.

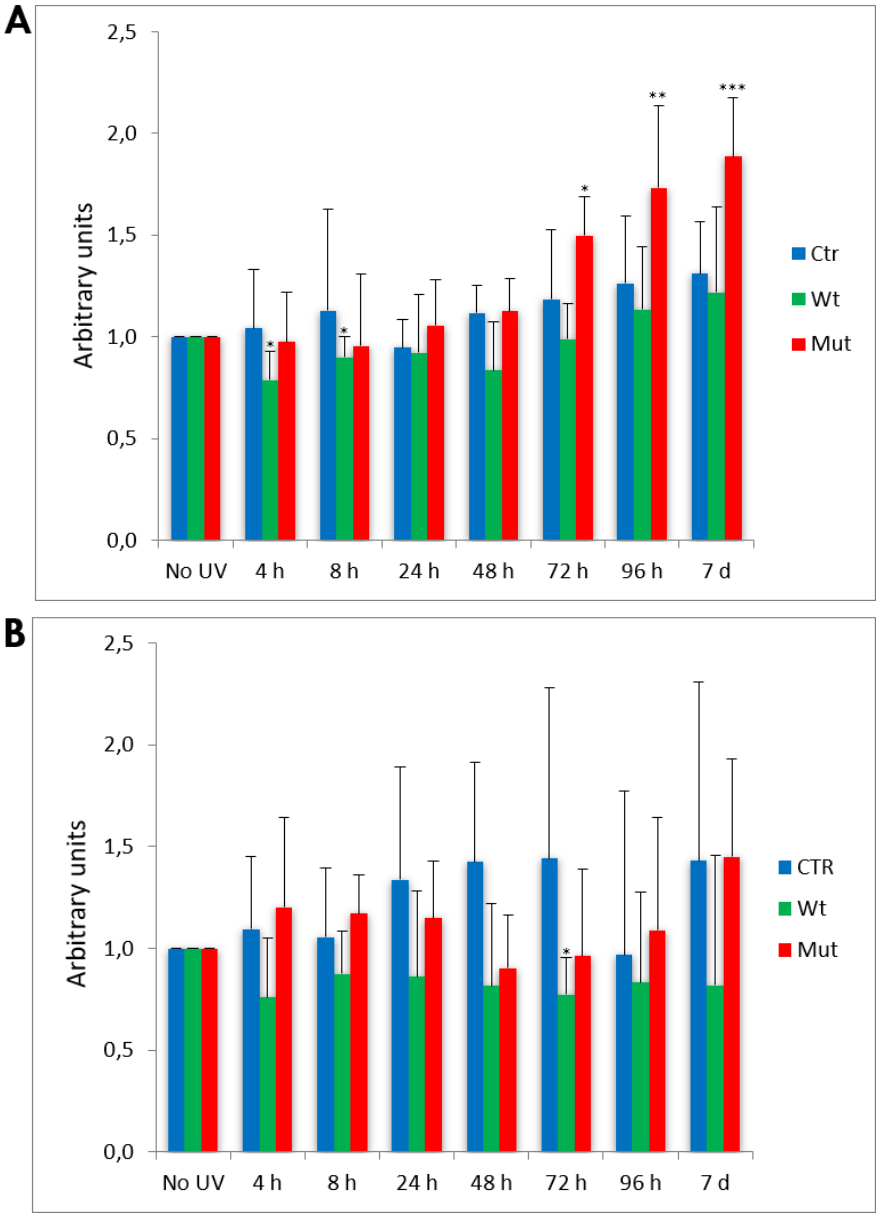

Figure 32 Statistical analysis of MMPs-9 (**A**) and 2 (**B**) activity in HEK293 CTR (blue bar), DDB2^{Wt} (green bar) and DDB2^{PCNA-} (red bar) stable clones obtained by gelatin zymography experiments. N=3 independent experiments; data are mean ± S.D., UV irradiated cells *vs*. not irradiated cells * $p < 0.05$, ** $p < 0.01$, *** $p < 0.0001$

Until 48 h after UV-induced DNA damage, the MMPs activation was quite similar in all the three cell lines. In DDB2^{PCNA-} cells, the activity of MMP-9 was particularly increased starting from 72 h after UV-damage, and this trend was maintained until 7 d. At this time, MMP-9 activity was almost 2-fold higher compared to its negative control (Figure 32 A). Statistical analysis confirmed that the increase is time dependent and was also significant.
Instead, both MMPs in the wild-type clone did not show an important activation: the values obtained remained almost similar to its basal level. Only in the MMP-9 it was found a little increase in its digestion activity 96 h and 7 d after UV-induced DNA damage, but this was not significant.
In irradiated control cells, an increase in MMP-2 activity was found; however, in all recovery times not significant values were found (Figure 32 B).

4.9 Evaluation of migration capability in irradiated HEK293

Wound healing experiments have demonstrated that irradiated HEK293 DDB2^{Wt} and, even more the mutated stable clone, acquired both proliferation and migration advantages.
To dissect whether these cells could be able to migrate, upon UV damage, a Boyden chamber assay was performed.
For this reason, a 48-Well Micro Chemotaxis chamber was assembled with a polycarbonate membrane pretreated with collagen type I. HEK293 (CTR, DDB2^{Wt} and DDB2^{PCNA-}) were irradiated (10 J/m^2), counted and seeded in the top wells of the chamber. Not irradiated cells were also used as control. Different concentrations of FBS were employed as chemoattractant factor.

Figure 33 showed preliminary results obtained from Boyden chamber assay:

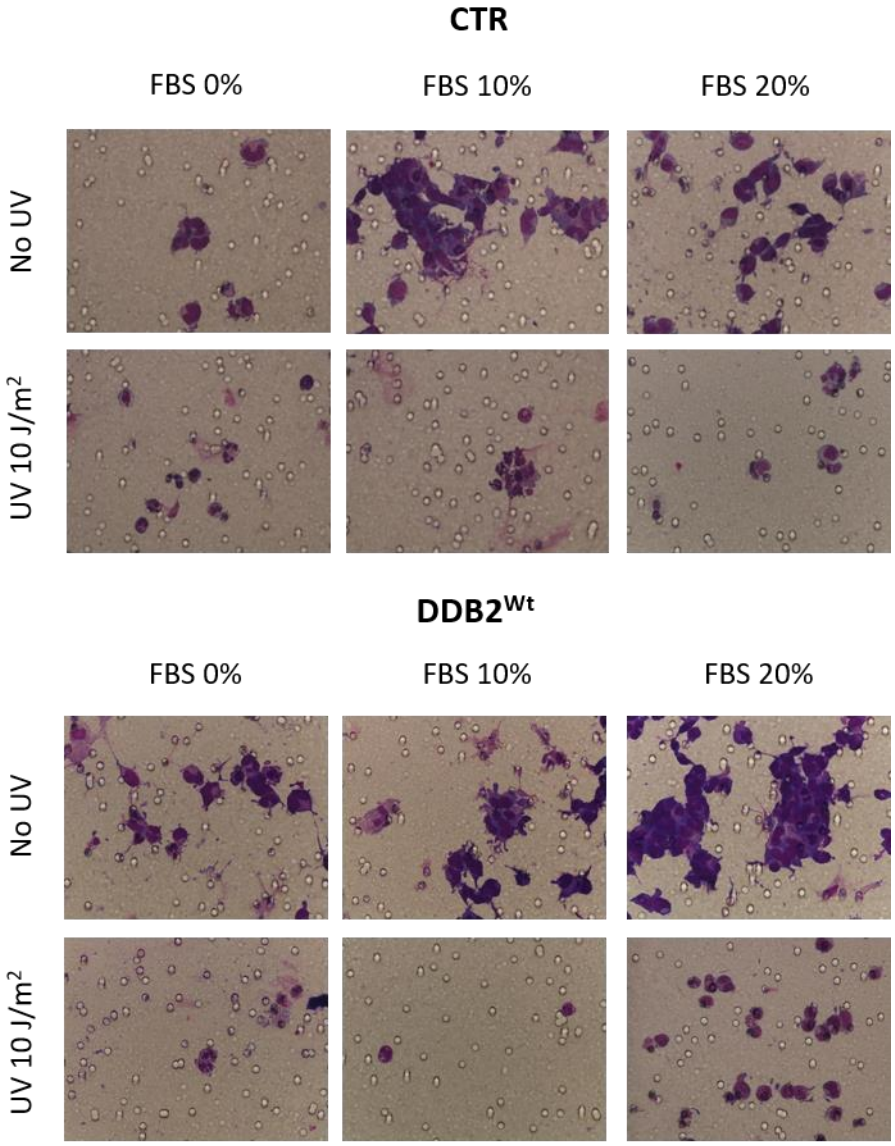
CTR
FBS 0%
FBS 10%
FBS 20%
No UV
UV 10 J/m2
DDB2Wt
FBS 0%
FBS 10%
FBS 20%
No UV
UV 10 J/m2

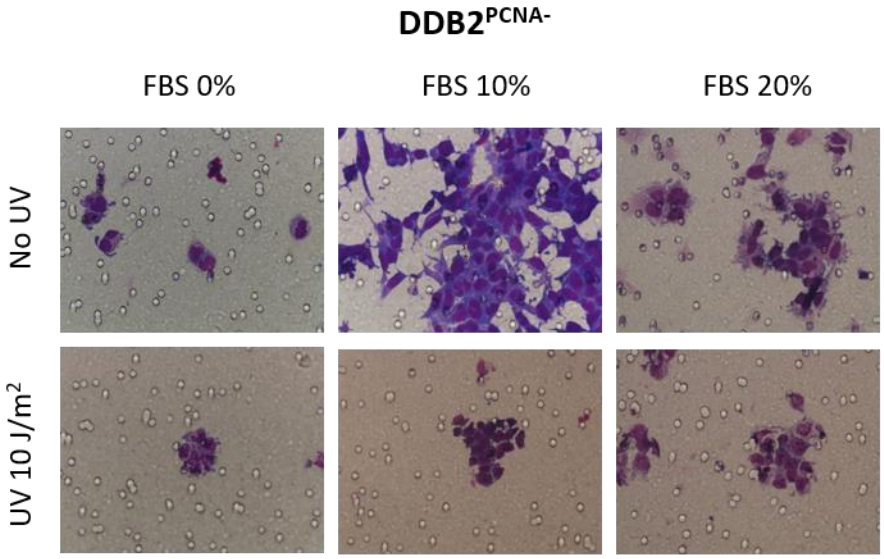

Figure 33 Boyden chamber assay in irradiated or not irradiated HEK293 CTR, $DDB2^{Wt}$ and $DDB2^{PCNA-}$ stably transfected clones with some FBS concentrations (0, 10 and 20%) as chemoattractant factors. 10^5 cells were seeded in each top wells of the chamber and, after 24 h of incubation, the polycarbonate membrane was fixed and stained. Representative images of cell migration assay (x40 magnification objective). N=2 independent experiments

All the three cell lines not irradiated cells were able to migrate, as demonstrated in each upper panels of **Figure 33**; these data confirm the ability of HEK293 cells to migrate under chemoattractant *stimulus*. In CTR and $DDB2^{Wt}$ cells, the migration pattern was correlated with the percentage of FBS: more migrated cells were observed when the FBS was more concentrated. Instead, in the mutated clone the better concentration of FBS for cells was 10%.

After UV irradiation, many cells in the three samples showed evident signs of suffering or death, such as apoptotic bodies or cytoplasmic membrane fragmentation. However, cells expressing mutated protein showed the best migration ability. Indeed, these cells were more able to migrate, as demonstrated by an increased number of cells migrated. Interestingly, these cells showed a different behaviour compared to control cell line or $DDB2^{Wt}$ clone; in fact, their migration pattern was mainly characterized by a cluster

of cells instead of single cell, as demonstrated in the lower panel of DDB2^{PCNA-} samples in **Figure 33**. Furthermore, it seems that the number of migrated cells was directly proportional to the concentration of chemoattractant factor.

Cell expressing DDB2^{Wt} protein showed a migration capability although lower than mutated one; moreover, only singular cells were found in the polycarbonate membrane compared to mutated clone. As it was observed in not irradiated cells, also irradiated cells showed a correlation between the number of migrated cells and the concentration of FBS.

Conversely, irradiated control cells were not able to migrate; furthermore, the few migrated cells were almost all dead.

IV. A novel possible role of DDB2

4.10 A novel putative role of DDB2

To study the possile involvement of DDB2 protein in TC-NER, the other subpathway of NER process, the host cell reactivation (HCR) assay and co-localization analysis were performed.

4.10.1 Evaluation of DNA Damage Response to UV lesions

HCR assay was employed to evaluate the DNA Damage Response (DDR) to UV irradiation in HEK293 stable clones (DDB2^{Wt} and DDB2^{PCNA-}).

Cells were co-transfected with pmRFP-N2 plasmid and not irradiated pEGFP-N1 or UV-pEGFP-N1 constructs; then, 16 or 48 h later, samples were harvested for "*in vivo*" cytofluorimetric analysis.

In particular, it was evaluated and compared the capability of HEK293 cells to express the GFP starting by UV-GFP plasmid transfection. The production of RFP protein was used as a positive control, to ensure that the transfection protocol was properly working.

In **Figure 34** representative flow cytometry graphs of GFP, derived from irradiated pEGFP-N1 construct, and RFP fluorescence are shown (Bassi E *et al*. 2019).
In the upper panel (**Figure 34 A**), the cytofluorimetric analysis was carried out 16 h after co-transfection: no significant differences were found in GFP and RPF production comparing both HEK293 $DDB2^{Wt}$ and $DDB2^{PCNA-}$ stable clones, suggesting that the inability to interact with PCNA, in DDB2 mutated protein, does not influence the protein expression at early stage of the repair process.

In $DDB2^{Wt}$ stable clone, 48 h after transfection, the ability to repair UV-DNA lesions was reactivated; **Figure 34 B** demonstrates that the encoding of the reporter gene was switched on in these cells. On the contrary, GFP expression in the mutated clone was remarkable reduced, indicating that its DNA damage response was impaired (**Figure 34 B**).

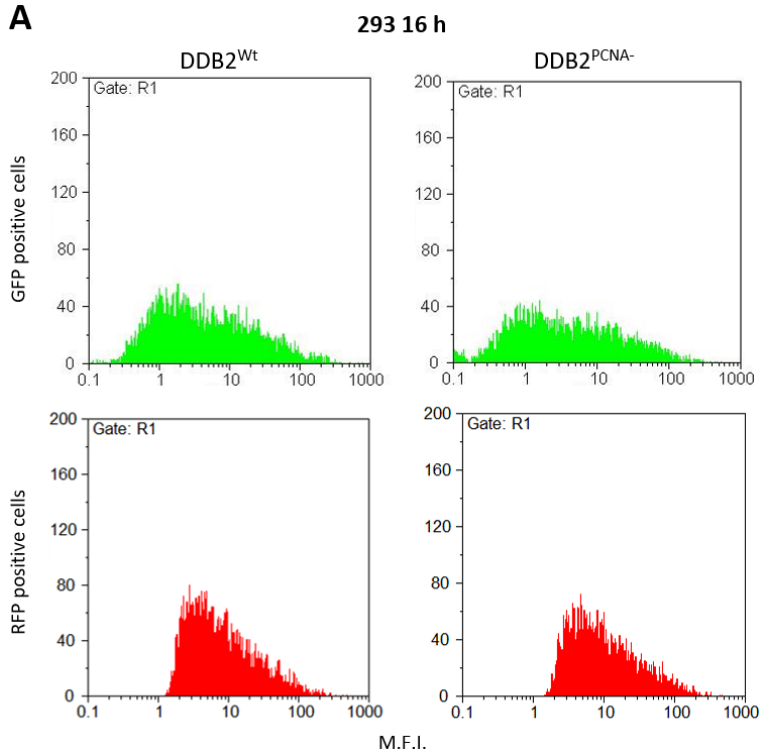
A
293 16 h
DDB2Wt
DDB2PCNA-
GFP positive cells
RFP positive cells
Gate: R1
M.F.I.

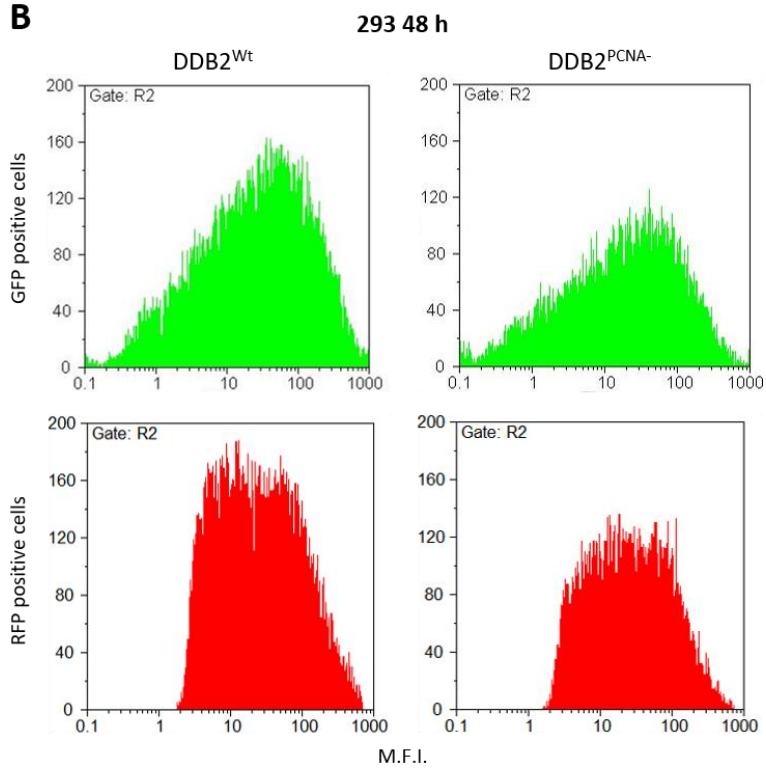

Figure 34 Cytofluorimetric "*in vivo*" monoparametric analysis, representative images: mean fluorescence intensity (MFI) of GFP (green) derived from UV-pEGFP-N1 construct and RFP (red), produced in HEK293 $DDB2^{Wt}$ and $DDB2^{PCNA-}$ stable clones, respectively. The analysis was performed after 16 (A) or 48 h (B) from co-transfection. N=3 independent experiments

Figure 35 shows the ratio between GFP expression from the irradiated and not irradiated pEGFP-N1 constructs after normalization with RFP and statistical analysis: in $DDB2^{PCNA-}$ clone the expression of the fusion protein was significantly reduced (36.1%) compared to the wild-type stable clone (46.1%), 48 h after co-transfection (Bassi E *et al*. 2019).

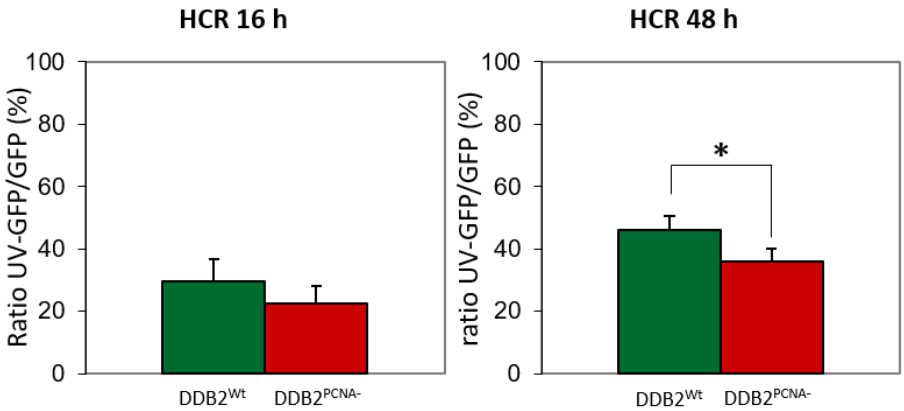

Figure 35 Ratio between UV-GFP (derived from repaired gene reporter) and GFP (encoded from not irradiated plasmid) produced in $DDB2^{Wt}$ (green bar) or $DDB2^{PCNA-}$ (burgundy bar) stable clones, after normalization with RFP production, expressed in percentage. Cells were harvested 16 or 48 h after co-transfection for the "*in vivo*" FACS analysis. N=3 independent experiments; HEK293 $DDB2^{Wt}$ *vs*. HEK293 $DDB2^{PCNA-}$ 16 and 48 h, respectively. Data are mean ± S.D., * $p < 0.05$

4.10.2 Study of co-localization between DDB2 and Polymerase II proteins

RNA Polymerase II stalling triggers the activation of repair machinery in TC-NER followed UV-DNA lesions. This protein is a damage sensor in transcribed DNA region.

Starting by this evidence, we wondered whether DDB2 could play a possible role in TC-NER, studying its potential cooperation with Polymerase II by immunofluorescence technique.

HeLa cells were transiently transfected with $DDB2^{Wt}$ or $DDB2^{PCNA-}$ constructs and locally UV-irradiated. After 30 or 60 min, cells were fixed and immunostained for immunofluorescence and confocal microscopies observation.

DDB2 wild-type protein was perfectly recruited ad damaged sites and

overlapped with RNA Polymerase II already 30 min after DNA damage response activation, as shown in the upper panel of **Figure 36** (Bassi E *et al*. 2019). The kinetic recruitment of both damage sensors, in wild-type stable clone, was properly well-timed: the fluorescence intensity of both proteins decreased 60 min after locally irradiation.

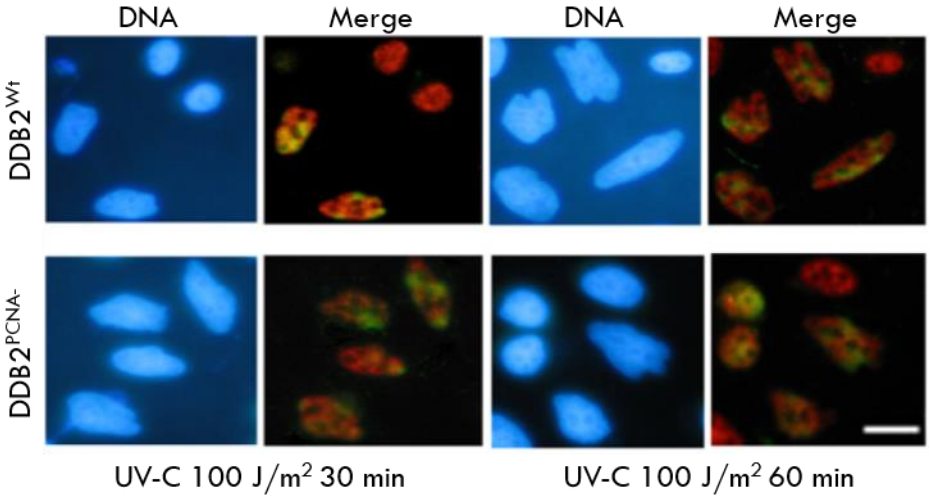

Figure 36 Co-localization between DDB2 (green fluorescence) and RNA Polymerase II (red fluorescence) analysed by immunofluorescence microscopy. Scale bar 20 µm

Whereas, DDB2 mutated clone showed an impairment localization of both proteins to DNA damaged sites 30 and 60 min recovery times (**Figure 36**, lower panel). Cells were locally irradiated, as demonstrated by the *foci* formation, although Polymerase II was widely diffused in HeLa nuclei (**Figure 36**, merge).

To study in depth and confirm the co-localization of the above proteins, a confocal analysis was performed (**Figure 37**) (Bassi E *et al*. 2019).
In **Figure 37 A** some representative images of both stable clones are shown.

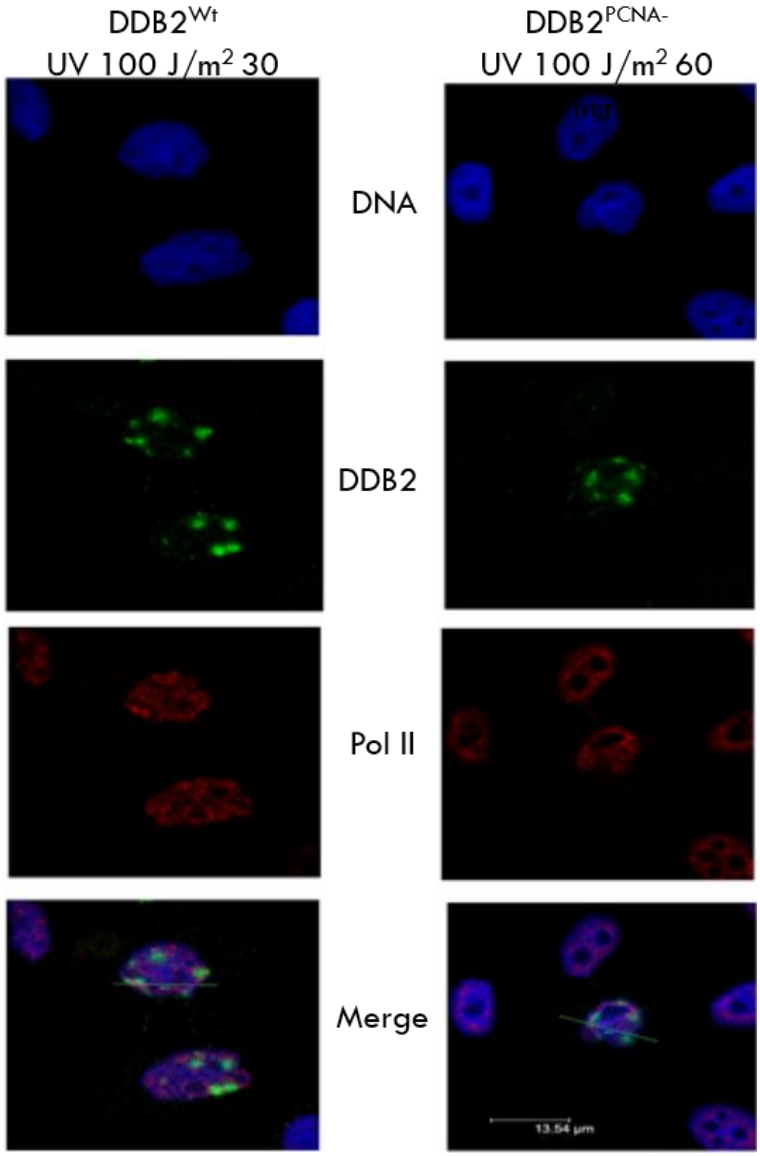
DDB2Wt
UV 100 J/m2 30
DDB2PCNA-
UV 100 J/m2 60
DNA
DDB2
Pol II
Merge
13.54 µm

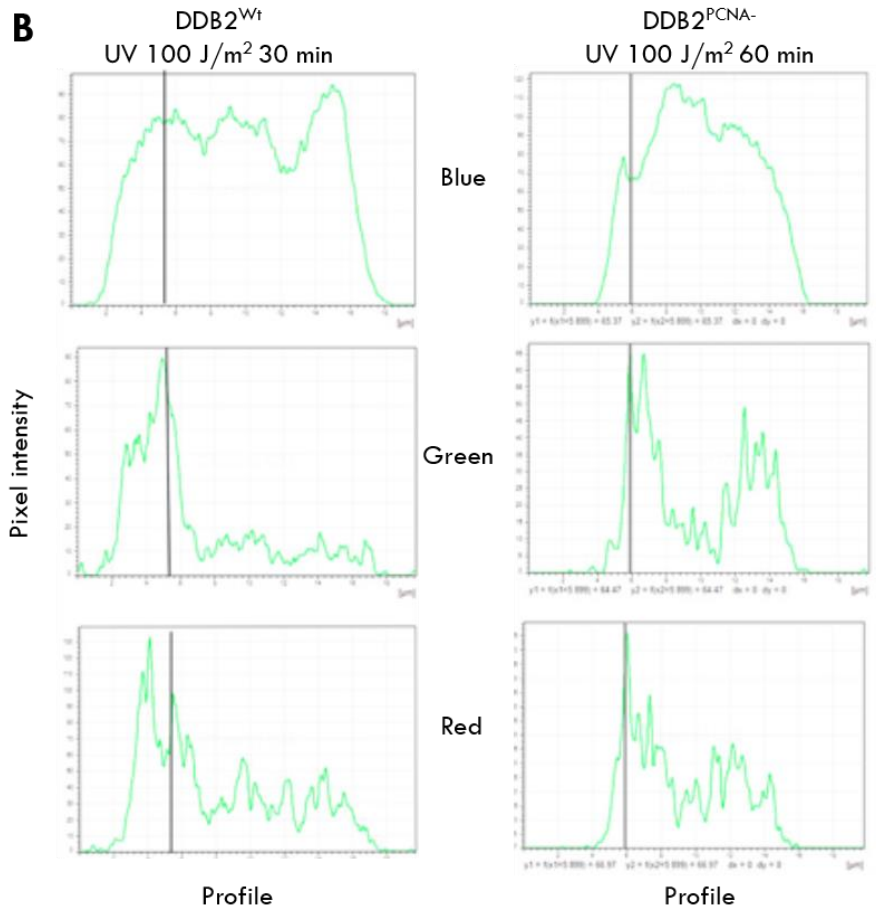

Figure 37 Co-localization analysis of DDB2 and Polymerase II by confocal microscopy, representative images. (**A**) Recruitment to DNA lesions of Polymerase II (red fluorescence) and $DDB2^{Wt}$ or $DDB2^{PCNA-}$ (green fluorescence) 30 or 60 min upon UV irradiation, respectively. (**B**) Pixel intensity representation by confocal analysis. N=3 independent experiments

In $DDB2^{Wt}$ clone the best co-localization was mainly found 30 min after UV-DNA damage with 52% of positive cells; instead, the mutated clone shown a delayed recruitment of both proteins compared to wild-type clone, because the better results were obtained only 60 min after DNA damage.

Moreover, analysing the pixel intensity of green (DDB2) and red (Polymerase II) fluorescence, it was not observed a perfect protein overlapping in the mutated clone even 1 h upon DNA damage (Figure 37 B).

5. Discussion

UV irradiation is one of the most damaging agents that activates a type of DNA damage response (DDR), the Nucleotide Excision Repair (NER). In particular, DDB2 protein is responsible to recognize and bind UV-photolesions - cyclobutane pyrimidine dimers (CPDs) or 6-4 photoproducts (6-4 PPs) - leading to the activation of Global Genome-NER (GG-NER) process, a subpathway of NER (Wittschieben BØ *et al*. 2005; Feltes BC and Bonatto D 2015; Sugasawa K 2016; Paul D *et al*. 2019).
DDB2 protein is characterized by the presence of a PCNA protein interacting-box (PIP-box) in its sequence, which allows the direct interaction with PCNA (Cazzalini O *et al*. 2014). It has been demonstrated that this functional interaction is essential for DDB2 proteasome-mediated degradation, after UV damage, allowing the recruitment of the following NER factors (Cazzalini O *et al*. 2014).
In our laboratory, it was previously demonstrated that a mutated DDB2 ($DDB2^{PCNA-}$) protein, unable to bind PCNA, showed a delayed kinetic recruitment to UV DNA lesions compared to a functional DDB2 ($DDB2^{Wt}$) protein (Perucca P *et al*. 2018); these data suggest that, in cells expressing $DDB2^{PCNA-}$, the NER process is ineffective.

In the first part of my PhD project, I attempted to investigate the role and consequences of DDB2-PCNA association in several steps of GG-NER pathway, after UV-C damage. Collected data demonstrated that the inability of DDB2 to interact with PCNA affected not only the early phase of NER, but also determining delay in the repair process evident until the final step. The delayed recruitment of $DDB2^{PCNA-}$ protein to DNA damaged sites at the early phase of NER (Perucca P *et al*. 2018), was confirmed and explained by the inefficient DNA binding affinity of mutated DDB2 protein. In fact, by two different electrophoretic mobility shift (EMSA) assays, both DDB2 mutated recombinant protein than HEK293 $DDB2^{PCNA-}$ cell extract, have highlighted a

lower capability to bind UV lesions compared to wild-type samples. In particular, the inefficient binding affinity observed in mutated cell extract compared to HEK293 DDB2^{Wt} after 30 min from UV damage, was still significantly maintained 1 h later.

As reported in literature (Sugasawa K *et al*. 1998; Araki M *et al*. 2001; Sugasawa K *et al*. 2001; Sugasawa K *et al*. 2002), XPC protein is essential during the recognition of the lesion process in GG-NER and its recruitment is facilitate by a proper and well-timed DDB2 degradation (Sugasawa K *et al*. 2005; Wang QE *et al*. 2005; El-Mahdy MA *et al*. 2006); accordingly to this evidence, co-localization studies between DDB2 and XPC proteins to UV photolesions, have demonstrated that the presence of a DDB2 mutated protein caused a delay in the initiation step of NER mechanism compared to cells expressing DDB2^{Wt} protein (Perucca P *et al*. 2018).

Remarkably, to understand whether DDB2 mutated protein could also altered a late NER phase, co-localization analysis between DDB2 and XPG proteins and immunoprecipitation experiments were performed (Bassi E *et al*. 2019). My results revealed that both DDB2 proteins were able to interact with XPG; in particular, in cells expressing DDB2^{Wt} protein a correct and well-timed co-localization between two proteins was found 10 min after UV-C exposure. On the contrary, DDB2^{PCNA-} protein and the endonuclease were not perfectly overlapping even 30 min after UV irradiation. These results suggest that the loss of DDB2-PCNA interaction affects also a late phase in NER. Furthermore, it has been demonstrated by several papers (Matsuda N *et al*. 2005; Sugasawa K *et al*. 2005; El-Mahdy MA *et al*. 2006; Wang QE *et al*. 2007; Han C *et al*. 2015), that a proper recruitment of late NER factors depends by the degradation of DDB2 protein. According to this evidence, the DDB2^{PCNA-} protein accumulation observed in cells (Cazzalini O *et al*. 2014), could justify the delayed recruitment of XPG. Moreover, these data are in agreement with our recent paper (Perucca P *et al*. 2018), in which it was demonstrated that DDB2^{PCNA-} positive cells were able to remove fewer CPDs molecules compared to cells expressing DDB2^{Wt} protein.

Taking together, my findings have demonstrated that the loss of DDB2-PCNA interaction affects the mainly steps of GG-NER: starting by the initial recognition step, passing through the incision of the DNA damaged fragment and, finally, arriving at the removal of UV photolesions.

Although DDB2 contribution is still debated, it is well known that the protein is also implicated in cancer biology; in particular, several papers have correlated DDB2 expression levels to cancer initiation and progression (Yoon T *et al*. 2005; Ennen M *et al*. 2013; Roy N *et al*. 2013).

Starting from this evidence, in the second and third section of my PhD project, we speculated whether DDB2-PCNA association can influence cell behaviour after UV-damage induction.

By a clonogenic assay, it was demonstrated that HEK293 cells stably expressing $DDB2^{PCNA-}$ protein, were more able to form colonies with larger dimension, compared to $DDB2^{Wt}$ clone or control cell line, highlighting an unexpected UV resistance (Perucca P *et al*. 2018). Moreover, mutated cells were more prone to proliferate, as evidenced by the high and significant percentage of positive pospho-histone 3 cells, a marker of mitosis, that was found. The data is in agreement with a paper published by our research group (Perucca P *et al*. 2015), in which it was demonstrated that the exogenous expression of a DDB2 mutated protein induced an increase of positive cells in the S-phase with a reduction of cell cycle length; in addition, we also recently reported that the uncontrolled cell growth of mutated clone is related to a failure in the activation of a correct and well-timed cell cycle checkpoint signaling (Perucca P *et al*. 2018).

Intriguingly, the analysis of cell morphological features has underlined a significant presence of atypical mitoses in the mutated clone and, as reported in literature, this characteristic is a typical hallmark frequently observed in cancer cells (Batistatou A 2004).

The morphological analysis of cells as also highlighted an increase cell viability of $DDB2^{Wt}$, and, even more, $DDB2^{PCNA-}$ stable clones after UV damage, characterized by a lower number of dead cells compared to control cell line.

Finally, atypical mitoses were more evident and numerous in the presence of DDB2 mutated protein, highlighting an atypical feature.

In conclusion, these findings have demonstrated that the mutated clone could be more prone to proliferate developing numerous colonies with a tumour-like phenotype.

Cells expressing DDB2 mutated protein are more prone to proliferate but less able to remove UV photolesions. Starting from this evidence, we speculated

whether proliferative advantage of these cells could be related not only to an increase UV resistance, but also to a possible activation of a DNA damage tolerance process, the Translesion DNA Synthesis (TLS).

For this purpose, I investigated the interaction between DDB2 and Polymerase η, which is involved in TLS process, applying different approaches.

It was demonstrated, by confocal analysis, that $DDB2^{PCNA-}$ and Polymerase η were in proximity to each other, in fact they perfectly overlapped; these data were in agreement with immunoprecipitation experiments in which an interaction between the above proteins was significantly evident compared to wild-type stable clone and positive control samples. Remarkably, Proximity Ligation Assay (PLA) confirmed a strong and direct interaction between Polymerase η and DDB2 mutated protein. In addition, this association was found in numerous $DDB2^{PCNA-}$ positive cells containing until 40 of positive events per cell.

Interestingly, cells expressing exogenous DDB2 protein, both wild-type and, even more, the mutated form, showed a marked cell proliferation and motility abilities in wound healing assay. In agreement with previously obtained data, in the mutated clone were also evident a dense multilayer of growing cells, thus confirming its increase resistance to UV irradiation (Perucca P *et al*. 2018). Moreover, in this clone the expression levels of E-cadherin and Vimentin proteins, which are considered the main epithelial or mesenchymal markers respectively, were modified, suggesting a possible influence of DDB2-PCNA interaction in the activation of epithelial to mesenchymal transition (EMT) process. Remarkable, it has been reported that epithelial tumours characterized by an aggressive phenotype are related to a loss of adhesion molecules expression (Strumane K *et al*. 2004), this evidence could explain the uncontrolled growth and motility of our DDB2 mutated stable clone. These results were strongly correlated to the activation of metalloproteinases (MMPs) 2 and, even more MMP-9 that in the mutated clone was particularly evident. Both MMPs are essential in EMT process (Chambers AF and Matrisian LM 1997; Duffy MJ *et al*. 2008), specifically during the invasion step of cancer cells (Gialeli C *et al*. 2011), since these proteases are responsible to digest extracellular matrix (ECM).

Furthermore, the migration ability of DDB2^{PCNA-} positive cells was confirmed by Boyden chamber assay. In fact, only the irradiated cells expressing DDB2 mutated protein were able to migrate; unexpectedly, the migration pattern of these cells was characterized by a cluster of cells instead of single cell, suggesting a possible correlation to an aggressive cell behaviour (Hegerfeldt Y *et al*., 2002; Langbein L *et al*. 2003; Friedl P 2004) and to an increased digestion activity of MMPs (Sabeh F *et al*. 2004; Wolf K *et al*. 2007; Wolf K and Friedl P 2008).
Finally, our preliminary results (data not shown) have demonstrated that cells expressing DDB2^{PCNA-} protein are characterized not only by an aggressive tumour-like phenotype, but they are also more prone to interact with some ECM components after UV damage induction.

Then, in the last section of my thesis, I wondered whether the inability of DDB2 protein to directly interact with PCNA could also affects the cellular repair process of actively transcribed genes.
For this purpose, a host cell reactivation (HCR) assay was performed. This interesting technique is widely used in molecular biology to test the capabilities of intact cells - the host - to repair a damaged reporter gene. The method can be applied for several conditions; for instance, it was performed to investigate the homologous recombination ability of different human cancer cell lines (Slebos RJ and Taylor JA 2001); another study has demonstrated, by HCR assay, that fibroblasts derived from Cockayne syndrome patients differently respond to several damaging agents (Spivak G and Hanawalt PC 2006).
Specifically, in our experiments, we used, as reporter gene, the green fluorescent protein (GFP), either UV-damaged or undamaged, the red fluorescent protein (RFP) as a positive control of transfection and, the repair ability of both HEK293 stable clones (DDB2^{Wt} and DDB2^{PCNA-}) was "*in vivo*" measured by cytofluorimeter, following the experimental design of Burger and colleagues (Burger K *et al*. 2010). Our results have demonstrated that wild-type stable clone was able to repair UV damaged GFP, suggesting that in these cells the repair machinery was properly working. Conversely, 48 h after co-transfection, significant reduction in UV-GFP expression was found in the mutated clone, suggesting that the loss of DDB2-PCNA interaction modifies

the DDR. It seems that the presence of a mutated DDB2 protein delays the repair ability in an "*in vivo*" cellular system, as shown by the defective expression of reporter gene. These findings are consistent with our previous results obtained by "*in vitro*" approaches (Perucca P *et al*. 2018). In our experimental model it was possible to focus on the influence of a mutated NER factor ($DDB2^{PCNA-}$) in the intact repair machinery of cells, providing evidence that the HCR assay could be a useful tool to dissect and study several phases of NER process or other repair pathways.

Furthermore, we also verify the recruitment and the possible co-localization between DDB2 and RNA Polymerase II, which stalled at UV-damaged transcribed DNA fragment, triggering the repair machinery activation.

As expected, a well-timed and perfect co-localization of above proteins was found in wild-type stable clone, suggesting a possible cooperation between the two damage protein sensors. Moreover, the fluorescence signals of both proteins were decreased 60 min after UV irradiation, to allow a proper and well-timed recruitment of other proteins involved in the next NER phases. Instead, the co-presence of both proteins was not observed in positive $DDB2^{PCNA-}$ cells even 1 h after UV irradiation; in addition, as demonstrated by confocal analysis, the mutated protein was not perfectly overlapped with Polymerase II, leaving to suppose that in the mutated clone the repair process is later activated.

All these findings have demonstrated that a functional DDB2 protein cooperates with Polymerase II, implying a possible cooperation between the two subpathways of NER - GG-NER and TC-NER - in the early phase; besides a possible cooperation between different DDR pathways was reported by several studies (Simonelli V *et al*. 2016; Limpose K *et al*. 2017).

6. Conclusions and perspectives

In this first part of my PhD thesis, it was demonstrated that the loss of DDB2-PCNA interaction, negatively influences not only the early steps of NER pathway, but also the late phases of the repair process.

In the second and third section, I focused the attention mainly on the phenotype and behaviour of irradiated HEK293 cells.
In particular, I demonstrated, by wound healing experiments and Boyden chamber assay, that the loss of DDB2-PCNA interaction confers to irradiated cells, proliferation and motility advantages with an increased resistance to UV irradiation. Moreover, in DDB2 mutated stable clone it was found a higher number of cells in mitosis with atypical features.
Furthermore, it seems that $DDB2^{PCNA-}$ is involved in the activation of EMT program, since positive $DDB2^{PCNA-}$ cells expressed lower levels of E-cadherin related to an increased activity of MMPs, the MMP-9 especially.
In addition, our recent experiments have demonstrated that the mutated DDB2 protein may be involved in the TLS process, since an interaction between Polymerase η and DDB2 mutated protein was found.

Moreover, the loss of DDB2-PCNA association appears to be implicated also in the repair process of actively transcribed gene. Indeed, when cells stably express the wild-type DDB2 protein, a correct repair process of damaged DNA and a well-timed co-localization with Polymerase II were found; on the contrary, in the presence of the mutated DDB2 protein the repair process of damaged reporter gene was affected, as demonstrated by HCR assay. In addition, the recruitment of mutated DDB2 protein to damaged sites was not perfectly co-localized with Polymerase II.

Altogether, my data suggest that the DDB2-PCNA interaction is crucial to perform a correct DNA damage response avoiding the genome instability,

involved in tumour onset and progression.

In the next future, to understand the marked cellular proliferation and motility in the presence of $DDB2^{PCNA-}$ protein, I will try to investigate what molecular signalling pathways are activated after UV damage induction.
Moreover, I would like to study in depth the possible interaction between DDB2 protein, both wild-type and mutated form, with some extracellular matrix component employing several approaches.
Finally, after demonstrating that DDB2 mutated protein directly interacts with Polymerase η, it will be interesting to evaluate the possible activation of this Polymerase.

References

Aboussekhra A, Biggerstaff M, Shivji MKK, Vilpo JA, Moncollin V, Podust VN, Protic M, Hubscher U, Egly J-M, Wood RD. Mammalian DNA nucleotide excision repair reconstituted with purified protein components. Cell. 1995; 80:859-868

Anindya R, Mari PO, Kristensen U, Kool H, Giglia-Mari G, Mullenders LH, Fousteri M, Vermeulen W, Egly JM, Svejstrup JQ. A ubiquitin-binding domain in Cockayne syndrome B required for transcription-coupled nucleotide excision repair. Mol Cell. 2010;38:637-648

Araki M, Masutani C, Takemura M, Uchida A, Sugasawa K, Kondoh J, Ohkuma Y, Hanaoka F. Centrosome protein centrin 2/caltractin 1 is part of the xeroderma pigmentosum group C complex that initiates global genome nucleotide excision repair. J Biol Chem. 2001;276:18665-18672

Araujo SJ, Nigg EA, Wood RD. Strong functional interaction of TFIIH with XPC and XPG in human nucleotide excision repair, without a preassembled repairosome. Mol Cell Biol. 2001;21:2281-2291

Araujo SJ, Tirode F, Coin F, Pospiech H, Syvaoja JE, Stucki M, Hubscher U, Egly JM, Wood RD. Nucleotide excision repair of DNA with recombinant human proteins: definition of the minimal set of factors, active forms of TFIIH, and modulation by CAK. Genes Dev. 2000;14:349-359

Ashour ME, Atteya R, El-Khamisy SF. Topoisomerase-mediated chromosomal break repair: an emerging player in many games. Nat Rev Cancer. 2015;15:137-151

Auclair Y, Rouget R, Drobetsky EA. ATR kinase as master regulator of nucleotide excision repair during S phase of the cell cycle. Cell Cycle. 2009;8:1865-1871

Barakat BM, Wang QE, Han C, Milum K, Yin DT, Zhao Q, Wani G, Arafa el-SA, El-Mahdy MA, Wani AA. Overexpression of DDB2 enhances the sensitivity of human ovarian cancer cells to cisplatin by augmenting cellular apoptosis. Int J Cancer. 2010;127:977-988

Bassi E, Perucca P, Guardamagna I, Prosperi E, Stivala LA, Cazzalini O. Exploring new potential role of DDB2 by Host Cell Reactivation assay in human tumorigenic cells. BMC Cancer. 2019;19:1013

Batistatou A. Mitoses and cancer. Med Hypotheses. 2004;63:281-282

Beerens N, Hoeijmakers JH, Kanaar R, Vermeulen W, Wyman C. The CSB protein actively wraps DNA. J Biol Chem. 2005;280:4722-4729

Bergmann E, Egly JM. Trichothiodystrophy, a transcription syndrome. Trends Genet. 2001;17:279-286

Besaratinia A, Yoon JI, Schroeder C, Bradforth SE, Cockburn M, Pfeifer GP. Wavelenght dependence of ultraviolet radiation-induced DNA damage as determined by laser irradiation suggests that cyclobutane pyrimidine dimers are the principal DNA lesions produced by terrestrial sunlight. FASEB J. 2011;25:3079-3091

Bi X, Barkley LR, Slater DM, Tateishi S, Yamaizumi M, Ohmori H, Vaziri C. Rad18 regulates DNA polymerase κ and is required for recovery from S-phase checkpoint-mediated arrest. Mol Cell Biol. 2006;26:3527-3540

Bienko M, Green CM, Crosetto N, Rudolf F, Zapart G, Coull B, Kannouche P, Wider G, Peter M, Lehmann AR, Hofmann K, Dikic I. Ubiquitin-binding domains in Y-family polymerases regulate translesion synthesis. Science. 2005;310:1821-1824

Bienko M, Green CM, Sabbioneda S, Crosetto N, Matic I, Hibbert RG, Begovic T, Niimi A, Mann M, Lehmann AR, Dikic I. Regulation of translesion synthesis DNA polymerase η by monoubiquitination. Mol Cell. 2010;37:396-407

Biertümpfel C, Zhao Y, Kondo Y, Ramón-Maiques S, Gregory M, Lee JY, Masutani C, Lehmann AR, Hanaoka F, Yang W. Structure and mechanism of human DNA polymerase η. Nature. 2010;465:1044-1048

Botta E, Nardo T, Broughton BC, Marinoni S, Lehmann AR, Stefanini M. Analysis of mutations in the XPD gene in Italian patients with trichothiodystrophy: site of mutation correlates with repair deficiency, but gene dosage appears to determine clinical severity. Am J Hum Genet. 1998;63:1036-1048

Bresson A, Fuchs RP. Lesion bypass in yeast cells: pol eta participates in a multi-DNA polymerase process. EMBO J. 2002;21:3881-3887

Brueckner F, Hennecke U, Carell T, Cramer P. CPD damage recognition by

transcribing RNA polymerase II. Science. 2007;315:859-862

Bukowska B, Karwowski T. Actual state of knowledge in the field of diseases related with defective nucleotide excision repair. Life Sci. 2018;195:6-18

Burger K, Matt K, Keiser N, Gebhard D, Bergemann J. A modified fluorimetric host cell reactivation assay to determine the repair capacity of primary keratinocytes, melanocytes and fibroblasts. BMC Biotechnol. 2010;10:46

Cadet J, Douki T. Formation of UV-induced DNA damage contributing to skin cancer development. Photochem Photobiol. 2018;17:1816-1841

Cazzalini O, Perucca P, Mocchi R, Sommatis S, Prosperi E, Stivala LA. DDB2 association with PCNA is required for its degradation after UV-induced DNA damage. Cell Cycle. 2014;13:240-248

Chambers AF, Matrisian LM. Changing views of the role of matrix metalloproteinases in metastasis. J Natl Cancer Inst. 1997;89:1260-1270

Chao C, Hergenhahn M, Kaeser MD, Wu Z, Saito S, Iggo R, Hollstein M, Appella E, Xu Y. Cell type- and promoter-specific roles of Ser18 phosphorylation in regulating p53 responses. J Biol Chem. 2003;278:41028-41033

Chatterjee N, Walker GC. Mechanisms of DNA damage, repair and mutagenesis. Environ Mol Mutagen. 2017;58:235-263

Cheung AC, Cramer P. Structural basis of RNA polymerase II backtracking, arrest and reactivation. Nature. 2011;471:249-253

Citterio E, Van Den Boom V, Schnitzler G, Kanaar R, Bonte E, Kingston RE, Hoeijmakers JH, Vermeulen W. ATP-dependent chromatin remodeling by the Cockayne syndrome B DNA repair transcription-coupling factor. Mol Cell Biol. 2000;20:7643-7653

Cleaver JE. Defective repair replication of DNA in Xeroderma pigmentosum. Nature. 1968;218:652-656

Crovato F, Borrone C, Rebora A. Trichothiodystrophy-BIDS, IBIDS and PIBIDS? Br J Dermatol. 1983;108:247

Cui T, Srivastava AK, Han C, Wu D, Wani N, Liu L, Gao Z, Qu M, Zou N, Zhang X, Yi P, Yu J, Bell EH, Yang SM, Maloney DJ *et al*. DDB2 represses ovarian cancer cell dedifferentiation by suppressing ALDH1A1. Cell Death Dis. 2018;9:561

Datta A, Bagchi S, Nag A, Shiyanov P, Adami GR, Yoon T, Raychaudhuri P. The p48 subunit of the damaged-DNA binding protein DDB associates with the CBP/p300 family of histone acetyltransferase. Mutat Res. 2001;486:89-97

de Laat WL, Appeldoorn E, Sugasawa K, Weterings E, Jaspers NG, Hoeijmakers JH. DNA-binding polarity of human replication protein A positions nucleases in nucleotide excision repair. Genes Dev. 1998;12:2598-2609

Dean M, Fojo T, Bates S. Tumour stem cells and drug resistance. Nat Rev Cancer. 2005;5:275-284

Dehez F, Gattuso H, Bignon E, Morell C, Dumont E, Monari A. Conformational polymorphism or structural invariance in DNA photoinduced lesions: implications for repair rates. Nucleic Acids Res. 2017;45:3654-3662

Donahue BA, Yin S, Taylor JS, Reines D, Hanawalt PC. Transcript cleavage by RNA polymerase II arrested by a cyclobutane pyrimidine dimer in theDNAtemplate. Proc Natl Acad Sci U S A. 1994;91:8502-8506

Drapkin R, Reardon JT, Ansari A, Huang JC, Zawel L, Ahn K, Sancar A, Reinberg D. Dual role of TFIIH in DNA excision repair and in transcription by RNA polymerase II. Nature. 1994;368:769-772

Dualan R, Brody T, Keeney S, Nichols A, Admon A, Linn S. Chromosomal localization and cDNA cloning of the genes (*DDB1* and *DDB2*) for the p127 and p48 subunits of a human damage-specific DNA-binding protein. Genomics. 1995;29:62-69

Duffy MJ, McGowan PM, Gallagher WM. Cancer invasion and metastasis: changing views. J Pathol. 2008;214:283-293

El-Mahdy MA, Zhu Q, Wang QE, Wani G, Praetorius-Ibba M, Wani AA. Cullin 4A-mediated proteolysis of DDB2 protein at DNA damage sites regulates in vivo lesion recognition by XPC. J Biol Chem. 2006;281:13404-13411

Ennen M, Klotz R, Touche N, Pinel S, Barbieux C, Besancenot V, Brunner E, Thiebaut D, Jung AC, Ledrappier S, Domenjoud L, Abecassis J, Plénat F, Grandemange S, Becuwe P. DDB2: a novel regulator of NF-κB and breast tumor invasion. Cancer Res. 2013;73:5040-5052

Evans E, Fellows J, Coffer A, Wood RD. Open complex formation around a lesion during nucleotide excision repair provides a structure for cleavage by human XPG protein. EMBO J. 1997;16:625-638

Faghri S, Tamura D, Kraemer TH, DiGiovanna JJ. Trichothiodystrophy: a systematic review of 112 published cases characterises a wide spectrum of clinical manifestations. J Med Genet. 2008;45:609-621

Fei J, Chen J. KIAA1530 protein is recruited by Cockayne syndrome complementation group protein A (CSA) to participate in transcription-coupled repair (TCR). J Biol Chem. 2012;287:35118-35126

Feltes BC, Bonatto D. Overview of xeroderma pigmentosum proteins architecture, mutations and post-translational modifications. Mutat Res Rev Mutat Res. 2015;763:306-320

Fischer ES, Scrima A, Böhm K, Matsumoto S, Lingaraju GM, Faty M, Yasuda T, Cavadini S, Wakasugi M, Hanaoka F, Iwai S, Gut H, Sugasawa K, Thomä NH. The molecular basis of CRL4DDB2/CSA ubiquitin ligase architecture, targeting, and activation. Cell. 2011;147:1024-1039

Fitch ME, Nakajima S, Yasui A, Ford JM. In vivo recruitment of XPC to UV-induced cyclobutene pyrimidine dimers by the DDB2 gene product. J Biol Chem. 2003;278:46906-46910

Fois A, Balestri P, Calvieri S, Zampetti M, Giustini S, Stefanini M, Lagomarsini P. Trichothiodystrophy without photosensitivity. Eur J Pediatr. 1988;147:439-441

Fousteri M, Vermeulen W, van Zeeland AA, Mullenders LH. Cockayne syndrome A and B proteins differentially regulate recruitment of chromatin remodeling and repair factors to stalled RNA polymerase II in vivo. Mol Cell. 2006;23:471-482

Friedberg EC, Walker GC, Siede W, Wood RD, Schultz RA, Ellenberger T. DNA Repair and Mutagenesis. ASM Press, Washington, D.C. 2006

Friedl P. Prespecification and plasticity: shifting mechanisms of cell migration. Curr Opin Cell Biol. 2004;16:14-23

Friedmann-Morvinski D, Verma IM. Dedifferentiation and reprogramming: origins of cancer stem cells. EMBO Rep. 2014;15:244-253

Ganesan A, Hanawalt P. Photobiological origins of the field of genomic maintenance. Photochem Photobiol. 2016;92:52-60

Gialeli C, Theocharis AD, Karamanos NK. Roles of matrix metalloproteinases in cancer progression and their pharmacological targeting. FEBS J. 2011;278:16-27

Giglia G, Dumaz N, Drougard C, Avril MF, Daya-Grosjean L, Sarasin A. p53

mutations in skin and internal tumors of xeroderma pigmentosum patients belonging to the complementation group C. Cancer Res. 1998;58:4402-4409

Gillet LC, Schärer OD. Molecular mechanism of mammalian global genome nucleotide excision repair. Chem Rev. 2006;106:253-276

Goodman MF, Woodgate R. Translesion DNA polymerases. Cold Spring Harb Perspect Biol. 2013;5:a010363

Groisman R, Kuraoka I, Chevallier O, Gaye N, Magnaldo T, Tanaka K, Kisselev AF, Harel-Bellan A, Nakatani Y. CSA-dependent degradation of CSB by the ubiquitin-proteasome pathway establishes a link between complementation factors of the Cockayne syndrome. Genes Dev. 2006;20:1429-1434

Groisman R, Polanowska J, Kuraoka I, Sawada J, Saijo M, Drapkin R, Kisselev AF, Tanaka K, Nakatani Y. The ubiquitin ligase activity in the DDB2 and CSA complexes is differentially regulated by the COP9 signalosome in response to DNA damage. Cell. 2003;113:357-367

Guo C, Tang TS, Bienko M, Parker JL, Bielen AB, Sonoda E, Takeda S, Ulrich HD, Dikic I, Friedberg EC. Ubiquitin-binding motifs in REV1 protein are required for its role in the tolerance of DNA damage. Mol Cell Biol. 2006;26:8892-8900

Han C, Wani G, Zhao R, Qian J, Sharma N, He J, Zhu Q, Wang QE, Wani AA. Cdt2-mediated XPG degradation promotes gap-filling DNA synthesis in nucleotide excision repair. Cell Cycle. 2015;14:1103-1115

Han C, Zhao R, Liu X, Srivastava A, Gong L, Mao H, Qu M, Zhao W, Yu J, Wang QE. DDB2 suppresses tumorigenicity by limiting the cancer stem cell population in ovarian cancer. Mol Cancer Res. 2014;12:784-794

Hayashi M, Araki S, Kohyama J, Shioda K, Fukatsu R. Oxidative nucleotide damage and superoxide dismutase expression in the brains of xeroderma pigmentosum group A and Cockayne syndrome. Brain Dev. 2005;27:34-38

Hayes S, Shiyanov P, Chen X, Raychaudhuri P. DDB, a putative DNA repair protein, can function as a transcriptional partner of E2F1. Mol Cell Biol. 1998;18:240-249

Hebra F, Kaposi M. On Disease of the Skin, Including Exanthemata. 61 New Sydenham Soc. 1874;252-258

Hegerfeldt Y, Tusch M, Brocker EB, Friedl P. Collective cell movement in primary melanoma explants: plasticity of cell-cell interaction, beta1-integrin function, and migration strategies. Cancer Res. 2002;62:2125-2130

Hermann PC, Huber SL, Heeschen C. Metastatic cancer stem cells: a new target for anti-cancer therapy? Cell Cycle. 2008;7:188-193

Hess MT, Schwitter U, Petretta M, Giese B, Naegeli H. Bipartite substrate discrimination by human nucleotide excision repair. Proc Natl Acad Sci U S A. 1997;94:6664-6669

Hoeijmakers JH. Genome maintenance mechanisms for preventing cancer. Nature 2001;411:366-374

Hwang BJ, Ford J, Hanawalt PC, Chu G. Expression of the p48 xeroderma pigmentosum gene is p53-dependent and is involved in global genomic repair. Proc Natl Acad Sci U S A. 1999;96:424-428

Jackson S., Xiong, Y. CRL4s: the CUL4-RING E3 ubiquitin ligases. Trends Biochem Sci. 2009;34:562-570

Janicijevic A, Sugasawa K, Shimizu Y, Hanaoka F, Wijgers N, Djurica M, Hoeijmakers JH, Wyman C. DNA bending by the human damage recognition complex XPC-HR23B. DNA Repair (Amst). 2003;2:325-336

Johnson RE, Haracska L, Prakash S, Prakash L. Role of DNA polymerase eta in the bypass of a (6-4) TT photoproduct. Mol Cell Biol. 2001;21:3558-3563

Johnson RE, Kondratick CM, Prakash S, Prakash L. hRAD30 mutations in the variant form of Xeroderma Pigmentosum. Science. 1999a;285:263-265

Johnson RE, Prakash S, Prakash L. Efficient bypass of a thymine-thymine dimer by yeast DNA polymerase, Pol eta. Science. 1999b;283:1001-1004

Jung YS, Hakem A, Hakem R, Chen X. Pirh2 E3 ubiquitin ligase monoubiquitinates DNA polymerase η to suppress Translesion DNA Synthesis. Mol Cell Biol. 2011; 19:3997-4006

Kannouche PL, Wing J, Lehmann AR. Interaction of human DNA polymerase eta with monoubiquitinated PCNA: A possible mechanism for the polymerase switch in response to DNA damage. Mol Cell. 2004;14:491-500

Kapetanaki MG, Guerrero-Santoro J, Bisi DC, Hsieh CL, Rapic-Otrin V, Levine AS. The DDB1-CUL4A-DDB2 ubiquitin ligase is deficient in xeroderma

pigmentosum group E and targets histone H2A at UV-damaged DNA sites. Proc Natl Acad Sci U S A. 2006;103:2588-2593

Karass M, Naguib MM, Elawabdeh N, Cundiff CA, Thomason J, Steelman CK, Cone R, Schwenkter A, Jordan C, Shehata BM. Xeroderma pigmentosa: three new cases with an in depth review of the genetic and clinical characteristics of the disease. Fetal Pediatr Pathol. 2015;34:120-127

Karikkineth AC, Scheibye-Knudsen M, Fivenson E, Croteau DL, Bohr VA. Cockayne syndrome: clinical features, model systems and pathways. Ageing Res Rev. 2017;33:3-17

Korzhnev DM, Hadden MK. Targeting the Translesion Synthesis Pathway for the Development of Anti-Cancer Chemotherapeutics. J Med Chem. 2016;59:9321-9336

Kraemer KH, Patronas NJ, Schiffmann R, Brooks BP, Tamura D, DiGiovanna JJ. Xeroderma pigmentosum, trichothiodystrophy and Cockayne syndrome. A complex genotype-phenotype relationship. Neuroscience. 2007;145:1388-1396

Kunkel TA. Considering the cancer consequences of altered DNA polymerase function. Cancer Cell. 2003;3:105-110

Kuraoka I, Ito S, Wada T, Hayashida M, Lee L, Saijo M, Nakatsu Y, Matsumoto M, Matsunaga T, Handa H, Qin J, Nakatani Y, Tanaka K. Isolation of XAB2 complex involved in pre-mRNA splicing, transcription, and transcription-coupled repair. J Biol Chem. 2008;283:940-50

Kusumoto R, Masutani C, Sugasawa K, Iwai S, Araki M, Uchida A, Mizukoshi T, Hanaoka F. Diversity of the damage recognition step in the global genomic nucleotide excision repair in vitro. Mutat Res. 2001;485:219-227

Langbein L, Pape UF, Grund C, Kuhn C, Praetzel S, Moll I, Moll R, Franke WW. Tight junction-related structures in the absence of a lumen: occludin, claudins and tight junction plaque proteins in densely packed cell formations of stratified epithelia and squamous cell carcinomas. Eur J Cell Biol. 2003;82:385-400

Lans H, Marteijn JA, Vermeulen W. ATP-dependent chromatin remodelling in the DNA-damage response. Epigenetics Chromatin. 2012;5:4

Lehmann AR, Kirk-Bell S, Arlett CF, Paterson MC, Lohman PH, de Weerd-

Kastelein EA, Bootsma D. Xeroderma pigmentosum cells with normal levels of excision repair have a defect in DNA synthesis after UV-irradiation, Proc Natl Acad Sci U S A. 1975;72:219-223

Lehmann AR, McGibbon D, Stefanini M. Xeroderma pigmentosum. Orphanet J Rare Dis. 2011;6:70

Li JM, Jin, J. CRL ubiquitin ligases and DNA damage response. Front Oncol. 2012;2:29

Li W, Selvam K, Ko T, Li S. Transcription bypass of DNA lesions enhances cell survival but attenuates transcription coupled DNA repair. Nucleic Acids Res. 2014;42:13242-13253

Lim JH, West KL, Rubinstein Y, Bergel M, Postnikov YV, Bustin M. Chromosomal protein HMGN1 enhances the acetylation of lysine 14 in histone H3. EMBO J. 2005;24:3038-3048

Limpose KL, Corbett AH, Doetsch PW. BERing the burden of damage: Pathway crosstalk and post-translational modification of base excision repair proteins regulate DNA damage management. DNA Repair (Amst). 2017;56:51-64

Liu W, Nichols A, Graham J, Dualan R, Abbas A, Linn S. Nuclear transport of human DDB protein induced by ultraviolet light. J Biol Chem. 2000;275:21429-21434

Luijsterburg MS, Lindh M, Acs K, Vrouwe MG, Pines A, van Attikum H, Mullenders LH, Dantuma NP. DDB2 promotes chromatin decondensation at UV-induced DNA damage. J Cell Biol. 2012;197:267-281

Mao P, Wyrick J, Roberts SA, Smerdon MJ. UV-induced DNA damage and mutagenesis in chromatin. Photochem Photobiol. 2017;93:216-228

Masutani C, Kusumoto R, Yamada A, Dohmae N, Yokoi M, Yuasa M, Araki M, Iwai S, Takio K, Hanaoka F. The XPV (xeroderma pigmentosum variant) gene encodes human DNA polymerase η. Nature. 1999;399:700-704

Matsuda N, Azuma K, Saijo M, Iemura S, Hioki Y, Natsume T, Chiba T, Tanaka K, Tanaka K. DDB2, the xeroderma pigmentosum group E gene product, is directly ubiquitylated by Cullin 4A-based ubiquitin ligase complex. DNA Repair (Amst). 2005;4:537-545

Min C, Eddy SF, Sherr DH, Sonenshein GE. NF-kappaB and epithelial to

mesenchymal transition of cancer. J Cell Biochem. 2008;104:733-744

Moser J, Kool H, Giakzidis I, Caldecott K, Mullenders LH, Fousteri MI. Sealing of chromosomal DNA nicks during nucleotide excision repair requires XRCC1 and DNA ligase III alpha in a cell-cycle-specific manner. Mol Cell. 2007;27:311-323

Mu D, Park C-H, Matsunaga T, Hsu DS, Reardon JT, Sancar A. Reconstitution of human DNA repair excision nuclease in a highly defined system. J Biol Chem. 1995;270:2415-2418

Nakano K, Vousden KH. PUMA, a novel proapoptotic gene, is induced by p53. Mol Cell. 2001;7:683-694

Nakatsu Y, Asahina H, Citterio E, Rademakers S, Vermeulen W, Kamiuchi S, Yeo JP, Khaw MC, Saijo M, Kodo N, Matsuda T, Hoeijmakers JH, Tanaka K. XAB2, a novel tetracopeptide repeat protein involved in transcription-coupled DNA repair and transcription. J Biol Chem. 2000;45:34931-34937

Neuwald A, Poleksic A. PSI-BLAST searches using hidden Markov models of structural repeats: prediction of an unusual sliding DNA clamp and of β-propellers in UV-damaged DNA-binding protein. Nucleic Acids Res. 2000;28:3570-3580

Ng JM, Vermeulen W, van der Horst GT, Bergink S, Sugasawa K, Vrieling H, Hoeijmakers JH. A novel regulation mechanism of DNA repair by damage-induced and RAD23-dependent stabilization of xeroderma pigmentosum group C protein. Genes Dev. 2003;17:1630-1645

Nguyen LV, Vanner R, Dirks P, Eaves CJ. Cancer stem cells: an evolving concept. Nat Rev Cancer. 2012;12:133-143

O' Connor MJ. Targeting the DNA damage response in cancer. Mol Cell. 2015;60:547-560

Ogi T, Limsirichaikul S, Overmeer RM, Volker M, Takenaka K, Cloney R, Nakazawa Y, Niimi A, Miki Y, Jaspers NG, Mullenders LH, Yamashita S, Fousteri MI, Lehmann AR. Three DNA polymerases, recruited by different mechanisms, carry out NER repair synthesis in human cells. Mol Cell. 2010;37:714-727

Ortolan TG, Tongaonkar P, Lambertson D, Chen L, Schauber C, Madura K. The DNA repair protein rad23 is a negative regulator of multi-ubiquitin chain assembly. Nat Cell Biol. 2000; 2:601-608

Osakabe A, Tachiwana H, Kagawa W, Horikoshi N, Matsumoto S, Hasegawa M, Matsumoto N, Toga T, Yamamoto J, Hanaoka F, Thomä NH, Sugasawa K, Iwai S, Kurumizaka H. Structural basis of pyrimidine-pyrimidone (6-4) photoproduct recognition by the UV-DDB in the nucleosome. Sci Rep. 2015;5:16330

Otrin V, McLenigan M, Takao M, Levine A, Protic M. Translocation of a UV-damaged DNA-binding protein in a tight association with chromatin after treatment of mammalian cells with UV light. J Cell Sci. 1997;110:1159-1168

Park H, Zhang K, Ren Y, Nadji S, Sinha N, Taylor JS, Kang C. Crystal structure of a DNA decamer containing a cis-syn thymine dimer. Proc Natl Acad Sci U S A. 2002;99:15965-15970

Paul D, Mu H, Zhao H, Ouerfelli O, Jeffrey PD, Broyde S, Min JH. Structure and mechanism of pyrimidine-pyrimidone (6-4) photoproduct recognition by the Rad4/XPC nucleotide excision repair complex. Nucleic Acids Res. 2019;47:6015-6028

Perucca P, Mocchi R, Guardamagna I, Bassi E, Sommatis S, Nardo T, Prosperi E, Stivala LA, Cazzalini O. A damaged DNA protein 2 mutation disrupting interaction with proliferating-cell nuclear antigen affects DNA repair and confers proliferation advantage. Biochim Biophys Acta Mol Cel Res. 2018;1865:898-907

Perucca P, Sommatis S, Mocchi R, Prosperi E, Stivala LA, Cazzalini O. A DDB2 mutant protein unable to interact with PCNA promotes cell cycle progression of human transformed embryonic kidney cells. Cell Cycle 2015;14:3920-3928

Petruseva IO, Evdokimov AN, Lavrik OI. Molecular Mechanism of Global Genome Nucleotide Excision Repair. Acta Naturae. 2014;6:23-34

Plesca D, Mazumder S, Almasan A. DNA Damage Response and Apoptosis. Methods Enzymol. 2008;446:107-122

Plosky BS, Vidal A, Fernández de Henestrosa AR, McLenigan MP, McDonald JP, Mead S, Woodgate R. Controlling the subcellular localization of DNA polymerases ι and η *via* interactions with ubiquitin. EMBO J. 2006;25:2847-2855

Pustovalova Y, Magalhaes MT, D'Souza S, Rizzo AA, Korza G, Walker GC, Korzhnev DM. Interaction between the Rev1 C-Terminal Domain and

the PolD3 Subunit of Polζ Suggests a Mechanism of Polymerase Exchange upon Rev1/Polζ-Dependent Translesion Synthesis. Biochemistry. 2016;55:2043-2053

Quinet A, Lerner LK, Martins DJ, Menck CF. Filling gaps in translesion DNA synthesis in human cells. Mutat Res Gen Tox En. 2018;836:127-142

Quinet A, Martins DJ, Vessoni AT, Biard D, Sarasin A, Stary A, Menck CF. Translesion synthesis mechanisms depend on the nature of DNA damage in UV-irradiated human cells. Nucleic Acids Res. 2016;44:5717-5731

Rapic-Otrin V, McLenigan MP, Bisi DC, Gonzalez M, Levine AS. Sequential binding of UV DNA damage binding factor and degradation of the p48 subunit as early events after UV irradiation. Nucleic Acids Res. 2002;30:2588-2598

Reardon JT, Sancar A. Recognition and repair of cyclobutene thymine dimer, a major cause of skin cancer, by the human excision nuclease. Genes Dev. 2003;17:2539-2551

Riedl T, Hanaoka F, Egly JM. The comics and goings of nucleotide excision repair factors on damaged DNA. EMBO J. 2003;22:5293-5303

Roos WP, Thomas AD, Kaina B. DNA damage and the balance between survival and death in cancer biology. Nat Rev Cancer. 2016;16:20-33

Roos WP, Tsaalbi-Shtylik A, Tsaryk R, Güvercin F, de Wind N, Kaina B. The translesion polymerase Rev3L in the tolerance of alkylating anticancer drugs. Mol Pharmacol. 2009;76:927-934

Rothwell PJ, Waksman G. Structure and mechanism of DNA polymerases. Adv Protein Chem. 2005;71:401-440

Roy N, Bommi PV, Bhat UG, Bhattacharjee S, Elangovan I, Li J, Patra KC, Kopanja D, Blunier A, Benya R, Bagchi S, Raychaudhuri P. DDB2 suppresses epithelial-to-mesenchymal transition in colon cancer. Can Res. 2013;73:3771-3782

Sabeh F, Ota I, Holmbeck K, Birkedal-Hansen H, Soloway P, Balbin M, Lopez-Otin C, Shapiro S, Inada M, Krane S, Allen E, Chung D, Weiss SJ. Tumor cell traffic through the extracellular matrix is controlled by the membrane-anchored collagenase MT1-MMP. J Cell Biol. 2004;167:769-781

Sale JE. Competition, collaboration and coordination-determining how cells

bypass DNA damage. J Cell Sci. 2012;125:1633-1643

Sale JE. Translesion DNA synthesis and mutagenesis in eukaryotes. Cold Spring Harb Perspect Biol. 2013;5:a012708

Sanz-Murillo M, Xu J, Belogurov GA, Calvo O, Gil-Carton D, Moreno-Morcillo M, Wang D, Fernandez-Tornero C. Structural basis of RNA polymerase I stalling at UV light-induced DNA damage. Proc Natl Acad Sci U S A. 2018;115:8972-8977

Schärer OD. Nucleotide excision repair in eukaryotes. Cold Spring Harb Perspect Biol. 2013;5:a012609

Schärer OD, Campbell AJ. Wedging out DNA damage. Nat Struct Mol Biol. 2009;16:102-104

Scheibye-Knudsen M, Ramamoorthy M, Sykora P, Maynard S, Lin PC, Minor RK, Wilson DM 3rd, Cooper M, Spencer R, de Cabo R, Croteau DL, Bohr VA. Cockayne syndrome group B protein prevents the accumulation of damaged mitochondria by promoting mitochondrial autophagy. J Exp Med. 2012;209:855-869

Schwertman P, Lagarou A, Dekkers DH, Raams A, van der Hoek AC, Laffeber C, Hoeijmakers JH, Demmers JA, Fousteri M, Vermeulen W, Marteijn JA. UV-sensitive syndrome protein UVSSA recruits USP7 to regulate transcription-coupled repair. Nat Genet. 2012;44:598-602

Scrima A, Konicková R, Czyzewski BK, Kawasaki Y, Jeffrey PD, Groisman R, Nakatani Y, Iwai S, Pavletich NP, Thomä NH. Structural basis of UV DNA-damage recognition by the DDB1-DDB2 complex. Cell. 2008;135:1213-1223

Shachar S, Ziv O, Avkin S, Adar S, Wittschieben J, Reissner T, Chaney S, Friedberg EC, Wang Z, Carell T, Geacintov N, Livneh Z. Two-polymerase mechanisms dictate error-free and error-prone translesion DNA synthesis in mammals. EMBO J. 2009;28:383-393

Shiyanov P, Hayes SA, Donepudi M, Nichols AF, Linn S, Slagle BL, Raychaudhuri P. The naturally occurring mutants of DDB are impaired in stimulating nuclear import of the p125 subunit and E2F1-activated transcription. Mol Cell Biol. 1999;19:4935-4943

Sigurdsson S, Dirac-Svejstrup AB, Svejstrup JQ. Evidence that transcript cleavage is essential for RNA polymerase II transcription and cell viability. Mol Cell. 2010;38:202-210

Sijbers AM, De Laat WL, Ariza RR, Biggerstaff M, Wei YF, Moggs JG, Carter KC, Shell BK, Evans E, De Jong MC, Rademakers S, De Rooij J, Jaspers NGJ, Hoeijmakers JHJ, Wood RD. Xeroderma pigmentosum group F caused by a defect in a structure-specific DNA repair endonuclease. Cell. 1996;86:811-822

Silva IA, Bai S, McLean K, Yang K, Griffith K, Thomas D, Ginestier C, Johnston C, Kueck A, Reynolds RK, Wicha MS, Buckanovich RJ. Aldehyde dehydrogenase in combination with CD133 defines angiogenic ovarian cancer stem cells that portend poor patient survival. Cancer Res. 2011;71:3991-4001

Silverstein TD, Johnson RE, Jain R, Prakash L, Prakash S, Aggarwal AK. Structural basis for the suppression of skin cancers by DNA polymerase eta. Nature. 2010;465:1039-1043

Simonelli V, Leuzzi G, Basile G, D'Errico M, Fortini P, Franchitto A, Viti V, Brown AR, Parlanti E, Pascucci B, Palli D, Giuliani A, Palombo F, Sobol RW, Dogliotti E. Crosstalk between mismatch repair and base excision repair in human gastric cancer. Oncotarget. 2016;8:84827-84840

Slebos RJ, Taylor JA. A novel host cell reactivation assay to assess homologous recombination capacity in human cancer cell lines. Biochem Biophys Res Commun. 2001;281:212-219

Soria G, Speroni J, Podhajcer OL, Prives C, Gottifredi V. p21 differentially regulates DNA replication and DNA-repair-associated processes after UV irradiation. J Cell Sci. 2008;121:3271-3282

Spivak G. Nucleotide excision repair in humans. DNA Repair (Amst). 2015;36:13-18

Spivak G, Hanawalt PC. Host cell reactivation of plasmids containing oxidative DNA lesions is defective in Cockayne syndrome but normal in UV-sensitive syndrome fibroblasts. DNA Repair (Amst). 2006;5:13-22

Staresincic L, Fagbemi AF, Enzlin JH, Gourdin AM, Wijgers N, Dunand-Sauthier I, Giglia-Mari G, Clarkson SG, Vermeulen W, Scharer OD. Coordination of dual incision and repair synthesis in human nucleotide excision repair. EMBO J. 2009;28:1111-1120

Stary A, Kannouche P, Lehmann AR, Sarasin A. Role of DNA Polymerase η in the UV Mutation Spectrum in Human Cells. J Biol Chem. 2003;278:18767-18775

Stefanini M, Botta E, Lanzafame M, Orioli D. Trichothiodystrophy: from basic mechanisms to clinical implications. DNA Repair (Amst). 2010;9:2-10

Stingele J, Habermann B, Jentsch S. DNA– protein crosslink repair: proteases as DNA repair enzymes. Trends Biochem Sci. 2015;40:67–71

Stoyanova T, Roy N, Kopanja D, Raychaudhuri P, Bagchi S. DDB2 (Damage DNA binding protein 2) in nucleotide excision repair and DNA damage response. Cell Cycle. 2009;8:4067-4071

Stoyanova T, Yoon T, Kopanja D, Mokyr MB, Raychaudhuri P. The Xeroderma pigmentosum group E gene product DDB2 activates nucleotide excision repair by regulating the level of p21Waf1/Cip1. Mol Cell Biol. 2008;28:177-187

Strumane K, Berx G, Van Roy F. Cadherins in cancer. In: Behrens J, Nelson J. (Eds.). Cell Adhesion, Heidelberg: Springer-Verlag; 2004;165:69-103

Su Y, Patra A, Harp JM, Egli M, Guengerich FP. Roles of residues Arg-61 and Gln-38 of human DNA polymerase η in bypass of deoxyguanosine and 7,8-Dihydro-8-oxo-2′-deoxyguanosine. J Biol Chem. 2015;290:15921-15933

Sugasawa K. Molecular mechanisms of DNA damage recognition for mammalian nucleotide excision repair. DNA Repair (Amst). 2016;44:110-117

Sugasawa K, Ng JM, Masutani C, Iwai S, Van der Spek P, Eker A, Hanoaka F, Bootsma D, Hoeijmakers JHJ. Xeroderma pigmentosum group C complex is the initiator of global genome nucleotide excision repair. Mol Cell. 1998;2:223-232

Sugasawa K, Okamoto T, Shimizu Y, Masutani C, Iwai S, Hanaoka F. A multistep damage recognition mechanism for global genomic nucleotide excision repair. Genes Dev. 2001;15:507-521

Sugasawa K, Okuda Y, Saijo M, Nishi R,Matsuda N, Chu G, Mori T, Iwai S, Tanaka K, Hanaoka F. UV-induced ubiquitylation of XPC protein mediated by UV-DDB-ubiquitin ligase complex. Cell. 2005;121:387-400

Sugasawa K, Shimizu Y, Iwai S, Hanaoka F. A molecular mechanism for DNA damage recognition by the xeroderma pigmentosum group C protein complex. DNA Repair (Amst). 2002;1:95-107

Takao M, Abramic M, Moos M, Otrin V, Wootton J, McLenigan M, Levine A, Protic M. A 127 kDa component of a UV-damaged DNA-binding

complex, which is defective in some xeroderma pigmentosum group E patients, is homologous to a slime mold protein. Nucleic Acids Res. 1993;21:4111-4118

Tan T, Chu G. p53 binds and activates the xeroderma pigmentosum DDB2 gene in humans but not mice. Mol Cell Biol. 2002;22:3247-3254

Tapias A, Auriol J, Forget D, Enzlin JH, Schärer OD, Coin F, Coulombe B, Egly JM. Ordered conformational changes in damaged DNA induced by nucleotide excision repair factors. J Biol Chem. 2004;279:19074-19083

Tofuku Y, Nobeyama Y, Kamide R, Moriwaki S, Nakagawa H. Xeroderma pigmentosum complementation group F: report of a case and review of Japanese patients. J Dermatol. 2015;42:897-899

Trieschmann L, Martin B, Bustin M. The chromatin unfolding domain of chromosomal protein HMG-14 targets the N-terminal tail of histone H3 in nucleosomes. Proc Natl Acad Sci U S A. 1998;95:5468-5473

Tsai C, Smider V, Joon Hwang B, Chu G. Electrophoretic Mobility Shift Assays for Protein-DNA Complexes Involved in DNA Repair. Methods Mol Biol. 2012;920:53-78

Tsodikov OV, Ivanov D, Orelli B, Staresincic L, Shoshani I, Oberman R, Scharer OD, Wagner G, Ellenberger T. Structural basis for the recruitment of ERCC1-XPF to nucleotide excision repair complexes by XPA. EMBO J. 2007;26:4768-4776

Uchida A, Sugasawa K, Masutani C, Dohmae N, Araki M, Yokoi M, Ohkuma Y, Hanaoka F. The carboxy-terminal domain of XPC protein plays a crucial role in nucleotide excision repair through interactions with transcription factor IIH. DNA Repair (Amst). 2002;1:449-461

van den Boom V, Citterio E, Hoogstraten D, Zotter A, Egly JM, van Cappellen WA, Hoeijmakers JH, Houtsmuller AB, Vermeulen W. DNA damage stabilizes interaction of CSB with the transcription elongation machinery. J Cell Biol. 2004;166:27-36

van Hoffen A, Venema J, Meschini R, van Zeeland AA, Mullenders LH. Transcription-coupled repair removes both cyclobutane pyrimidine dimers and 6-4-photoproducts with equal efficiency and in a sequential way from transcribed DNA in xeroderma pigmentosum group-C fibroblasts. EMBO J. 1995;14:360-367

Vasiliou V, Nebert DW. Analysis and update of the human aldehyde

dehydrogenase (ALDH) gene family. Hum Genom. 2005;2,138-143

Vermeulen W, Fousteri M. Mammalian Transcription-Coupled Excision Repair. Cold Spring Harb Perspect Biol. 2013;5:a012625

Volker M, Mone MJ, Karmakar P, Van Hoffen A, Schul W, Vermeulen W, Hoeijmakers JH, van Driel R, Van Zeeland AA, Mullenders LH. Sequential assembly of the nucleotide excision repair factors in vivo. Mol Cell. 2001;8:213-224

Vuillaume M, Calvayrac R, Best-Belpomme M, Tarroux P, Hubert M, Decroix Y, Sarasin A. Deficiency in the catalase activity of xeroderma pigmentosum cell and simian virus 40-transformed human cell extracts. Cancer Res. 1986;46:538-544

Wakasugi M, Kawashima A, Morioka H, Linn S, Sancar A, Mori T, Nikaido O, Matsunaga T. DDB accumulates at DNA damage sites immediately after UV irradiation and directly stimulates nucleotide excision repair. J Biol Chem. 2002;277:1637-1640

Wakasugi M, Sancar A. Assembly, subunit composition, and footprint of human DNA repair excision nuclease. Proc Natl Acad Sci U S A. 1998;95:6669-6674

Wang H, Zhai L, Xu J, Joo H-Y, Jackson S, Erdjument-Bromage H, Tempst P, Xiong Y, Zhang Y. Histone H3 and H4 ubiquitylation by the CUL4-DDB-ROC1 ubiquitin ligase facilitates cellular response to DNA damage. Mol Cell. 2006;22:383-394

Wang QE, Praetorius-Ibba M, Zhu Q, El-Mahdy MA, Wani G, Zhao Q, Qin S, Patnaik S, Wani AA. Ubiquitylation-independent degradation of Xeroderma pigmentosum group C protein is required for efficient nucleotide excision repair. Nucleic Acids Res. 2007;35:5338-5350

Wang QE, Wani MA, Chen J, Zhu Q, Wani G, El-Mahdy MA, Wani AA. Cellular ubiquitination and proteasomal functions positively modulate mammalian nucleotide excision repair. Mol Carcinog. 2005;42:53-64

Washington MT, Johnson RE, Prakash L, Prakash S. Human DINB1-encoded DNA polymerase kappa is a promiscuous extender of mispaired primer termini. Proc Natl Acad Sci U S A. 2002;99:1910-1914

Watanabe K, Tateishi S, Kawasuji M, Tsurimoto T, Inoue H, Yamaizumi M. Rad18 guides polη to replication stalling sites through physical interaction and PCNA monoubiquitination. EMBO J. 2004;23:3886-

3896

Waters LS, Minesinger BK, Wiltrout ME, D'Souza S, Woodruff RV, Walker GC. Eukaryotic translesion polymerases and their roles and regulation in DNA damage tolerance. Microbiol Mol Biol Rev. 2009;73:134-154

Waters LS, Walker GC. The critical mutagenic translesion DNA polymerase Rev1 is highly expressed during G(2)/M phase rather than S phase. Proc Natl Acad Sci U S A. 2006;103:8971-8976

Wilson BT, Stark Z, Sutton RE, Danda S, Ekbote AV, Elsayed SM, Gibson L, Goodship JA, Jackson AP, Keng WT, King MD, McCann E, Motojima T, Murray JE, Omata T *et al*. The Cockayne Syndrome Natural History (CoSyNH) study: clinical findings in 102 individuals and recommendations for care. Genet Med. 2016;18:483-493

Wittschieben BØ, Iwai S, Wood RD. DDB1-DDB2 (xeroderma pigmentosum group E) protein complex recognizes a cyclobutane pyrimidine dimer, mismatches, apurinic/apyrimidinic sites, and compound lesions in DNA. J Biol Chem. 2005;280:39982-39989

Wojtaszek J, Lee CJ, D'Souza S, Minesinger B, Kim H, D'Andrea AD, Walker GC, Zhou P. Structural basis of Rev1-mediated assembly of a quaternary vertebrate translesion polymerase complex consisting of Rev1, heterodimeric polymerase (Pol) zeta, and Pol kappa. J Biol Chem. 2012a;287:33836-33846

Wojtaszek J, Liu J, D'Souza S, Wang S, Xue Y, Walker GC, Zhou P. Multifaceted recognition of vertebrate Rev1 by translesion polymerases zeta and kappa. J Biol Chem. 2012b;287:26400-26408

Wolf K, Friedl P. Tube travel: the role of proteases in individual and collective cancer cell invasion. Cancer Res. 2008;68:7247-7249

Wolf K, Wu YI, Liu Y, Geiger J, Tam E, Overall C, Stack MS, Friedl P. Multi-step pericellular proteolysis controls the transition from individual to collective cancer cell invasion. Nat Cell Biol 2007;9:893-904

Xu J, Lahiri I, Wang W, Wier A, Cianfrocco MA, Chong J, Hare AA, Dervan PB, DiMaio F, Leschziner AE, Wang D. Structural basis for the initiation of eukaryotic transcription-coupled DNA repair. Nature. 2017;551:653-657

Yang H, Liu J, Jing J, Wang Z, Li Y, Gou K, Feng X, Yuan Y, Xing C. Expression in DDB2 Protein in the Initiation, Progression, and Prognosis of Colorectal

Cancer. Dig Dis Sci. 2018;63:2959-2968

Yang W, Woodgate R. What a difference a decade makes: insights into translesion DNA synthesis. Proc Natl Acad Sci U S A. 2007;104:15591-15598

Ye X, Weinberg RA. Epithelial-Mesenchymal Plasticity: A central regulator of cancer progression. Trends. Cell Biol. 2015;25:675-686

Yokoi M, Masutani C, Maekawa T, Sugasawa K, Ohkuma Y, Hanaoka F. The Xeroderma pigmentosum group C protein complex XPC-HR23B plays an important role in the recruitment of transcription factor IIH to damaged DNA. J Biol Chem. 2000;275:9870-9875

Yoon JH, Park J, Conde J, Wakamiya M, Prakash L, Prakash S. Rev1 promotes replication through UV lesions in conjunction with DNA polymerases η, ι, and κ but not DNA polymerase ζ. Genes Dev. 2015;29:2588-2602

Yoon JH, Prakash L. Error-free replicative bypass by DNA polymerase ζ in mouse and human cells. Res Commun. 2010;24:123-128

Yoon T, Chakrabortty A, Franks R, Valli T, Kiyokawa H, Raychaudhuri P. Tumor-prone phenotype of the DDB2-deficient mice. Oncogene. 2005;24:469-478

You YH, Lee DH, Yoon JH, Nakajima S, Yasui A, Pfeifer GP. Cyclobutane pyrimidine dimers are responsible for the vast majority of mutations induced by UVB irradiation in mammalian cells. J Biol Chem. 2001;276:44688-44694

Zhang X, Horibata K, Saijo M, Ishigami C, Ukai A, Kanno S, Tahara H, Neilan EG, Honma M, Nohmi T, Yasui A, Tanaka K. Mutations in UVSSA cause UV-sensitive syndrome and destabilize ERCC6 in transcription-coupled DNA repair. Nat Genet. 2012;44:593-597

Zhao Y, Biertumpfel C, Gregory MT, Hua YJ, Hanaoka F, Yang W. Structural basis of human DNA polymerase eta-mediated chemoresistance to cisplatin. Proc Natl Acad Sci U S A. 2012;109:7269-7274

Zhu Q, Wani G, Arab HH, El-Mahdy MA, Ray, A, Wani AA. Chromatin restoration following nucleotide excision repair involves the incorporation of ubiquitinated H2A at damaged genomic sites. DNA Repair (Amst). 2009;8:262-273

List of original manuscripts

Bassi E, Perucca P, Guardamagna I, Prosperi E, Stivala LA, Cazzalini O. (2019). "Exploring new potential role of DDB2 by Host Cell Reactivation assay in human tumorigenic cells". *BMC Cancer,* 19; 1013. doi: 10.1186/s12885-019-6258-0.

Perucca P, Mocchi R, Guardamagna I, Bassi E, Sommatis S, Nardo T, Prosperi E, Stivala LA, Cazzalini O. (2018). "A damaged DNA binding protein 2 mutation disrupting interaction with proliferating-cell nuclear antigen affects DNA repair and confers proliferation advantage". *Biochimica et Biophysica Acta*, 1865; 898-907. doi: 10.1016/j.bbamcr.2018.03.012.

My contribution to manuscripts

In “Exploring new potential role of DDB2 by Host Cell Reactivation assay in human tumorigenic cells” I carried out cell culture and transfection procedures, immunofluorescence experiments. I performed the Host Cell Reactivation assay and I prepared samples for the flow cytometry analysis. I also analysed the data obtained by flow cytometry analysis. I wrote the “Methods” section.

In the article “A damaged DNA binding protein 2 mutation disrupting interaction with proliferating-cell nuclear antigen affects DNA repair and confers proliferation advantage” I carried out cell culture and transfection procedures, gel electrophoretic mobility shift assay, clonogenic assay. I also performed the May-Grünwald Giemsa staining to evaluate the morphological features of cells, wound healing assay and Western blot experiments.

Bassi et al. BMC Cancer (2019) 19:1013
https://doi.org/10.1186/s12885-019-6258-0

BMC Cancer

RESEARCH ARTICLE Open Access

Exploring new potential role of DDB2 by host cell reactivation assay in human tumorigenic cells

Elisabetta Bassi[1], Paola Perucca[1], Isabella Guardamagna[1], Ennio Prosperi[2*], Lucia A. Stivala[1*] and Ornella Cazzalini[1*]

Abstract

Background: The Host Cell Reactivation assay (HCR) allows studying the DNA repair capability in different types of human cells. This assay was carried out to assess the ability in removing UV-lesions from DNA, thus verifying NER efficiency. Previously we have shown that DDB2, a protein involved in the Global Genome Repair, interacts directly with PCNA and, in human cells, the loss of this interaction affects DNA repair machinery. In addition, a mutant form unable to interact with PCNA ($DDB2^{PCNA-}$), has shown a reduced ability to interact with a UV-damaged DNA plasmid in vitro.

Methods: In this work, we have investigated whether DDB2 protein may influence the repair of a UV-damaged DNA plasmid into the cellular environment by applying the HCR method. To this end, human kidney 293 stable clones, expressing $DDB2^{Wt}$ or $DDB2^{PCNA-}$, were co-transfected with pmRFP-N2 and UV-irradiated pEGFP-reported plasmids. Moreover, the co-localization between DDB2 proteins and different NER factors recruited at DNA damaged sites was analysed by immunofluorescence and confocal microscopy.

Results: The results have shown that $DDB2^{Wt}$ recognize and repair the UV-induced lesions in plasmidic DNA transfected in the cells, whereas a delay in these processes were observed in the presence of $DDB2^{PCNA-}$, as also confirmed by the different extent of co-localization of $DDB2^{Wt}$ and some NER proteins (such as XPG), vs the DDB2 mutant form.

Conclusion: The HCR confirms itself as a very helpful approach to assess in the cellular context the effect of expressing mutant vs Wt NER proteins on the DNA damage response. Loss of interaction of DDB2 and PCNA affects negatively DNA repair efficiency.

Keywords: DNA damage response, DNA damaged binding protein 2, Global genome nucleotide excision repair, *Xeroderma Pigmentosum* group G, RNA polymerase II

Background

DNA damaged binding protein 2 (DDB2) plays a crucial role in DNA Damage Response (DDR) activated by UV radiation [1]. This protein is known to act as an important sensor in the Global Genome Nucleotide Excision Repair (GG-NER) by recognizing sites of UV-induced DNA lesions [2]. This function is shared with DDB1, which associates to DDB2 to form the heterodimeric UV-damaged DNA-binding protein complex (UV-DDB); this complex initiates GG-NER by recognizing photodimers (CPDs) and 6–4 photoproducts (PPs), the primary type of lesions induced by UV irradiation. The distortion of the double helix caused by the CPDs is smaller than that of 6-4PPs, and their recognition is performed by the synchronized work of UV-DDB complex and XPC protein [3]. Mutations in NER genes are linked to human genetic diseases (e.g. Xeroderma pigmentosum) as well as cancer predisposition [4–6].

The mutagenic effect of UV is efficiently neutralized by DNA repair processes involving not only GG-NER but also the transcription-coupled nucleotide excision repair (TC-NER), a sub-pathway that preferentially removes DNA lesions generated in highly transcribed DNA regions

*Correspondence: prosperi@igm.cnr.it; luciaanna.stivala@unipv.it; ornella.cazzalini@unipv.it
[1]Istituto di Genetica Molecolare (IGM) del CNR, Pavia, Italy
[2]Dipartimento di Medicina Molecolare, Unità di Immunologia e Patologia generale, Università degli Studi di Pavia, Pavia, Italy

BMC

© The Author(s). 2019 **Open Access**. This article is distributed under the terms of the Creative Commons Attribution 4.0 International License (http://creativecommons.org/licenses/by/4.0/), which permits unrestricted use, distribution, and reproduction in any medium, provided you give appropriate credit to the original author(s) and the source, provide a link to the Creative Commons license, and indicate if changes were made. The Creative Commons Public Domain Dedication waiver (http://creativecommons.org/publicdomain/zero/1.0/) applies to the data made available in this article, unless otherwise stated.

[7]. At the molecular level, both these processes are promoted and regulated by various post-translational modifications of NER factors and chromatin substrate. While GG-NER employs UV-DDB heterodimer and XPC complex to initiate the DNA repair process, TC-NER utilizes elongating RNA polymerase II (Pol II) and Cockayne syndrome B (CSB) proteins as damage sensors [8].

We have previously demonstrated that the interaction between DDB2 and PCNA is important to remove DNA lesions by NER. In fact, a mutated form of DDB2, unable to interact with PCNA ($DDB2^{PCNA-}$), causes a delay in UV-induced NER process activation and confers proliferative and migratory advantages in HEK293 stable clone expressing $DDB2^{PCNA-}$ [9, 10].

In addition, using gel electrophoretic motility shift assay, we showed that $DDB2^{Wt}$ recombinant protein retains the ability to bind directly plasmidic UV-damaged DNA, but not the DDB2 mutated form [10]. Nevertheless, this finding does not prove that $DDB2^{PCNA-}$ since the mutant form at the cellular level localized to DNA damage sites and interact with DDB1 [10]. To clarify this issue, we decided to apply a transfection-based assay, named Host Cell Reactivation (HCR), to investigate DNA lesions removal efficacy in the presence of $DDB2^{Wt}$ protein or DDB2 mutated one. This method allows studying the DNA repair capability in different types of human cells [11] and may be employed as a marker for genetic instability and cancer risk [12, 13]. A subsequent adaptation to FACS technology further improved its sensitivity, compared to the previous luminometer method [14]. The HCR assay assesses repair of a transcriptionally active genes and, once applied to UV lesions, it measures the capacity of the host cells to perform NER [15].

In order to investigate whether DDB2 protein interacts with nude plasmidic UV-damaged DNA in cellular environment and whether the mutation in DDB2 interferes with DNA repair kinetic, we used two stable clones of HEK293 expressing $DDB2^{Wt}$ or $DDB2^{PCNA-}$. HCR assay was performed co-transfecting these cells with UV-C irradiated pEGFP-N1 and not irradiated pmRFP-N2 plasmids. To further elucidate the ability of $DDB2^{Wt}$ and mutant form to interact with transcription machinery, co-localization to the UV-damaged sites between RNA polymerase II (Pol II), a protein sensor of DNA lesions in transcribed genes, was also considered. Finally, DDB2 recruitment and co-localization with XPG was detected to assess potential modifications in the DNA excision step kinetic.

Methods

Cell lines and transfection

HEK293 (Human Embryonic Kidney) cell line was purchased from the European Tissue culture Collection (ECACC) (catalogue code: 85120602). Cells were cultured in Dulbecco's modified Eagle's medium (DMEM, Sigma) supplemented with 10% foetal bovine serum (Life Technologies-Gibco), 2 mM l-glutamine (Life Technologies-Gibco), 100 U/ml penicillin, 100 μg/ml streptomycin in a 5% CO_2 atmosphere.

Cell lines (50% confluent) were stably transfected with $DDB2^{Wt}$ construct kindly provided by dr. Q. Wang [16] or the mutated form $DDB2^{PCNA-}$ using Effectene transfection reagent (Qiagen). $DDB2^{PCNA-}$ mutated in PIP-BOX region was produced in our laboratory, as previously described [9].

HeLa S3 cell line was purchased from European Tissue Culture Collection (ECACC, catalogue code: 87110901). HeLa cells were cultured as above, seeded on coverslips (70% confluent) and transiently transfected with DDB2 wild-type or mutated form constructs as previously described [9]. Both cell lines were periodically tested for mycoplasma contamination.

UV plasmid preparation

pEGFP-N1 (Clontech) was irradiated in 10.5 μl of TE buffer (10 mM Tris–HCl, 1 mM EDTA, pH 8.0) at a DNA concentration of 2.85 μg/μl with 800 J/m^2 UV-C lamp (Philips TUV-9) emitting mainly at 254 nm, as measured with a DCRX radiometer (Spectronics). Ethanol (70%) was added to DNA for the precipitation. After 15 min in freezer, DNA was centrifuged at 15500 g for 15 min at 4 °C (Allegra 21R, Beckman Coulter). The pellet was left to air dry overnight, whereas the supernatant was stored at −20 °C. Pellet was re-suspended in 15 μl of TE buffer and the DNA was quantified by spectrophotometer (POLARstar Omega, BMG LABTECH). The supernatant was pelleted by centrifugation (Allegra 21R, Beckman Coulter) and quantified.

Host cell reactivation assay and cytofluorimetric analysis

HEK293, stably transfected with $DDB2^{Wt}$ or $DDB2^{PCNA-}$ construct, were co-transfected with pmRFP-N2 (as a positive control), kindly provided by Professor Cardoso, and pEGFP-N1 or UV-pEGFP-N1 (as previously described) employing Effectene transfection reagent (Qiagen).

After 16 and 48 h, the cells were harvested from Petri dishes and centrifuged at 200 g for 3 min (Centrifuge 4236, Alc), the pellets were gently re-suspended on phosphate-buffered saline (PBS) for in vivo flow cytofluorimetry measurements (CyFlow® SL, Sysmex Partec GmbH). Only RFP positive cells were considered for the subsequent analysis in which the ratio between the mean fluorescence intensity (MFI) for the RFP and GFP protein were calculated. After normalization (MFI GFP/MFI RFP), relative expression of GFP protein was computed by comparing the normalized MFI of the UV-irradiated

to the normalized MFI of unirradiated plasmid, thereby detecting the restored plasmidic DNA [14, 15].

Immunofluorescence and confocal microscopy

HeLa cells, seeded on coverslips and transiently transfected as reported above, were locally irradiated at 100 J/m^2 by laying on top of cells an Isopore polycarbonate filters (Millipore) with 3 μm pores. At the end of 5, 10, 30 and 60 min (recovery time for XPG) or 30 and 60 min (recovery time for Pol II), the cells were washed twice in cold PBS, lysed with 0.5% Triton X-100 (Sigma-Aldrich) in cold PBS for 30 min at 4°C in agitation, fixed with freshly made 2% paraformaldehyde and preserved in Ethanol (70%) at − 20 °C for permeabilization.

Next, the samples were washed twice with cold PBS and blocked in PBST buffer (PBS, 0.2% Tween 20) containing 1% bovine serum albumin (BSA) with gentle shaking, and then incubated for 1 h with specific antibodies: mouse monoclonal anti-RNA polymerase II (anti-Pol II, 1:100, Covance, RRID:AB_10013665), rabbit polyclonal anti-XPE/DDB2 (1:100, Novus Biologicals; NBP2−38854) and rabbit polyclonal anti-XPG (1:200, RRID: AB_1080609), all diluted in PBST buffer/BSA. After three washing, each reaction was followed by incubation for 30 min with anti-mouse Alexa Fluor 594 (1:200, RRID: AB_141607) or anti-rabbit Alexa Fluor 488 (1:200, Molecular Probes, RRID: AB_141708). After immunoreactions and washing, the samples were incubated with Hoechst 33258 dye (0.5 μg/ml) for 10 min at room temperature with mild agitation and then washed in PBS. Slides were mounted in Mowiol (Calbiochem) containing 0.25% 1, 4-diazabicyclo-octane (Aldrich) as antifading agent. Images of fixed cells were taken with a Nikon Eclipse E400 fluorescence microscope equipped with a Canon Power Shot A590 IS digital camera. Fluorescence signals were acquired with a TCS SP5 II Leica confocal

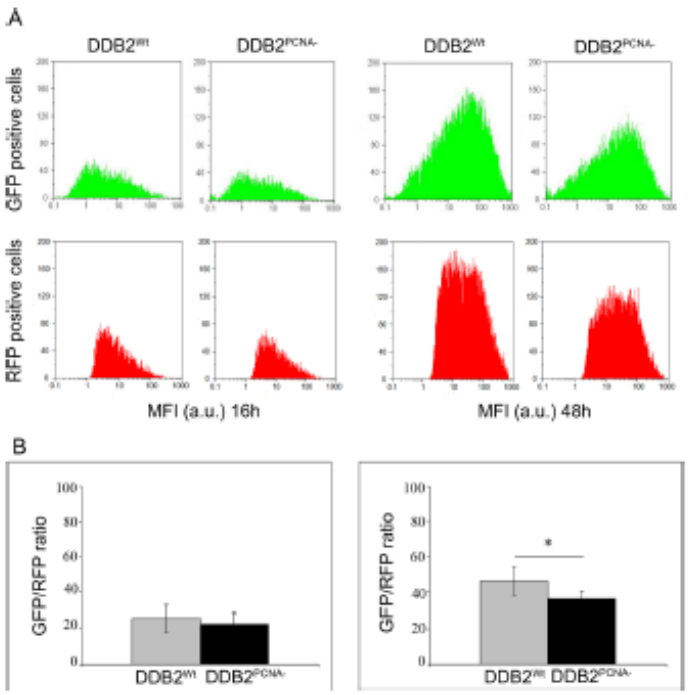

Fig. 1 NER process is impaired when DDB2-PCNA interaction is lost. HEK293 stable clones expressing DDB2 wild-type (DDB2^{WT}) or mutated protein (DDB2^{PCNA-}) were transiently transfected with pEFGP-N1 UV-irradiated plasmid and pmRFP-N2 control plasmid. At 16 and 48 h after transfection, the cells were collected and analysed using in vivo cytofluorimetric protocol (see Materials and Methods section). In **a** GFP and RFP positive cells are reported and the MFI is shown. **b** Statistical analysis of GFP/RFP ratio from three independent experiments is reported. * $p < 0.05$

microscope, at 0.3 μm intervals. Image analysis was performed using the LAS AF software.

Results

DNA damage response is delayed in the presence of DDB2 mutated protein

To evaluate the UV-induced DNA damage response, we performed experiments using irradiated or not irradiated pEGFP-N1 plasmid co-transfected with pmRFP-N2 construct in HEK293 stable clones expressing $DDB2^{Wt}$ or $DDB2^{PCNA-}$ protein. Flow cytometry analysis of GFP and RFP expression, performed at 16 and 48 h after plasmidic DNA-damaged transfection, highlights the production of the green fluorescent protein, indicating the ability of these cells to repair DNA lesions in irradiated pEGFP-N1 plasmid (Fig. 1). In the panel A, monoparametric analysis of the green (GFP positive cells) and red (RFP positive cells) shows no significant differences in the two cell clones at 16 h after transfection. At this time, the presence of DDB2 mutated protein does not influence the repair ability since it produced similar results as wild-type protein. In contrast, the analysis performed 48 h after transfection highlights a significant reduction of DNA damage repair capability in the presence of the mutated protein (Fig. 1b). Considering the ratio of GFP/RFP fluorescence, the GFP protein synthesis is more efficient in the presence of $DDB2^{Wt}$; instead, the loss of DDB2-PCNA interaction determines a reduction of reported gene reactivation after UV irradiation.

DDB2 and RNA polymerase II co-localization is prevented without PCNA involvement

HeLa cells transiently transfected with pc-DNA3.1-$DDB2^{Wt}$ or pc-DNA3.1-$DDB2^{PCNA-}$ constructs were incubated with anti-DDB2 and anti-RNA Pol II antibodies for 30 min and 1 h after UV-C local irradiation. The immunofluorescence analysis shows that $DDB2^{Wt}$ and Pol II were already recruited at DNA damaged sites at 30 min after DNA damage, and their co-localization were still detectable at 1 h after UV irradiation, even if the signal appears to be reduced (Fig. 2a). In the presence of DDB2 mutated protein, the cells did not show well-defined spots of co-localization at both 30 and 60 min (Fig. 2b).

To better evaluate the recruitment kinetics at DNA damaged sites of the above proteins, confocal analysis was performed as shown in Fig. 3. The co-localization between $DDB2^{Wt}$ and Pol II occurs mainly at 30 min after UV irradiation (Fig. 3a); at this time, 52% of cells were positive for colocalization. On the contrary, in the presence of $DDB2^{PCNA-}$ protein, only 1 h after damage, the pixel intensity profile showed a not complete co-localization. In fact, the green and red signals were partially overlapped (Fig. 3b). This

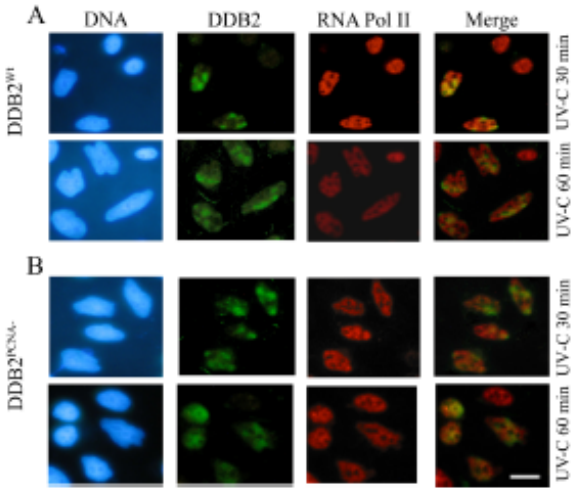

Fig. 2 $DDB2^{PCNA-}$ and Polymerase II proteins partially co-localize in irradiated cells. Immunofluorescence analysis of HeLa cells transiently transfected with constructs expressing $DDB2^{Wt}$ or $DDB2^{PCNA-}$ protein, as indicated. Cells were UV-C local irradiated and analysed 30 min and 1 h later. In **a** representative images obtained from cells expressing $DDB2^{Wt}$ protein. In **b** results from HeLa transfected with pc-DNA3.1-$DDB2^{PCNA-}$ construct are shown. Scale bar = 20 μm. Data are at least from three independent experiments

Bassi et al. BMC Cancer (2019) 19:1013

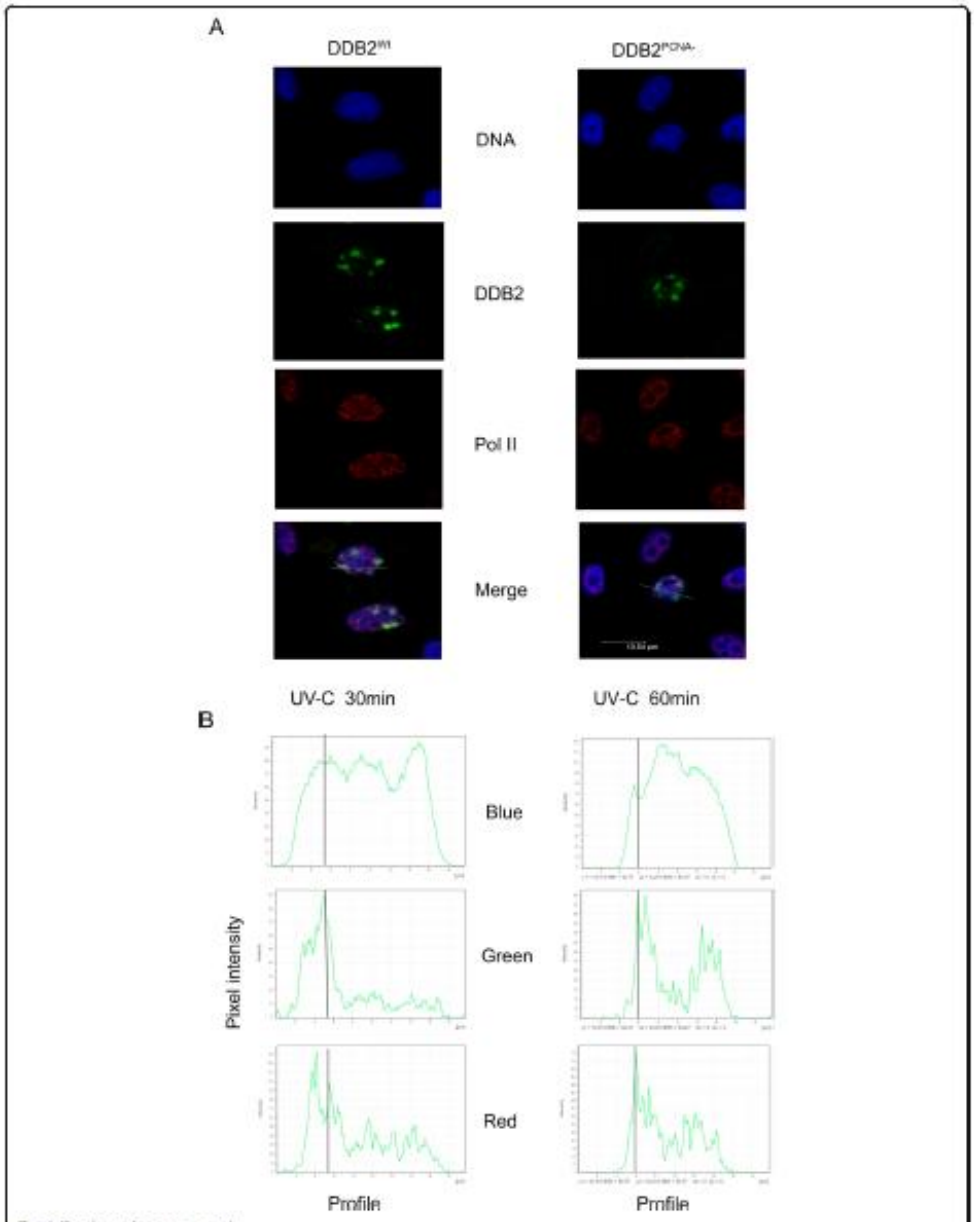

Fig. 3 (See legend on next page.)

(See figure on previous page.)
Fig. 3 The loss of DDB2-PCNA interaction determines defects in NER pathway. HeLa cells transiently transfected with pc-DNA3.1-DDB2^{Wt} or pc-DNA3.1-DDB2^{PCNA-} constructs and UV-C local irradiated were analysed 30 min and 1 h after damage. In **a** representative co-localization analysis between DDB2 and Polymerase II proteins after UV-induced damages as obtained by confocal microscopy. The co-localization analyses are reported in panel (**b**). Data are at least from three independent experiments

finding confirms a delay in this co-presence at DNA damage foci.

DDB2-PCNA interaction facilitates the appropriate maintenance of the late NER-phase

To evaluate the potential influence of DDB2-PCNA interaction on the late NER steps, we investigate the interaction between DDB2 and XPG, a protein involved in the incision phase of NER process. HeLa cells transiently expressing DDB2^{Wt} or DDB2^{PCNA-} protein were local irradiated and analysed by fluorescence and confocal microscopies at different recovery times.

Figure 4a shows representative images of the immunofluorescence analysis. The time course after irradiation indicate that DDB2^{Wt} protein is recruited at DNA damaged sites together with the endonuclease XPG. Confocal microscopy confirmed a better co-localization between DDB2^{Wt} and XPG proteins at 10 min after UV irradiation (Fig. 4b), whereas the recruitment at the damage sites appears postponed at 30 min with regards to XPG and DDB2^{PCNA-}. Furthermore, in the last case, the confocal analysis indicated that the two proteins recruited at DNA damaged sites are very closed but not completely overlapped since the profile of the peak intensity reveal that the better fluorescent signals are not superimposable. These data demonstrate that the loss of DDB2-PCNA interaction influences the late phase of NER process.

Discussion

NER process is a highly versatile and complex system removing different types of DNA lesions [17]. UV-induced damages trigger NER process using both sub-pathways TC-NER and GG-NER. The first one is fast and efficient in removing lesions from transcribed regions determining a block of transcription [18].

The role of DDB2 in GG-NER is widely described and this protein is crucial to recognize and remove DNA UV-lesions [19, 20]. We have previously demonstrated that DDB2-PCNA interaction is i) required for DDB2 degradation [9], ii) likely involved in cell cycle progression [21], iii) able to affects DNA repair and iv) implicated in conferring proliferation and migration advantages [10]. In addition, using UV-damaged plasmidic DNA, DDB2^{PCNA-} recombinant protein showed both defective lesion recognition and DNA binding [10].

In this work we applied HRC assay to evaluate plasmidic DNA repair capacity of DDB2 protein and its mutated form. In the past, several approaches based on transfected damaged-DNA have been used to this end. After the initial demonstration on HCR efficiency for studying NER process activation in whole cells [11] or fractionated cell extracts transfected with UV-damaged plasmid DNA [11], different attempts to improve HCR assay have been further developed. Among them, a fluorescent method for detecting cellular ability to incise the damaged strand by NER mechanism [22], as well as a plasmid-type fluorescent probe [23] were proposed.

Based on our results, the re-activated expression of GFP protein in the stable clone producing DDB2^{Wt} demonstrated that DNA lesions are removed from transfected irradiated plasmidic DNA and, therefore, the transcription process is restored. It is known from the literature, that HCR assay, when performed after UV damage, measures the ability of the host cells to complete NER [15]. Our results demonstrated that this capability is influenced by DDB2-PCNA interaction; in fact, the cells expressing DDB2^{PCNA-} protein showed a significant reduction of GFP expression, as shown by the low GFP protein level measured by flow cytometry. By this experimental approach we demonstrated that both DDB2^{Wt} and DDB2^{PCNA-} proteins may intervene on nude UV-damaged plasmidic DNA inserted in human cells. Importantly, the DDB2^{PCNA-} mutant protein causes a delayed repair, confirming our previously published data obtained in an in vitro model [10]. In addition, our data support that the HCR method can be an efficient tool for investigating the role of NER mutant proteins in DNA repair. One advantage of this technical approach is that only the transfected DNA is damaged, while host cells are not irradiated and, therefore, they own intact cellular synthesis machinery and biochemical processes.

Interestingly, the co-localization between DDB2^{Wt} and RNA Pol II protein, as highlighted by confocal analysis at 30 min after UV irradiation, allows us to confirm the co-presence of these proteins at DNA damaged sites. This finding suggests a putative cooperation in DNA repair processes between TC-NER and GG-NER. Cooperation between other repair pathways have already been reported, as well as functional links between apparently separate signalling pathways converging toward a single global DNA damage response [24, 25]. In the presence of DDB2 mutated protein this cooperation is slower and its co-localization with RNA Pol II at DNA damaged sites appears incomplete even one hour after irradiation, thus suggesting a delay in the repair process.

Bassi et al. BMC Cancer (2019) 19:1013

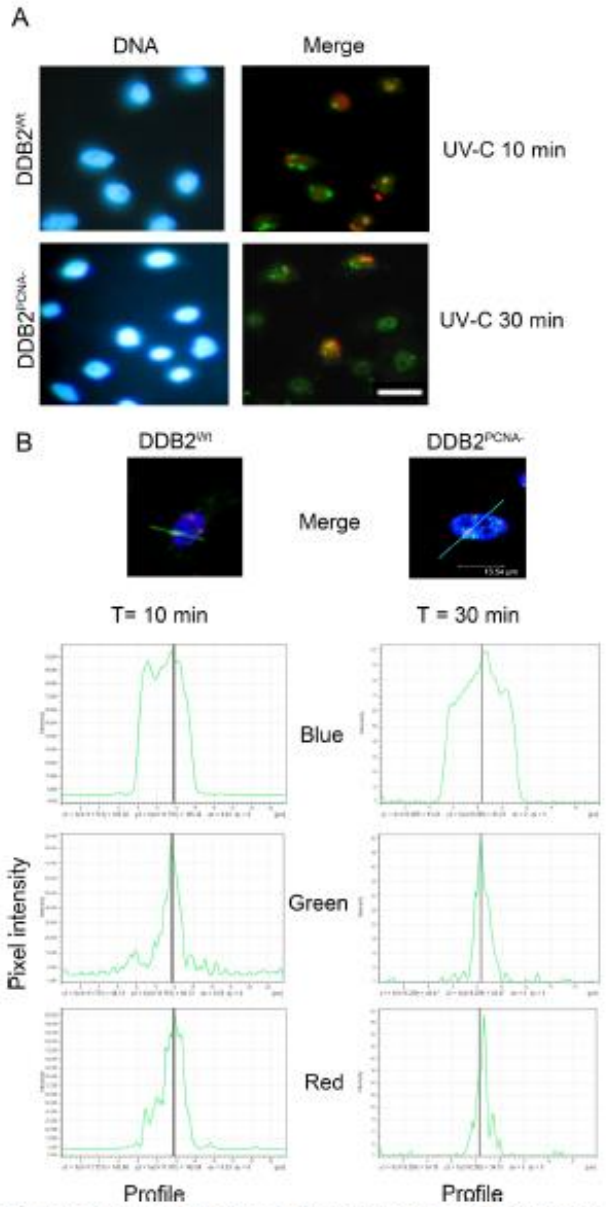

Fig. 4 DDB2-PCNA binding influences the late phase of repair process. Representative analysis obtained from transfected and irradiated HeLa cells using immunofluorescence microscope (**a**). Scale bar = 20 μm. In **b** confocal images and analysis are reported. The peaks exemplify the co-localization studies between DDB2 and XPG proteins. Data are at least from three independent experiments

To verify whether this different DNA damage response occurs also in the next phase of the NER and, in particular, in the excision of DNA lesions, DDB2-XPG co-localization was also considered. Although early report indicated that DDB2 is not required for XPG recruitment [26], this does not mean that co-localization may occur thereafter, as suggested by our results with DDB2^{Wt} and further supported by the evidence that loss of DDB2-PCNA interaction determines a delay on the XPG recruitment on DNA lesions. Since XPG-mediated excision of DNA containing the lesions is fundamental for the fast DNA re-synthesis to correct the errors [27], our results suggest that DDB2 may influence not only the recognition, but also the next step of the NER, confirming the results observed in delayed GG-NER process [9, 10].

Conclusions

In conclusion, this work reports two new findings. First, the HCR data allowed highlighting the importance of the DDB2-PCNA interaction to complete correctly NER process. The second result is that HCR approach is useful to study how mutations in NER proteins may influence genome stability.

Abbreviations

DDB2: DNA damaged binding protein 2; DDR: DNA Damage Response; GG-NER: Global Genome Nucleotide Excision Repair; HCR: Host Cell Reactivation assay; HEK: Human Embryonic Kidney; MFI: Mean Fluorescence Intensity; PCNA: Proliferating Cell Nuclear Antigen; Pol II: RNA Polymerase II; TC-NER: Transcriptional Coupled Nucleotide Excision Repair; XPG: *Xeroderma Pigmentosum* group G

Acknowledgements

The authors wish to thank P. Vaghi, Centro Grandi Strumenti Università di Pavia, for technical assistance to confocal microscopy.

Authors' contributions

EB, PP and IG carried out cell culture and transfection experiments; HCR experiments were performed by EB; immunofluorescence experiments were performed by PP and EB. Flow cytometry analysis was carried out by EP. EP, LAS and OC wrote the manuscript. All the authors contributed to the design of the project. All the authors have read and approved the manuscript.

Funding

This research was supported by a Grant from the Italian Ministry of Education, University and Research (MIUR) to the Department of Molecular Medicine of the University of Pavia under the initiative "Dipartimenti di Eccellenza (2018–2022)". This work was in part supported by AIRC (n° 17041 to EP). No role of the funding body in this study.

Availability of data and materials

The datasets used and/or analysed during the current study are available from the corresponding authors on reasonable request.

Ethics approval and consent to participate

Not applicable.

Consent for publication

Not applicable.

Competing interests

The authors declare that they have no competing interests.

Received: 18 April 2019 Accepted: 14 October 2019
Published online: 29 October 2019

References

1. Wang QE, Zhu Q, Wani G, Chen J, Wani AA. UV radiation-induced XPC translocation within chromatin is mediated by damaged-DNA binding protein, DDB2. Carcinogenesis. 2004;25(6):1033–43.
2. Abouselkhra A, Wood RD. Detection of nucleotide excision repair incisions in human fibroblasts by immunostaining for PCNA. Exp Cell Res. 1995; 221(2):326–32.
3. Wakasugi M, Kawashima A, Morioka H, Linn S, Sancar A, Mori T, Nikaido O, Matsunaga T. DDB accumulates at DNA damage sites immediately after UV irradiation and directly stimulates nucleotide excision repair. J Biol Chem. 2002;277(3):1637–40.
4. Cleaver JE, Lam ET, Revet I. Disorders of nucleotide excision repair: the genetic and molecular basis of heterogeneity. Nat Rev Genet. 2009; 10(11):756–68.
5. Basu AK. DNA Damage, Mutagenesis and Cancer. Int J Mol Sci. 2018;19(4). https://doi.org/10.3390/ijms19040970
6. Broustas CG, Lieberman HB. DNA damage response genes and the development of cancer metastasis. Radiat Res. 2014;181(2):111–30.
7. Lagerwerf S, Vrouwe MG, Overmeer RM, Fousteri MI, Mullenders LH. DNA damage response and transcription. DNA Repair (Amst). 2011; 10(7):743–50.
8. Mullenders LHF. Solar UV damage to cellular DNA: from mechanisms to biological effects. Photochem Photobiol Sci. 2018;17(12):1842–52.
9. Cazzalini O, Perucca P, Mocchi R, Sommatis S, Prosperi E, Stivala LA. DDB2 association with PCNA is required for its degradation after UV-induced DNA damage. Cell Cycle. 2014;13(2):240–8.
10. Perucca P, Mocchi R, Guardamagna I, Bassi E, Sommatis S, Nardo T, Prosperi E, Stivala LA, Cazzalini O. A damaged DNA binding protein 2 mutation disrupting interaction with proliferating-cell nuclear antigen affects DNA repair and confers proliferation advantage. Biochim Biophys Acta Mol Cell Res. 2018;1865(6):898–907.
11. Roguev A, Russev G. Two-wavelength fluorescence assay for DNA repair. Anal Biochem. 2000;287(2):313–8.
12. Wei Q, Spitz MR. The role of DNA repair capacity in susceptibility to lung cancer: a review. Cancer Metastasis Rev. 1997;16(3–4):295–307.
13. Ankathil R, Jyothish B, Madhavan J, Nair MK. Deficient DNA repair capacity: a predisposing factor and high risk predictive marker in familial colorectal cancer. J Exp Clin Cancer Res. 1999;18(1):33–7.
14. Burger K, Matt K, Keiser N, Gebhard D, Bergemann J. A modified fluorimetric host cell reactivation assay to determine the repair capacity of primary keratinocytes, melanocytes and fibroblasts. BMC Biotechnol. 2010;10:46–57.
15. Johnson JM, Latimer JJ. Analysis of DNA repair using transfection-based host cell reactivation. Methods Mol Biol. 2005;291:321–35.
16. Barakat BM, Wang QE, Han C, Milum K, Yin DT, Zhao Q, Wani G, Arafa E-S, El-Mahdy MA, Wani AA. Overexpression of DDB2 enhances the sensitivity of human ovarian cancer cells to cisplatin by augmenting cellular apoptosis. Int J Cancer. 2010;127(4):977–88.
17. Kusakabe M, Onishi Y, Tada H, Kurihara F, Kusao K, Furukawa M, Iwai S, Yokoi M, Sakai W, Sugasawa K. Mechanism and regulation of DNA damage recognition in nucleotide excision repair. Genes Environ. 2019;41:2.
18. Wang W, Xu J, Chong J, Wang D. Structural basis of DNA lesion recognition for eukaryotic transcription-coupled nucleotide excision repair. DNA Repair. 2018;71:43–55.
19. Stoyanova T, Roy N, Kopanja D, Bagchi S, Raychaudhuri P. DDB2 decides cell fate following DNA damage. Proc Natl Acad Sci U S A. 2009;106(26):10690–5.
20. Stoyanova T, Roy N, Kopanja D, Raychaudhuri P, Bagchi S. DDB2 (damaged-DNA binding protein 2) in nucleotide excision repair and DNA damage response. Cell Cycle. 2009;8(24):4067–71.
21. Perucca P, Sommatis S, Mocchi R, Prosperi E, Stivala LA, Cazzalini O. A DDB2 mutant protein unable to interact with PCNA promotes cell cycle progression of human transformed embryonic kidney cells. Cell Cycle. 2015; 14(24):3920–8.
22. Toga T, Kuraoka I, Watanabe S, Nakano E, Takeuchi S, Nishigori C, Sugasawa K, Iwai S. Fluorescence detection of cellular nucleotide excision repair of damaged DNA. Sci Rep. 2014;4:5578.
23. Tawarahara H, Kuraoka I, Iwai S. Facile preparation of a fluorescent probe to detect the cellular ability of nucleotide excision repair. Anal Biochem. 2017;526:71–4.

24. Simonelli V, Leuzzi G, Basile G, D'Errico M, Fortini P, Franchitto A, Vitli V, Brown AR, Parlanti E, Pascucci B, et al. Crosstalk between mismatch repair and base excision repair in human gastric cancer. Oncotarget. 2017;8(49):84827–40.
25. Fortini P, Dogliotti E. Base damage and single-strand break repair: mechanisms and functional significance of short- and long-patch repair subpathways. DNA Repair (Amst). 2007;6(4):398–409.
26. Zotter A, Luijsterburg MS, Warmerdam DO, Ibrahim S, Nigg A, van Cappellen WA, Hoeijmakers JH, van Driel R, Vermeulen W, Houtsmuller AB. Recruitment of the nucleotide excision repair endonuclease XPG to sites of UV-induced dna damage depends on functional TFIIH. Mol Cell Biol. 2006; 26(23):8868–79.
27. Riedl T, Hanaoka F, Egly JM. The comings and goings of nucleotide excision repair factors on damaged DNA. EMBO J. 2003;22(10):5293–303.

Publisher's Note

Springer Nature remains neutral with regard to jurisdictional claims in published maps and institutional affiliations.

Ready to submit your research? Choose BMC and benefit from:

- fast, convenient online submission
- thorough peer review by experienced researchers in your field
- rapid publication on acceptance
- support for research data, including large and complex data types
- gold Open Access which fosters wider collaboration and increased citations
- maximum visibility for your research: over 100M website views per year

At BMC, research is always in progress.

Learn more biomedcentral.com/submissions

BMC

BBA - Molecular Cell Research 1865 (2018) 898–907

Contents lists available at ScienceDirect

BBA - Molecular Cell Research

journal homepage: www.elsevier.com/locate/bbamcr

A damaged DNA binding protein 2 mutation disrupting interaction with proliferating-cell nuclear antigen affects DNA repair and confers proliferation advantage

Paola Perucca[a,1], Roberto Mocchi[a,1,2], Isabella Guardamagna[a], Elisabetta Bassi[a], Sabrina Sommatis[a,2], Tiziana Nardo[b], Ennio Prosperi[b,*], Lucia Anna Stivala[a,*], Ornella Cazzalini[a,*]

[a] Dipartimento di Medicina Molecolare, Unità di Immunologia e Patologia generale, Università degli Studi di Pavia, Pavia, Italy
[b] Istituto di Genetica Molecolare (IGM) del CNR, Pavia, Italy

ARTICLE INFO

Keywords:
DDB2
PCNA
NER
Genome instability
UV damage

ABSTRACT

In mammalian cells, Nucleotide Excision Repair (NER) plays a role in removing DNA damage induced by UV radiation. In Global Genome-NER subpathway, DDB2 protein forms a complex with DDB1 (UV-DDB), recognizing photolesions. During DNA repair, DDB2 interacts directly with PCNA through a conserved region in N-terminal tail and this interaction is important for DDB2 degradation. In this work, we sought to investigate the role of DDB2-PCNA association in DNA repair and cell proliferation after UV-induced DNA damage. To this end, stable clones expressing $DDB2^{WT}$ and $DDB2^{PCNA-}$ were used. We have found that cells expressing a mutant DDB2 show inefficient photolesions removal, and a concomitant lack of binding to damaged DNA *in vitro*. Unexpected cellular behaviour after DNA damage, such as UV-resistance, increased cell growth and motility were found in $DDB2^{PCNA-}$ stable cell clones, in which the most significant defects in cell cycle checkpoint were observed, suggesting a role in the new cellular phenotype. Based on these findings, we propose that DDB2-PCNA interaction may contribute to a correct DNA damage response for maintaining genome integrity.

1. Introduction

Genome integrity and its duplication fidelity are of fundamental importance for correct transmission of genetic information. Many factors, both exogenous and endogenous, can endanger the integrity of the genetic material by inducing DNA damage. To remove these lesions, mammalian cells have developed different DNA repair pathways and, among them, Nucleotide Excision Repair (NER) is specialised in removing DNA photoproducts induced by UV radiation [1,2]. In the global genome NER (GG-NER), the sub-pathway responsible for repair of transcriptionally inactive regions of the genome as well as the non-transcribed strands of expressed genes, DDB2 protein carries out a crucial role [3]. This factor forms with DDB1 and Cullin4A (Cul4A) the complex UV-DDB that recognizes both Cyclobutane Pyrimidine Dimers (CPDs) and 6-4 Photoproducts (6-4PPs), the major UV-lesions [4–6]. The complex formation is important not only for the damage recognition associated to the faster XPC recruitment, but also for the chromatin remodelling, thus facilitating the admission and binding of the repair factors [7]. In addition, the UV-DDB complex has a role in ubiquitination of DDB2 and XPC proteins [8,9] and in the same post-translational modification of H2A, H3 and H4 histones [10]. Furthermore, the homology of DDB2 with proteins that allow the reorganization of the chromatin has been demonstrated and the UV-DDB complex interaction with the STAGA complex has been observed [11].

DDB2 is involved in the early stages of damage recognition caused by UV radiation and in the early recruitment of the GG-NER repair proteins [12]. However, a possible role for DDB2 in tumorigenesis is under debate since different DDB2 expression levels in human cancer are reported [13–15]. In addition, experimental data highlight the DDB2 involvement in the epithelial to mesenchymal transition in cancer cells [16], whereas its overexpression limits stem cells abundance in cancer, thereby leading to the repression of tumorigenesis

Abbreviations: DDB2, damaged DNA binding protein 2; $DDB2^{WT}$, DDB2 wild-type protein; $DDB2^{PCNA-}$, DDB2 unable to interact with PCNA protein; CPDs, Cyclobutane Pyrimidine Dimers; Cul4A, Cullin 4A; NER, Nucleotide Excision Repair; PCNA, Proliferating Cellular Nuclear Antigen; PIP, PCNA Interacting Protein; 6-4PPs, 6-4 Photoproducts; UDS, Unscheduled DNA Synthesis; XPC, Xeroderma Pigmentosum group C

* Corresponding authors.
E-mail addresses: prosperi@igm.cnr.it (E. Prosperi), lucianna.stivala@unipv.it (L.A. Stivala), ornella.cazzalini@unipv.it (O. Cazzalini).
[1] Perucca P. and Mocchi R. contributed equally to this work.
[2] Present address: UB-CARE S.r.l., Spin-off University of Pavia, Pavia.

https://doi.org/10.1016/j.bbamcr.2018.03.012
Received 30 August 2017; Received in revised form 21 March 2018; Accepted 26 March 2018
Available online 28 March 2018
0167-4889/ © 2018 Elsevier B.V. All rights reserved.

[17].

Recently, we have demonstrated that DDB2 interacts with PCNA [18], and that the expression of a mutant form abolishing this interaction ($DDB2^{PCNA-}$), promoted cell proliferation [19].

In this work, we sought to study the effect of $DDB2^{PCNA-}$ protein expression on DNA repair efficiency and on cell proliferation and migration after DNA damage. For this reason, $DDB2^{PCNA-}$ transiently or stably transfected epithelial cells were irradiated with UV-C and DNA repair efficiency was evaluated both by CPDs removal and Unscheduled DNA Synthesis (UDS). In addition, $DDB2^{PCNA-}$ binding capability to DNA damaged sites was explored in *in vitro* assay. Finally, cell damage response to UV irradiation was investigated in terms of cell clonogenic efficiency, proliferation and motility.

We demonstrate that the loss of the interaction between DDB2 and PCNA influences different aspects of the DNA damage response: i) delaying the removal of UV-induced DNA damage; ii) determining an increase in UV-resistance; and iii) conferring a proliferation advantage, as determined by changes in cell growth and motility. These results suggest that the interaction between PCNA and DDB2 contributes to preserve genome stability by promoting DNA repair and by controlling cell cycle checkpoints.

2. Materials and methods

2.1. Cell lines and transfection

HeLa S3 cell line was cultured in Dulbecco's modified Eagle's medium (DMEM, Sigma) supplemented with 10% foetal bovine serum (Life Technologies-Gibco), 2 mM L-glutamine (Life Technologies-Gibco), 100 U/ml penicillin, 100 μg/ml streptomycin in a 5% CO_2 atmosphere.

HeLa S3 cells seeded on coverslips or Petri dishes (70% confluent) were transiently transfected with the $DDB2^{WT}$ kindly provided by Q. Wang [13], or the mutated DDB2 form ($DDB2^{PCNA-}$) using Effectene transfection reagent (Qiagen). DDB2 mutated in the PIP-box sequence was produced as previously described [18].

The irradiation was usually performed 24 h after transfection. Cell exposure to UV-C was performed with a lamp (Philips TUV-9) emitting mainly at 254 nm, at doses of 10, 30 or 100 J/m^2, as measured with a DCRX radiometer (Spectronics). Localized irradiation was performed by laying Isopore polycarbonate filters (Millipore) with 3 μm pores on top of the cells.

HEK293 (Human Embryonic Kidney) cell line was grown as above described. Cells (50% confluent) were stably transfected with the same constructs ($DDB2^{WT}$ and $DDB2^{PCNA-}$) [19].

2.2. Analysis of global genome repair (GG-NER)

HEK293 control cells or stably transfected with $DDB2^{WT}$ and $DDB2^{PCNA-}$ were seeded on coverslips or Petri dishes and 24 h later were washed in PBS, exposed to 30 J/m^2 of UV-C radiation, and harvested at 0 min, 0.5, 4, 8, 24 h.

The DNeasy tissue kit (Qiagen) was used to extract the DNA. The GG-NER efficiency was performed by an immunoblot assay of CPDs removal from DNA [20]. Briefly, DNA was denatured using PCR and blotted in triplicate on nitrocellulose using a Schleicher & Schuell apparatus that allows the DNA binding through a vacuum system. Membranes were fixed by heating at 70 °C for 90 min, blocked with 5% dry milk and incubated with the antibodies mouse monoclonal anti-CPDs (Kamiya Biomedical Company; RRID: AB_1233355), mouse anti Ig-G biotinylated (1:2000, Sigma) and streptavidinHRP (1:2000, Amersham Biosciences).

Reactive bands were visualized with the ECL system (Pierce) using a Li-Cor C-DiGit blot scanner and a densitometric analysis was performed with Li-Cor Image Studio Lite software.

2.3. Analysis of DNA repair by UDS determination

In control and transfected HEK293 cells, UDS was determined after irradiation (20 J/m^2), by incubating cells for 2 h in medium containing 1 ml [^{3}H]-thymidine (NEN, 10 Ci/ml specific activity), then chased for 1 h in medium containing 10 mM each cold thymidine and cytidine. Cells were then fixed in 4% formaldehyde and post-fixed in 70% ethanol. Samples were processed for autoradiography using an Ilford K2 emulsion, exposed for 4 days at 4 °C, and then developed and fixed before mounting on microscope slides. Autoradiographic granules were counted in 50 non-S phase cells showing DDB2 staining, in duplicate experiments [21].

2.4. Gel electrophoretic mobility shift assay

For the DNA binding assay, plasmid DNA (pEGFP-N1, Clontech) was irradiated at 800 J/m^2 and then mixed with each recombinant DDB2 (Wt or mutant form) and recombinant DDB1 human protein (Abnova). The reactions were conducted in 28 mM sodium phosphate (pH 7.5), containing 150 mM NaCl, 3.4 mM $MgCl_2$, 1.4 mM EDTA, 2% glycerol and 0.1 mg/ml BSA, at 30 °C for 30 min and 1 h. Gel electrophoresis was performed in TBE 1 × buffer and DNA was run on 1% agarose gel at 40 V for 3 h. The gel was photographed by transilluminator UST-20M-8E on Darkhood DH-30/32 (Biostep).

2.5. Immunofluorescence and confocal microscopy

HeLa cells seeded on coverslips and transiently transfected as described above, were locally irradiated (100 J/m^2) and re-incubated in whole medium for the indicated period of time (5, 10, 30, 60 and 240 min). The cells on coverslips were then washed twice in cold PBS, fixed, and lysed in buffer containing freshly made 2% paraformaldehyde, 0.5% Triton X-100 in PBS, 0.2 mM phenylmethylsulfonyl fluoride (PMSF), and 0.2 mM Na_3VO_4 for 30 min at 4 °C. Then, the samples were washed twice with cold PBS and treated with 2 M HCl at 37 °C for 10 min to denature the DNA, followed by a PBS rinse to remove HCl [22]. After re-hydration, the samples were blocked in PBST buffer (PBS, 0.2% Tween 20) containing 1% bovine serum albumin (BSA), and then incubated for 1 h with specific antibodies: goat polyclonal anti-DDB2 (1:100, Santa Cruz; RRID: AB_2088827), mouse monoclonal anti-CPDs (1:1000, Kamiya Biomedical Company; RRID: AB_1233355) and rabbit polyclonal anti-XPC (1:400, Sigma; RRID: AB_796183), all diluted in PBST buffer/BSA. After washing, each reaction was followed by incubation for 30 min with anti-mouse (Molecular Probes; RRID: AB_141607) or anti-rabbit (Molecular Probes; RRID: AB_141708) antibody conjugated with Alexa 488, anti-goat Alexa Fluor 594 (Molecular Probes; RRID: AB_14240). After immunoreactions, the cells were incubated with Hoechst 33258 dye (0.5 μg/ml) for 2 min at RT and washed in PBS. The slides were mounted in Mowiol (Calbiochem) containing 0.25% 1,4-diazabicyclo-octane (Aldrich) as antifading agent. Images of fixed cells were taken with a Nikon Eclipse E400 fluorescence microscope equipped with a Canon Power Shot A590 IS digital camera. Fluorescence signals were acquired with a TCS SP5 II Leica confocal microscope, at 0.3 μm intervals. Image analysis was performed using the LAS AF software.

2.6. Western blot and pull down

HeLa S3 and HEK293 cells were seeded at the density of 1 × 10^6 into 100 mm cell culture dishes. The day after, cells were washed with PBS and irradiated with a lamp at a dose of 10 or 30 J/m^2 UV-C. The medium was added to the cells, incubated at 37 °C to allow repair and harvested at the indicate post-UV irradiation times.

For blot analysis, the cells were directly lysed in SDS sample buffer (65 mM Tris-HCl pH 7.5, 1% SDS, 30 mM dithiothreitol (DTT), 10% glycerol, 0.02% Bromophenol Blue), or fractionated in soluble and

chromatin-bound fractions, as previously described [23] with minor modifications. The cells were lysed in hypotonic buffer containing 10 mM Tris-HCl (pH 7.4), 2.5 mM $MgCl_2$, 1 mM PMSF, 0.5% Nonidet NP-40, 0.2 mM Na_3VO_4, and a mixture of protease and phosphatase inhibitor cocktails (Sigma). After 10 min on ice, the cells were pelleted by low-speed centrifugation (200 g, 1 min), and the detergent-soluble fraction was recovered. Lysed cells were washed once in hypotonic buffer, followed by a second wash in 10 mM Tris-HCl buffer (pH 7.4), containing 150 mM NaCl, and protease/phosphatase inhibitor cocktails. The cell pellets were then incubated with DNaseI (20 U/10^6 cells) in 10 mM Tris-HCl (pH 7.4), 5 mM $MgCl_2$, and 10 mM NaCl for 15 min at 4 °C. After a brief sonication on ice, the samples were centrifuged again (13,000g, 1 min), and the supernatant containing the chromatin-bound fraction was collected. For immunoprecipitation, about 10^7 cells were re-suspended in 1 ml lysis buffer and fractionated as above. Equal amounts of each extract were incubated with anti-DDB2 rabbit polyclonal antibody (Santa Cruz; RRID: AB_2276986), pre-bound to protein G Dynabeads (Invitrogen). Half the amount of each antibody was used for chromatin-bound fractions. The reactions were performed for 3 h at 4 °C under constant agitation. The samples were then centrifuged at 14000g (30 min, 4 °C), and immunocomplexes were washed with ice-cold 50 mM Tris-HCl (pH 7.4) containing 150 mM NaCl, 0.5% Nonidet NP-40. Immunoprecipitated peptides were eluted in SDS sample buffer and resolved by SDS-PAGE (SDS-PAGE). Proteins were electro-transferred to nitrocellulose, then membranes were blocked for 30 min in 5% non-fat milk in PBST buffer and probed with the following primary antibodies: anti-DDB1 (1:1000, Genetex; RRID: AB_1950102), anti-DDB2 (1:500, Santa Cruz; RRID: AB_2088827), anti-PCNA (1:1000, Dako; RRID: AB_2160651), anti-CUL4A (1:500, Sigma; RRID: AB_1847339), anti-XPC (1:1000, Sigma; RRID: AB_796183), anti-p21 (1:500, Santa Cruz; RRID: AB_632121) and anti-actin (1:1000, Sigma; RRID: AB_476730), anti-P-Ser139-H2AX (Biol.egend, San Diego, CA; RRID: AB_315794), anti-P-Ser-317-Chk-1 (Cell Signalling; RRID: AB_331488), anti-P-Ser-345-Chk-1 (Cell Signalling; RRID: AB_330023) diluted 1:1000, anti-panH2AX (Santa Cruz) diluted 1:1000 and anti-panChk (Santa Cruz, RRID: AB_1121554) diluted 1:500. The membranes were then washed in PBST, incubated for 30 min with appropriate HRP-conjugated secondary antibodies: anti-mouse (DAKO), anti-goat and anti-rabbit (KPL) and revealed using enhanced chemiluminescence. All the pull-down experiments were performed at least 3 times. The densitometric analysis was performed using the public software ImageJ (http://rbs.info.nih.gov/nih-image).

2.7. Clonogenic efficiency

Control and stable transfected HEK293 cells were seeded (1×10^6) in 100 mm cell culture dishes. After two days, cells were exposed to 10 J/m^2 UV-C radiation and immediately trypsinized and harvested and re-seeded (5×10^2) in 60 mm cell culture dishes. The clonogenic efficiency was also assessed with cells that were not exposed to UV-C radiations [19]. After a period of 7–10 days, to prevent the cell confluence, the colonies were stained with Gentian Violet to count their number and to analyze their shape for each cell line. Cells were washes twice in PBS and the Petri dishes were covered with the dye for 20 min under constant stirring. Then, the dye was washed several times with distilled water and the colonies were air dried and counted.

To evaluate morphological features of colonies, control and stable transfected HEK293 cells were seeded (5×10^5) in 35 mm cell culture dishes containing a coverslip. After two days, cells were exposed to 10 J/m^2 UV-C radiation, immediately trypsinized, harvested and re-seeded (2×10^5) on coverslips. After 3 days, the samples were stained with May-Grünwald Giemsa using a standard protocol (May-Grünwald, Merck and Giemsa, Carlo Erba). Number of total cells per colony, dead cells and mitosis were counted and photographed under a digital microscope Nikon Eclipse 80i with a camera Nikon Digital Sight DS-Fi1.

2.8. Wound-healing assay

For cell motility assays, wound healing was performed using the Ibidi Culture-Insert (Madison, WI) according to the manufacturer's instructions. Control and stable transfected HEK293 cells were seeded (1×10^6) in 100 mm cell culture dishes. After two days, cells were exposed to 10 J/m^2 UV-C radiation and immediately trypsinized. 70 μl of cell suspension (7×10^4 cells) were applied to each culture-insert, allowing the cells to grow in the designated areas until a confluent layer was formed at 37 °C. Thereafter, the culture-insert was removed, creating a cell-free gap. Wound closure was monitored daily and photographed starting from 0 to 10 d with an inverted light microscope equipped with a Canon A590 IS camera (Tokyo, JP). The analysis was performed using the public software ImageJ (http://rbs.info.nih.gov/nih-image).

2.9. Statistical analysis

Results are expressed as mean ± standard deviation. Statistical significance was calculated using the Student *t*-test.

3. Results

3.1. Expression of DDB2^{PCNA-} impairs UV-lesion removal

In order to verify the capability of DDB2^{PCNA-} protein in removing the UV-induced DNA damage, untransfected control HEK293 and DDB2^{WT} or DDB2^{PCNA-} stable clones were irradiated and collected at different recovery times, as indicated in the Fig. 1A. Total DNA was extracted, quantified, spotted into nitrocellulose membrane and incubated with CPDs antibody (for detail see Material and Methods). Cells expressing DDB2^{WT} showed an efficient DNA repair, with > 40% of CPD removal at 24 h after UV radiation (Fig. 1A), even higher than that of control cells (about 30%). On the contrary, the mutant clone appeared very slow in repairing these DNA lesions. To exclude any effect of lesion dilution by DNA replication, we performed BrdU assays that show comparable results regarding the proliferation of the two stable clones (Fig. S1 in Supplementary Appendix).

Similarly, in UDS experiments (Fig. 1B and C), unscheduled DNA repair synthesis is strongly reduced in human cells expressing DDB2 mutant protein, whereas no significant modifications were observed in cells expressing DDB2^{WT} protein compared to control cells. These two different approaches demonstrated that the mutated form of DDB2 modifies the cellular response against UV-C induced lesions.

In order to evaluate whether DDB2^{PCNA-} affects directly damaged DNA binding, we performed gel electrophoretic motility shift assay. To this end, damaged plasmid DNA was incubated with each recombinant DDB2 proteins, in the presence of DDB1. DDB2^{WT} bound damaged DNA both 0.5 and 1 h after incubation, as demonstrated by the shift in migration of linearized DNA, which was not revealed in the presence of the mutant protein.

3.2. Impairment of DDB2^{PCNA-} recruitment at DNA damaged sites

To verify the DNA damage site recruitment of DDB2 exogenous proteins, we performed immunofluorescence time course experiments. To this end, we used HeLa cells since HEK293 cells do not adhere firmly on the glass surface. HeLa cells were transiently transfected with DDB2^{WT} or DDB2^{PCNA-} constructs, locally irradiated, lysed at different time points: 0.5, 1 and 4 h after UV damage and immunostained for DDB2. Fig. 2A shows that the highest percentage of DDB2 positive cells was detected at 1 h after damage in cells expressing DDB2 mutated; instead, the highest recruitment for DDB2^{WT} was observed at 0.5 h, as also evidenced by representative images obtained with confocal microscopy. To confirm this different behaviour, we performed co-localization studies using specific antibodies against DDB2 and CPDs. The

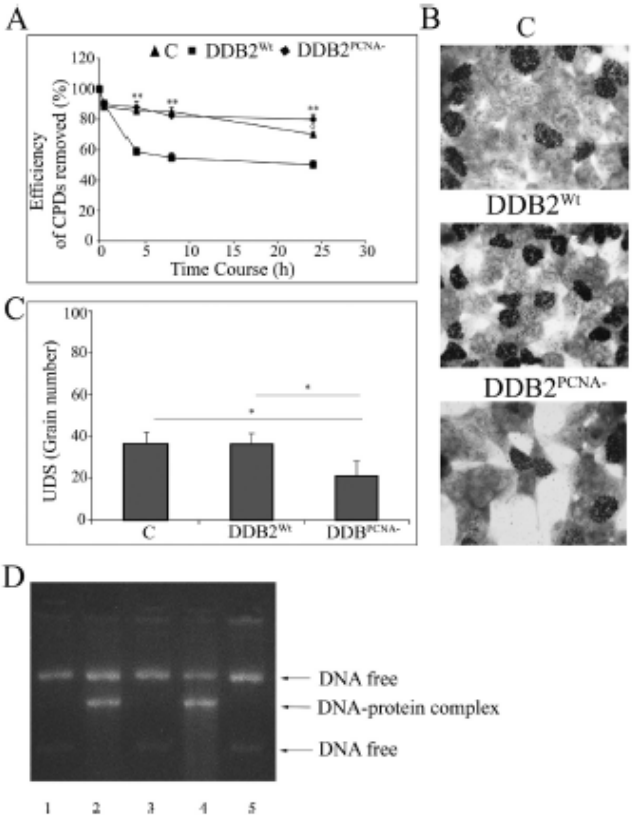

Fig. 1. Effect of the DDB2 mutation on the cells' efficiency to repair the DNA damage after UV-C irradiation. (A) HEK293 control cells, $DDB2^{Wt}$ and $DDB2^{PCNA-}$ stable clones were irradiated (20 J/m^2), collected at the indicated recovery times to detect CPDs removal from DNA. Data are mean ± S.D. from at least three independent experiments; values are expressed in percentage. Asterisks indicate $^*p < 0.05$ or $^{**}p < 0.01$ compared to $DDB2^{Wt}$ transfected cells. $^*p < 0.05$ compared to HEK293 control cells. (B) HEK293 control cells, $DDB2^{Wt}$ and $DDB2^{PCNA-}$ clones were UV-C irradiated (20 J/m^2), incubated for 2 h in [^{3}H] thymidine and then fixed. UDS is denoted by the presence of nuclear autoradiographic granules. (C) Quantification of UDS grains in nuclei of cells from HEK293 stable clones and control cells treated as above. Mean values of grain number (± S.D.) in triplicate samples are reported. (D) Gel electrophoretic mobility shift assay. Damaged plasmid DNA (lane 1), damaged DNA incubated for 30 min (lines 2–3) or 1 h (lanes 4–5) with DDB1 recombinant protein and $DDB2^{Wt}$ (lanes 2–4) or $DDB2^{PCNA-}$ proteins (lanes 3–5).

co-localization images (Figs. 2B and S2) showed that DDB2 mutated protein presents a delayed recruitment at DNA damage sites. In fact, a weak focalized co-localization begins to be detectable only 1 h after UV damage while a diffuse DDB2 staining in all the nuclear area is visible at earlier times. On the contrary, $DDB2^{Wt}$ is distinctly and significantly recruited at foci already 0.5 h after irradiation.

Time-course experiments to analyze the recruitment of DDB2 and XPC proteins (Fig. 2C) showed a very early chromatin association of XPC protein and $DDB2^{Wt}$, indicating 5 min after DNA damage as the best time for co-localization between these two NER proteins. Whereas, the recruitment of the two proteins occurred significantly only 1 h after UV-damage induction in the presence of the mutated form of DDB2 (Figs. 2C and S3 in Supplementary Appendix).

Altogether, the collected data show that the mutated $DDB2^{PCNA-}$ modifies the kinetic of co-localization with CPDs and/or XPC protein, thus suggesting a delay in the initiation of the repair process.

3.3. DDB2 mutation delays initiation of the NER process

In order to understand the mechanism underlying the different recruitment of DDB2 mutant protein, the interaction of DDB2 with crucial NER proteins was investigated. To this end, immunoprecipitation of proteins recruited at DNA was performed in HeLa cells expressing $DDB2^{Wt}$ or $DDB2^{PCNA-}$. In Fig. 3, soluble and chromatin bound fractions derived from irradiated cells, harvested at 0.5 and 1 h after UV damage, showed three important differences: i) the persistence of the $DDB2^{PCNA-}$ protein bound to the DNA until 1 h from the irradiation. As expected, no bands of PCNA were detectable in the specific lane, indicating that the protein is not able to immunoprecipitate with DDB2, and confirming that the mutation introduced in the PIP-box is actually able to prevent the interaction between the two proteins (Fig. 3D). (ii) The association between $DDB2^{PCNA-}$ and DDB1 was already detectable in the chromatin fraction immediately after the irradiation, and it increased with the recovery time after DNA damage. A similar trend was observed for XPC protein, whose interaction with $DDB2^{PCNA-}$ increased with time, reaching the highest value at 1 h. The latter result is markedly different from that obtained with the Wt protein, where the XPC level was maximum at 0.5 h (Fig. 3B). (iii) The last aspect, regarding $DDB2^{PCNA-}$/Cul4A interaction, showed again a shifted forward of their association, compared to the results obtained with $DDB2^{Wt}$, where already at 0.5 h the Cul4A protein level was of lower intensity (Fig. 3B). This early interaction between $DDB2^{Wt}$ and NER proteins has already been demonstrated [18]. Taken together, these results confirm a delay in NER machinery initiation when DDB2 presents a mutation in the PIP-box.

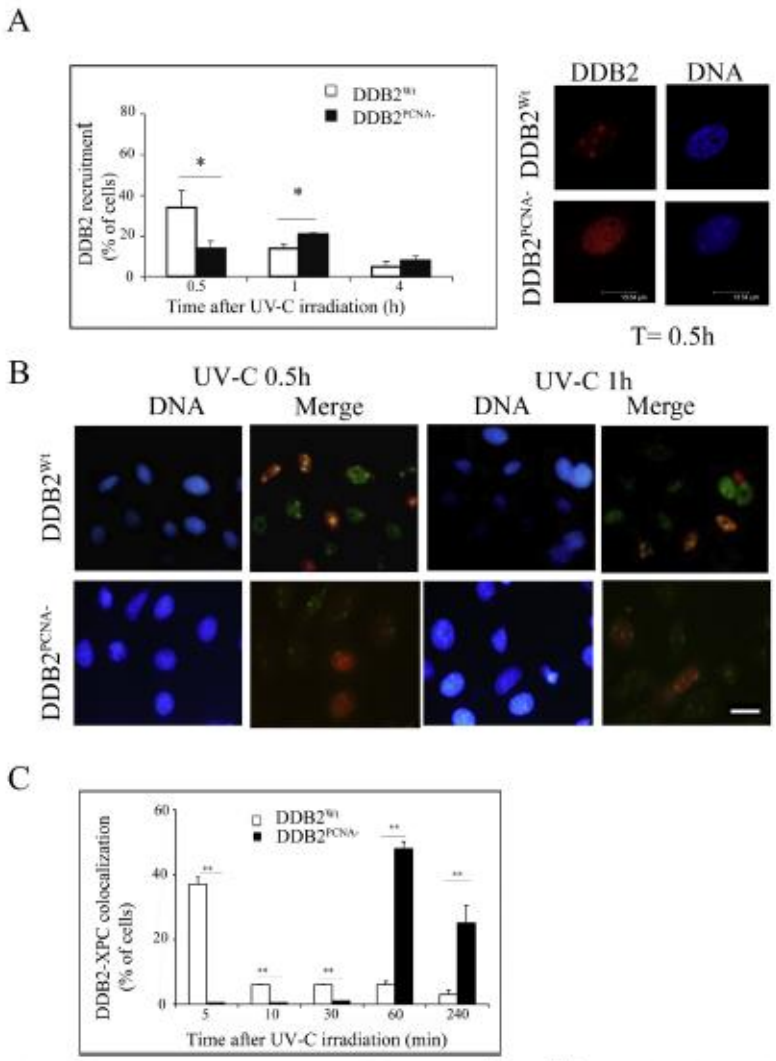

Fig. 2. Recruitment of DDB2 and NER proteins to DNA repair sites. (A) HeLa cells expressing DDB2^{WT} or DDB2^{PCNA-} were exposed to local UV-C radiation (100 J/m^2) through filters with 3 μm pores. After 0.5, 1 and 4 h, irradiated cells were extracted *in situ* and fixed for immunofluorescence staining with anti-DDB2 antibody. Results from DDB2^{WT} (empty bars) and DDB2^{PCNA-} (black bars) clones were shown. Besides, representative confocal images of the DDB2 recruitment (0.5 h after UV-C) on DNA damage site in DDB2^{WT} and DDB2^{PCNA-} cells were presented. Scale bar = 13.54 μm. (B) HeLa cells were transfected with pcDNA3.1-DDB2^{WT} or pcDNA3.1-DDB2^{PCNA-} expression vectors and 24 h later exposed to local UV-C radiation (100 J/m^2). Half and 1 h later, samples were extracted *in situ* and fixed for immunofluorescence determination CPDs (green) and DDB2 (red), respectively. In the merged images, spots of colocalization (yellow) are clearly visible. DNA (blue fluorescence) was stained with Hoechst 33258. Scale bar = 20 μm. (C) HeLa cells expressing DDB2 wild type or mutated form were locally irradiated (UV-C 100 J/m^2), DDB2-XPC co-localization was analyzed at 5, 10, 30, 60, 240 min after UV-C damage and the percentages of positive cells were reported. * $p < 0.05$ and ** $p < 0.01$. (For interpretation of the references to color in this figure legend, the reader is referred to the web version of this article.)

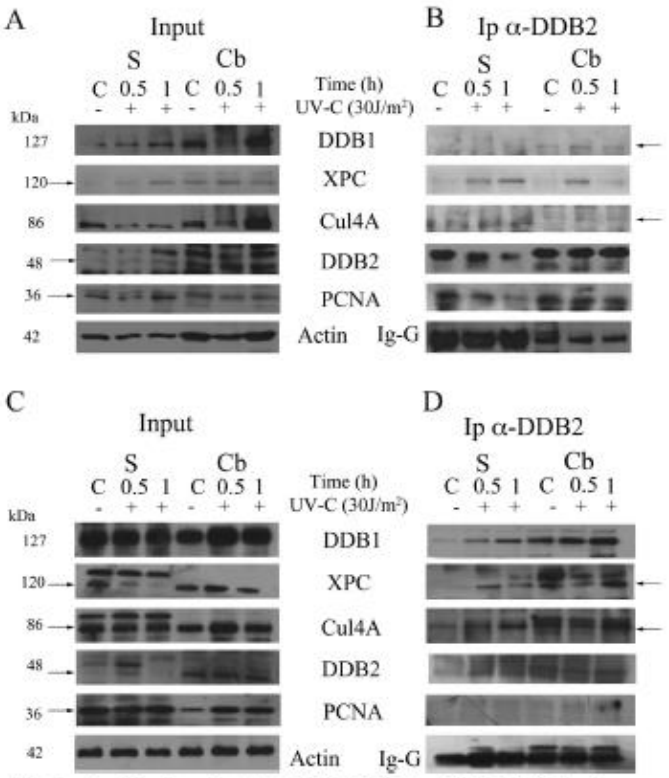

Fig. 3. DDB2 interaction with NER proteins. HeLa cells transfected with pcDNA3.1-DDB2^{WT} and pcDNA3.1-DDB2^{PCNA-} plasmids were grown for 24 h and collected 0.5 and 1 h after UV-C irradiation (30 J/m^2), as described in "Materials and Methods". Cells were fractionated in soluble (S) and chromatin-bound (Cb) samples for immunoprecipitation and analysed by Western blot. (A–C) Input load: 1/30 of cell extract. (B–D) Immunoprecipitation (Ip) with anti-DDB2 antibody on fractionated cell extracts, as indicated above. Arrows indicate the specific protein bands.

3.4. DDB2^{PCNA-} influences cell growth and motility after UV-C irradiation

We have previously shown that the expression of DDB2^{PCNA-} protein resulted in an increased cell proliferation [19]. To evaluate the effect of DDB2^{PCNA-} protein on cellular growth following DNA damage, we performed a clonogenic assay using HEK293 stable clones irradiated, seeded in 60 mm Petri dishes and incubated for 10 days to allow colony formation.

The results showed that stable DDB2^{PCNA-} clone produces more colonies, characterized also by a larger size, than those observed in cells expressing DDB2^{WT}. As expected, control cells did not grow after UV irradiation and only very few and faded colonies were present (Fig. 4A). All data are summarized in Fig. 4B in which is pointed out that the presence of exogenous DDB2, both wild-type and even more, the mutated form, unexpectedly determined an increase in cell survival after UV irradiation. Similarly, visual scoring of 3 days growing colonies stained with May-Grünwald Giemsa after UV-C irradiation confirmed that the number of cells per colony is higher in both wild-type and, even more, in the mutated clone respect to control cells. In contrast, dead cells are more numerous in the last one, and rare in DDB2^{PCNA-} stable clone. Finally, although the number of mitosis appeared comparable in the both clones, atypical forms are significantly increased in the DDB2 mutated cells (Fig. 4C and D).

Next, we investigated whether DDB2 stable expression could also influence cell motility. HEK293 stable clones exposed to UV-C radiation were seeded and wound healing assay was carried out. Fig. 4C shows representative images obtained by time-course experiments, starting from the cell wall (cell front) formation at time 0 until 10 days later. Cell motility, and consequently the ability to reconstitute the cell monolayer, started to be evident 7 days after UV irradiation, mainly in cells expressing exogenous DDB2 proteins. At this time, a higher cell motility and growth was observable in the presence of DDB2^{PCNA-}; in fact, cells were able to form dense multilayer of growing cells, evident in both cellular walls. The same feature was detectable two days later (9 d) in cells producing DDB2^{WT} when, in the presence of DDB2^{PCNA-}, the wound healing was entirely filled up.

In addition, the disordered and persistent growth in cells expressing DDB2 mutant protein suggests a major UV-C resistance acquired by this clone.

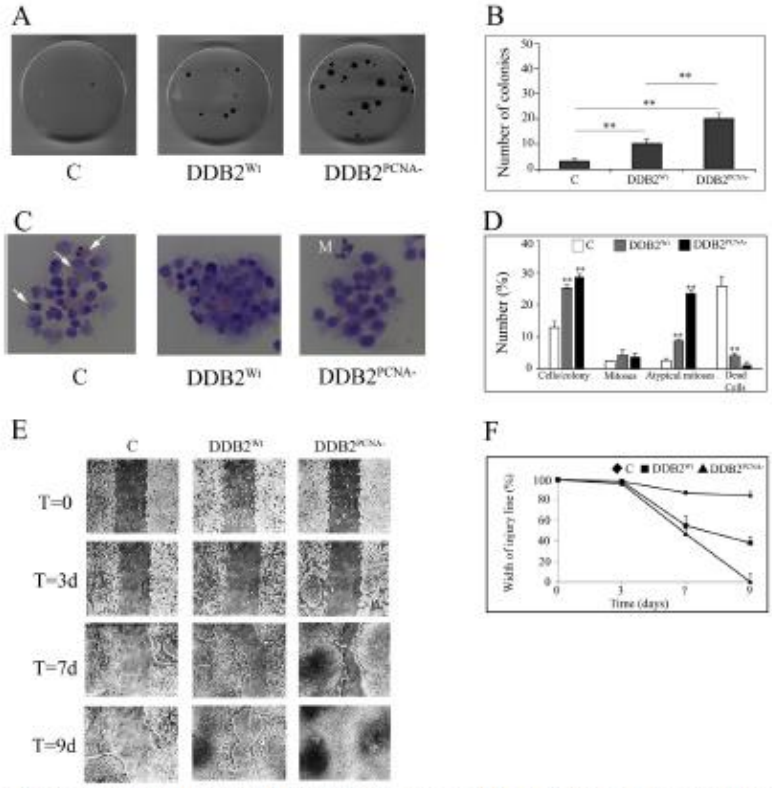

Fig. 4. Clonogenic efficiency and cell motility of DDB2^{WT} and DDB2^{PCNA-} clones after UV-induced DNA damage. HEK293 cells were seeded at the density of 1×10^6 into 100 mm cell culture dishes, irradiated (10 J/m^2 UV-C) and immediately harvested and re-seeded (5×10^5) both in 60 mm cell culture dishes for colony growth and (7×10^4) in culture-insert for wound-healing assay. (A) Representative images of colonies formed by control HEK293 cells, DDB2^{WT} and DDB2^{PCNA-} stable clones. After 10 days, the colonies were fixed, stained with crystal violet and then counted. Mean values (± S.D.) are reported from 3 independent experiments. (B) Number of colonies grown of DDB2^{WT} and DDB2^{PCNA-} clones vs. control cells. * $p < 0.05$ and ** $p < 0.01$. (C and D) Morphological features of May-Grünwald Giemsa-stained growing colonies of control, DDB2^{WT} and DDB2^{PCNA-} stable clones. Most of the cells in control colonies are dead (arrows) compared to the stable clones. Representative atypical mitosis (M) in DDB2^{PCNA-} stable clone. (E) Representative processed images of cell motility (× 10 magnification objective) of control HEK293 cells, DDB2^{WT} and mutated clones. (F) Migration rate quantification of HEK293 control and stable clones; data are the mean ± S.D. from at least three independent experiments, normalized to 100% wound closure for untreated cells.

3.5. Reduction on p21 protein level in the presence of DDB2^{PCNA-}

To further understand whether the above results could be dependent on cell cycle regulator factors, p21 protein level were investigated. Our previous data have demonstrated that lower level of this cell cycle inhibitor was related to high cell proliferation rate, in the presence of DDB2^{WT} and even more with the mutated form [19]. To perform a kinetic analysis of p21 protein level, cells were collected and its amount evaluated by Western blot analysis at 1, 3, 6 and 24 h after UV damage (Fig. 5A). The results reported in Fig. 5B show a rapid decrease in p21 levels, both in control and in DDB2^{WT} samples; the presence of DDB2^{PCNA-} appears to further reduce this protein. At longer times after UV-damage, p21 protein level remains low and similar in the control and DDB2 stable clones (Supplemental Fig. S4).

3.6. DDB2^{PCNA-} causes defective cell cycle checkpoints activation

To go further insight into the molecular pathway responsible for the loss of cell proliferation control after UV-C exposure, the expression of some key proteins involved in the checkpoints activation was investigated. In particular, the phosphorylated form of the histone H2AX (γ-H2AX), playing a key role in the signalling pathway of genomic damage, was the first protein analysed by Western blot (Fig 6A and B). For this purpose, HEK293 control cells and stable clones DDB2^{WT} and DDB2^{PCNA-} were irradiated with UV-C (10 J/m^2) and then recovered for 0.5 and 1 h. Cells of each non-irradiated line were kept as negative control. The results showed that the ectopic expression of DDB2^{WT} did not influence the activation kinetics of the histone H2AX, as compared with control cells in which a statistically significant increase was observed after the induction of DNA damage. High basal levels of γ-H2AX

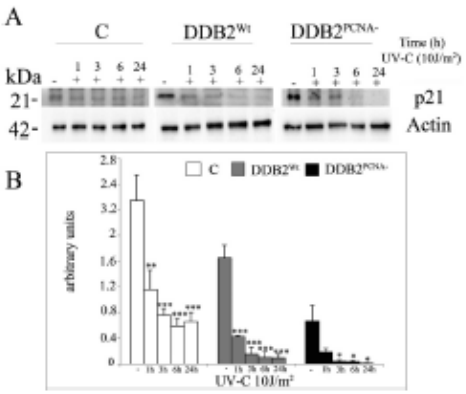

Fig. 5. p21 protein levels in control HEK293 cells, DDB2^{Wt} and DDB2^{PCNA-} stable clones at the indicated time point after UV-C irradiation. HEK293 control cells and DDB2 cell clones were plated (1×10^6) in 100 mm cell culture dishes, irradiated (10 J/m^2 UV-C) and harvested at different times. (A) Representative image from Western blot analysis of samples from control and DDB2 cell clones, in which the level of p21 and actin are shown. (B) p21 protein levels normalized to actin values through densitometric analysis. Mean values (± S.D.) are from 3 independent experiments. *$p < 0.05$ and **$p < 0.01$.

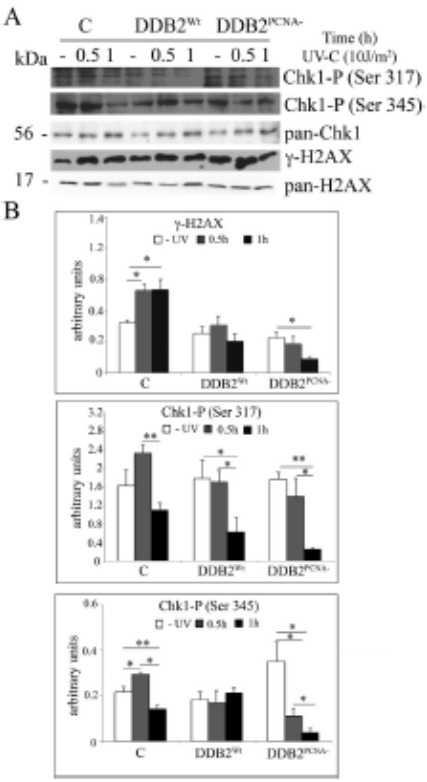

Fig. 6. Checkpoint activation in control HEK293 cells, DDB2^{Wt} and DDB2^{PCNA-} stable clones after UV-induced cell damage. HEK293 control cells and DDB2 cell clones were plated (1×10^6) in 100 mm cell culture dishes, irradiated (10 J/m^2 UV-C) and harvested at different times as indicated in the figure. In (A) representative images of γ-H2AX (Ser139), Chk1-P (Ser317), Chk1-P (Ser345) obtained by Western blot. (B) Protein levels normalized to pan-H2AX and pan-Chk1 values through densitometric analysis. Mean values (± S.D.), obtained from 3 independent experiments, were reported. *$p < 0.05$ and **$p < 0.01$.

was found in cells expressing the mutant form of DDB2 in which no further increase was found one hour after UV irradiation. These data suggest that loss of interaction between DDB2 and PCNA negatively affects the cell response that should be activated immediately after the damage.

Considering both mitotic activity and defective signalling of DNA damage in cells expressing DDB2^{PCNA-}, levels of the phosphorylated forms of Chk1 protein, that plays an important role in blocking cell cycle progression, were considered (Fig. 6A e B). Specifically, this protein is part of the G2/M phase checkpoint that monitors and regulates cellular mitosis. Fig. 6 shows the results of the analysis of the phosphorylated forms of Chk1 (Chk1-P) on both serine 317 (S317) and serine 345 (S345). The increase in the phosphorylation levels of this protein is comparable between the control and the stable DDB2^{Wt} clone, indicating that the checkpoint is correctly activated after the DNA damage. In the presence of DDB2^{PCNA-}, however, no activation is detected. In addition, the Chk1-P (S317), as well Chk1-P (S345) levels are low, opening to the hypothesis that the loss of control of this checkpoint could drive cells to mitosis, without repairing DNA damage.

4. Discussion

The UV rays are responsible for the induction of pyrimidine dimers which, if not removed, can cause genetic instability, mutations and the onset of skin cancer. In fact, some diseases with a defect of the NER machinery (e.g. *Xeroderma pigmentosum*) are characterized by high photosensitivity and high incidence of skin cancers [24].

The DDB2 role in tumorigenesis is still debated since different DDB2 expression levels in human cancer have been reported [13–15]. In addition, the DDB2 involvement in the epithelial to mesenchymal transition in cancer cells has been described [16] whereas its overexpression inhibits tumorigenesis [17].

We have previously demonstrated that mutations in DDB2 PIP-box, a conserved sequence useful to direct interaction with PCNA, promote cell cycle progression [19]. In the present study, we sought to investigate the role of DDB2-PCNA association in the cell response to UV-induced DNA damage. Our results have shown that expression of the mutant DDB2 form unable to interact with PCNA impaired DNA repair, that may be explained by inefficient binding to damaged DNA *in vitro*. Remarkably, the DDB2^{PCNA-} cells acquired uncontrolled cell growth, as indicated by an increased resistance to UV irradiation and also a more aggressive phenotype, as suggested by wound healing experiments. Explanation of such proliferative behaviour appears to be related to a defect in cell cycle checkpoint signalling, since DDB2^{PCNA-} cells show aberrant phosphorylation of H2AX and Chk1 both before and after UV-induced DNA damage. Interestingly, it has been previously reported that DDB2 influences checkpoint activation after UV-damage and, in particular, regulate H2AX and Chk1 phosphorylation [25]. In addition, it has been reported that DDB2 protein level can regulate Chk1 phosphorylation influencing ATR recruitment on chromatin, as well as in signalling checkpoint termination [26,27]. Therefore, our results are in agreement with these findings, and suggest that failure to correctly activate the cell cycle checkpoint could have provided the DDB2^{PCNA-}

cells with an enhanced proliferation and motility, two characteristic hallmarks of tumours. Accordingly, in DDB2^{PCNA-} irradiated cells a higher number of atypical mitosis has been detected in respect to the Wt stable clone or, even more, to control cells. Furthermore, UV-resistance phenotype of both clones is highlighted by the rare events of cell death. These results are also in agreement with the tumour-prone phenotype shown by DDB2-deficient mice, in which the inefficient DNA repair function has been related with the properties of increased cell proliferation and adhesion typical of the cancer phenotype [28,29].

Many papers have demonstrated that p21 has a role in modulating DNA repair process [30–34]. In particular, it has been reported a co-operation between DDB2 and p21 proteins in the cellular response to UV radiation [14,35], besides the DDB2 role in modulating p21 levels after DNA damage [12]. In our experimental model we have found that DDB2-PCNA interaction may have a role to prevent uncontrolled cell proliferation. In fact, in the presence of the DDB2 mutant protein, very low level of p21 was detected, associated to an increased cellular growth and motility.

Based on our results, we speculate that the DDB2-PCNA interaction may have a role in regulating cell cycle progression; in DDB2^{PCNA-} stable clone, the defective checkpoint activation, together with a delayed DNA repair process, could license the cells to enter mitosis even in the presence of unrepaired DNA. The results from clonogenic assay support this hypothesis, driving cells to acquire new capabilities such as uncontrolled cell growth and increased resistance to UV irradiation.

Taken together, the binding between DDB2 and PCNA could play a fundamental role in the correct removing of the UV-C induced DNA damage and its impairment may determine the acquisition of a phenotype characterized by proliferation advantage.

Supplementary data for this article can be accessed on the publisher's website. Supplementary data associated with this article can be found in the online version, at doi: https://doi.org/10.1016/j.bbamcr.2018.03.012

Transparency document

The http://dx.doi.org/10.1016/j.bbamcr.2018.03.012 associated with this article can be found in online version.

Acknowledgments

We thank P. Vaghi (Centro Grandi Strumenti, Università di Pavia) for help in confocal microscopy analysis and C. Scalera for technical help.

References

[1] A.F. Fagbemi, B. Orelli, O.D. Schärer, Regulation of endonuclease activity in human nucleotide excision repair, DNA Repair 10 (2011) 722–729, http://dx.doi.org/10.1016/j.dnarep.2011.04.022.
[2] R.D. Wood, Mammalian nucleotide excision repair proteins and interstrand cross-link repair, Environ. Mol. Mutagen. 51 (2010) 520–526, http://dx.doi.org/10.1002/em.20569.
[3] E.C. Friedberg, How nucleotide excision repair protects against cancer, Nat. Rev. Cancer 1 (2001) 22–33, http://dx.doi.org/10.1038/35094000.
[4] M.E. Fitch, S. Nakajima, A. Yasui, J.M. Ford, In vivo recruitment of XPC to UV-induced cyclobutane pyrimidine dimers by the DDB2 gene product, J. Biol. Chem. 278 (2003) 46906–46910, http://dx.doi.org/10.1074/jbc.M307254200.
[5] J. Moser, M. Volker, H. Kool, S. Alekseev, H. Vrieling, A. Yasui, A.A. van Zeeland, L.H. Mullenders, The UV-damaged DNA binding protein mediates efficient targeting of the nucleotide excision repair complex to UV-induced photolesions, DNA Repair 4 (2005) 571–582, http://dx.doi.org/10.1016/j.dnarep.2005.01.001.
[6] P. Shiyanov, A. Nag, P. Raychaudhuri, Cullin 4A associates with the UV damaged DNA-binding protein DDB, J. Biol. Chem. 274 (1999) 35309–35312.
[7] A. Datta, S. Bagchi, A. Nag, P. Shiyanov, G.R. Adami, T. Yoon, P. Raychaudhuri, The p48 subunit of the damaged-DNA binding protein DDB associates with the CBP/p300 family of histone acetyltransferase, Mutat. Res. 486 (2001) 89–97.
[8] K. Sugasawa, Y. Okuda, M. Saijo, R. Nishi, N. Matsuda, G. Chu, T. Mori, S. Iwai, K. Tanaka, K. Tanaka, F. Hanaoka, UV-induced ubiquitylation of XPC protein mediated by UV-DDB-ubiquitin ligase complex, Cell 121 (2005) 387–400, http://dx.doi.org/10.1016/j.cell.2005.02.035.
[9] J. Li, Q.E. Wang, Q. Zhu, M.A. El-Mahdy, G. Wani, M. Praetorius-Ibba, A.A. Wani, DNA damage binding protein component DDB1 participates in nucleotide excision repair through DDB2 DNA-binding and cullin 4A ubiquitin ligase activity, Cancer Res. 66 (2006) 8590–8597, http://dx.doi.org/10.1158/0008-5472.CAN-06-1115.
[10] M.G. Rapatonski, J. Guerrero-Santoro, D.C. Bisi, C.L. Hsieh, V. Rapic-Otrin, A.S. Levine, The DDB1-CUL4ADDB2 ubiquitin ligase is deficient in xeroderma pigmentosum group E and targets histone H2A at UV-damaged DNA sites, Proc. Natl. Acad. Sci. 103 (2006) 2588–2593, http://dx.doi.org/10.1073/pnas.0511160103.
[11] E. Martinez, V.B. Palhan, A. Tjernberg, E.S. Lymar, A.M. Gamper, T.K. Kundu, B.T. Chait, R.G. Roeder, Human STAGA complex is a chromatin - acetylating transcription coactivator that interacts with pre-mRNA splicing and DNA damage-binding factors in vivo, Mol. Cell. Biol. 21 (2001) 6782–6795, http://dx.doi.org/10.1128/MCB.21.20.6782-6795.2001.
[12] T. Stoyanova, T. Yoon, D. Kopanja, M.B. Mokyr, P. Raychaudhuri, The xeroderma pigmentosum group E gene product DDB2 activates nucleotide excision repair by regulating the level of p21Waf1/Cip1, Mol. Cell. Biol. 28 (2008) 177–187, http://dx.doi.org/10.1128/MCB.00880-07.
[13] B.M. Borakat, Q.E. Wang, C. Han, K. Milum, D.T. Yin, Q. Zhao, G. Wani, el-SA Arafa, M.A. El-Mahdy, A.A. Wani, Overexpression of DDB2 enhances the sensitivity of human ovarian cancer cells to cisplatin by augmenting cellular apoptosis, Int. J. Cancer 127 (2010) 977–988, http://dx.doi.org/10.1002/ijc.25112.
[14] T. Stoyanova, N. Roy, S. Bhattacharjee, D. Kopanja, T. Valli, S. Bagchi, P. Raychaudhuri, p21 cooperates with DDB2 protein in suppression of ultraviolet ray-induced skin malignancies, J. Biol. Chem. 287 (2012) 3019–3028, http://dx.doi.org/10.1074/jbc.M111.295816.
[15] M. Ennen, R. Klotz, N. Touche, S. Finel, C. Barbieux, V. Beauchemin, E. Brunner, D. Thiebaut, A.C. Jung, S. Ledoppier, L. Domenjoud, J. Abecassis, F. Flörsz, S. Grandemange, P. Becuwe, DDB2: a novel regulator of NF-kB and breast tumor invasion, Cancer Res. 73 (2013) 5040–5052, http://dx.doi.org/10.1158/0008-5472.CAN-12-3655.
[16] N. Roy, P.V. Bommi, U.G. Bhat, S. Bhattacharjee, I. Elangovan, J. Li, K.C. Patra, D. Kopanja, A. Blunier, R. Benya, S. Bagchi, P. Raychaudhuri, DDB2 suppresses epithelial-to-mesenchymal transition in colon cancer, Cancer Res. 73 (2013) 3771–3782, http://dx.doi.org/10.1158/0008-5472.CAN-12-4069.
[17] C. Han, R. Zhao, X. Liu, A. Srivastava, L. Gong, H. Mao, M. Qu, W. Zhao, J. Yu, Q.E. Wang, DDB2 suppresses tumorigenicity by limiting the cancer stem cell population in ovarian cancer, Mol. Cancer Res. 12 (2014) 784–794, http://dx.doi.org/10.1158/1541-7786.MCR-13-0638.
[18] O. Cazzalini, P. Perucca, R. Macchi, S. Sommatis, E. Prosperi, L.A. Stivala, DDB2 association with PCNA is required for its degradation after UV-induced DNA damage, Cell Cycle 13 (2014) 240–248, http://dx.doi.org/10.4161/cc.26987.
[19] P. Perucca, S. Sommatis, R. Macchi, E. Prosperi, L.A. Stivala, O. Cazzalini, A DDB2 mutant protein unable to interact with PCNA promotes cell cycle progression of human transformed embryonic kidney cells, Cell Cycle 14 (2015) 3920–3928, http://dx.doi.org/10.1080/15384101.2015.1120921.
[20] L.A. Stivala, F. Riva, O. Cazzalini, M. Savio, E. Prosperi, p21 (waf1/cip1)-null human fibroblasts are deficient in nucleotide excision repair downstream the recruitment of PCNA to DNA repair sites, Oncogene 20 (2001) 563–570, http://dx.doi.org/10.1038/sj.onc.1204132.
[21] O. Cazzalini, S. Sommatis, M. Tillhon, I. Dutto, A. Bachi, A. Rapp, T. Nardo, A.I. Scovassi, D. Necchi, M.C. Cardoso, L.A. Stivala, E. Prosperi, CBP and p300 acetylate PCNA to link its degradation with nucleotide excision repair synthesis, Nucleic Acids Res. 42 (2014) 8433–8448, http://dx.doi.org/10.1093/nar/gku533.
[22] Q. Wei, J.E. Lee, J.E. Gershenwald, M.I. Ross, P.F. Mansfield, S.S. Strom, L.E. Wang, Z. Gao, Y. Qiao, C.I. Amos, M.R. Spitz, M. Davis, Repair of UV light-induced DNA damage and risk of cutaneous malignant melanoma, J. Natl. Cancer Inst. 95 (2003) 308–315.
[23] F. Riva, M. Savio, O. Cazzalini, L.A. Stivala, I.A. Scovassi, L.S. Cox, B. Decommun, E. Prosperi, Distinct pools of proliferating cell nuclear antigen associated to DNA replication sites: interact with the p125 subunit of DNA polymerase delta or DNA ligase I, Exp. Cell Res. 293 (2004) 357–367.
[24] J. Tang, G. Chu, Xeroderma pigmentosum complementation group E and UV-damaged DNA-binding protein, DNA Repair 1 (2002) 601–616.
[25] A. Ray, K. Milum, A. Batra, G. Wani, A.A. Wani, NER initiation factors, DDB2 and XPC, regulate UV radiation response by recruiting ATR and ATM kinases to DNA damage sites, DNA Repair 12 (2013) 273–283, http://dx.doi.org/10.1016/j.dnarep.2013.01.003.
[26] N. Zou, G. Xie, T. Cui, A.K. Srivastava, M. Qu, L. Yang, S. Wei, Y. Zheng, Q.E. Wang, DDB2 increases radioresistance of NSCLC cells by enhancing DNA damage response, Tumour Biol. 37 (2016) 14183–14191, http://dx.doi.org/10.1007/s13277-016-5203-y.
[27] Q. Zhu, S. Wei, N. Sharma, G. Wani, J. He, A.A. Wani, A.A. Human, CRL4DDB2 ubiquitin ligase preferentially regulates post-repair chromatin restoration of H3K56Ac through recruitment of histone chaperone CAF-1, Oncotarget 8 (2017) 104525–104542.
[28] S.Y. Zhang, S.C. Liu, L.F. Al-Salasem, D. Holliman, J. Babb, X. Gao, A.J. Klein-Szanto, E2F-1: a proliferative marker of breast neoplasia, Cancer Epidemiol. Biomark. Prev. 9 (2000) 395–401.
[29] T. Yoon, A. Chakrabortty, R. Franks, T. Valli, H. Kiyokawa, P. Raychaudhuri, Tumor-prone phenotype of the DDB2-deficient mice, Oncogene 24 (2005) 469–478, http://dx.doi.org/10.1038/sj.onc.1208211.
[30] P. Perucca, O. Cazzalini, O. Mortusewicz, D. Necchi, M. Savio, T. Nardo, L.A. Stivala, H. Leonhardt, M.C. Cardoso, E. Prosperi, Spatiotemporal dynamics of p21CDKN1A protein recruitment to DNA-damage sites and interaction with proliferating cell nuclear antigen, J. Cell Sci. 119 (2006) 1517–1527, http://dx.doi.

org/10.1242/jcs.02868.
[31] O. Cazzalini, A.I. Scovassi, M. Savio, L.A. Stivala, E. Prosperi, Multiple roles of the cell cycle inhibitor p21(CDKN1A) in the DNA damage response, Mutat. Res. 704 (2010) 12–20, http://dx.doi.org/10.1016/j.mrrev.2010.01.009.
[32] G. Soria, V. Gottifredi, PCNA-coupled p21 degradation after DNA damage: the exception that confirms the rule? DNA Repair 9 (2010) 358–364, http://dx.doi.org/10.1016/j.dnarep.2009.12.003.
[33] A. Karimian, Y. Ahmadi, B. Yousefi, Multiple functions of p21 in cell cycle, apoptosis and transcriptional regulation after DNA damage, DNA Repair 42 (2016) 63–71, http://dx.doi.org/10.1016/j.dnarep.2016.04.008.
[34] A.G. Georgakilas, O.A. Martin, W.M. Bonner, p21: a two-faced genome guardian, Trends Mol. Med. 23 (2017) 310–319, http://dx.doi.org/10.1016/j.molmed.2017.02.001.
[35] H. Li, X.P. Zhang, F. Liu, Coordination between p21 and DDB2 in the cellular response to UV radiation, PLoS One 8 (2013) e80111, , http://dx.doi.org/10.1371/journal.pone.0080111.